Organisation and Mechanism of Bacterial Twin Arginine Translocases

James Paul Barnett BSc

A thesis submitted for the degree of Doctor of Philosophy

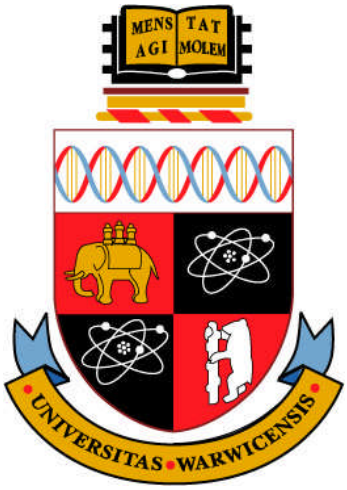

University of Warwick
Department of Biological Sciences

July 2009

Table of Contents

i Figures and Tables

ii Acknowledgments

First and foremost I thank Professor Colin Robinson for giving me the opportunity to complete this research and for his supervision throughout, including in the preparation of this manuscript.

I would also like to thank Prof. Oscar Kuipers and Dr. Robyn Eijlander for the gift of constructs for the over expression of the *B. subtilis* Tat proteins, without which this work would not have been possible.

I thank those members of the Robinson lab that have given assistance, advice, and encouragement during the course of this work. In particular I thank, Dr. Anja Nenninger, Dr. Lee Humphreys, Dr. Claire Barrett, Dr. Sharon Mendel, and Nishi Vashist who all made my time in the lab a memorable one.

I also thank Ryan for his help and support during the last three years, for reminding me that life exists outside the lab, and for his patience when work encroached into the rest of my life.

I thank my family, particularly my parents, for their love and support throughout my education and career as well as in life in general. I couldn't have done this without you!

Finally I would like to dedicate this thesis to my grandmother, Anne, who sadly passed away before its completion. Her enthusiasm for the natural world only encouraged my interest in biology.

iii Declaration

The work presented in this thesis is original, and was conducted by the author under the supervision of Professor Colin Robinson (University of Warwick).

None of the work presented in this thesis has been submitted previously for another degree.

This research was funded by a BBSRC Doctoral Training Account studentship.

All sources of information have been acknowledged by means of reference.

The confocal microscopy was performed with Dr. Anja Nenninger (University of Warwick).

Several of the plasmid constructs used in this study were provided by others as indicated in the text.

Part of this work has been published in the following journal articles:

Barnett, J. P., Eijlander, R. T., Kuipers, O. P. and Robinson, C. (2008) A minimal Tat system from a Gram-positive organism: A bifunctional TatA subunit participates in discrete TatAC and TatA complexes. *J. Biol. Chem*. **283**, 2534-42.

Barnett, J.P., van der Ploeg, R., Eijlander, R. T., Nenninger, A., Mendel, S., Rozeboom, R., Kuipers, O. P., van Dijl, J. M., and Robinson, C. (2009) The twin-arginine translocation (Tat) systems from Bacillus subtilis display a conserved mode of complex organization and similar substrate recognition requirements. *FEBS J*. **276**, 232-43.

iv Summary

The bacterial Tat pathway facilitates the translocation of pre-folded proteins over the cytoplasmic membrane. In Gram-negative bacteria, TatA, TatB and TatC (each an integral membrane protein) are the essential components. Most of our understanding of Tat function in bacteria has come from studies on *Escherichia coli*, a Gram-negative bacterium.

Gram-positive bacteria have Tat systems that are composed of just a single TatA and TatC protein. The absence of TatB suggests a different organisation and translocation mechanism to the Tat systems of Gram-negative bacteria.

Here the Tat pathway of *Bacillus subtilis*, a Gram-positive bacterium, was analysed in detail for the first time revealing important structural differences to the *E. coli* Tat pathway.

Complementation experiments reveal the Tat pathway of *B. subtilis* is active in *E. coli*, pointing to functional conservation between Gram-negative and Gram-positive bacteria.

The complexes formed by TatA and TatC in *B. subtilis* were investigated. TatA and TatC form a tight complex that is significantly smaller than its *E. coli* TatABC counterpart, possibly reflecting the presence of a different number of TatA and/or TatC units within this complex. TatA in *B. subtilis* like in *E. coli* also forms homo-oligomeric complexes separately from TatC. Unlike *E. coli* TatA complexes that vary enormously in size, the TatA complexes of Gram-positive bacteria are small and homogeneous in nature, suggesting an entirely different translocation mechanism involving a single defined translocon rather than a spectrum of size variants as proposed for *E. coli*.

The TatA proteins from Gram-positive bacteria may be bifunctional and perform the roles of *E. coli* TatA and TatB. Here the first direct evidence to support this hypothesis is presented and domains important for both TatA and TatB roles identified.

Finally a soluble population of TatA identified in *B. subtilis* was analysed and evidence is presented that suggests it maybe mis-localised.

v Abbreviations

AMP	Amphipathic Helix
APS	Ammonium persulphate
ATP	Adenosine triphosphate
BCA	Bicinchoninic acid
BN-PAGE	Blue Native PAGE
BSA	Bovine serum albumin
C-	Carboxy terminus
C	Cytoplasmic fraction
CD	Circular Dichroism
DDM	*n*-Dodecyl-*ß*-D-maltoside
DHFR	Dihydrofolate reductase
DMSO	Dimethyl sulphoxide
dNTP	Deoxynucleotide triphosphate
E	Elution fraction
ECL™	Enhanced chemifluoresence
EDTA	Ethylenediaminetetraacetic acid
EM	Electron microscopy
FPLC	Fast protein liquid chromatography
FT	Flow through fraction
GFP	Green fluorescent protein
GTP	Guanidine triphosphate
his / h	Hexahistidine tag
HRP	Horseradish peroxidise
IMVs	Inverted inner membrane vesicles
IPTG	Isopropylthiogalactosidase
kDa	kilo Dalton
LB	Luria Bertani medium
M	Membrane fraction
N-	Amino terminus
OD	Optical density
OG	*n*-Octylglucoside
P	Periplasmic fraction

PAGE	Polyacrylamide gel electrophoresis
PBSt	Phosphate buffered saline (0.01% Tween 20)
PCR	Polymerase chain reaction
PMF	Proton motive force
PVDF	Polyvinylidene fluoride membrane
RNA	Ribonucleic acid
rpm	Revolutions per minute
SDS	Sodium dodecyl sulphate
Sec	General secretory pathway
SRP	Signal recognition particle
Strep / s	Strep II tag
Tat	Twin arginine translocation
TCA	Trichloroacetic acid
TEMED	Tetramethylethylenediamine
TM	Transmembrane span
TMAO	Trimethylamine-*N*-oxide
TorA	Trimethylamine-*N*-oxide reductase
v/v	Volume per volume
W	Wash fraction
WT	Wild type
w/v	Weight per volume
YFP	Yellow fluorescent protein
Δ	Delta (gene deletion).

vi Amino acids

Amino acid	Single letter code	3 letter code
Alanine	A	Ala
Asparagine or Aspartic acid	B	Asx
Cysteine	C	Cys
Aspartic acid	D	Asp
Glutamic acid	E	Glu
Phenylalanine	F	Phe
Glycine	G	Gly
Histidine	H	His
Isoleucine	I	Ile
Lysine	K	Lys
Leucine	L	Leu
Methionine	M	Met
Asparagine	N	Asn
Proline	P	Pro
Glutamine	Q	Gln
Arginine	R	Arg
Serine	S	Ser
Threonine	T	Thr
Valine	V	Val
Tryptophan	W	Trp
Tyrosine	Y	Tyr
Glutamine or Glutamic acid	Z	Glx

Chapter 1

Introduction:
Protein Translocation in Prokaryotes

1.1 Bacterial protein translocation.

Protein translocation is an essential process in cellular life, even in the simplest prokaryotic organisms that lack the complex compartmentalisation of eukaryotic cells.

Bacteria are prokaryotes and they are broadly classified into two separate groups according to their ability to retain the dye Gram-stain. Those that retain Gram-stain are classified as Gram-positive bacteria whilst those that do not are classified as Gram-negative bacteria. Their cell walls have a different composition. In Gram-positive bacteria the cell is enclosed by a single membrane that is encapsulated by a thick cell wall layer of peptidoglycan and a co-anionic polymer. In this case non-cytoplasmic proteins can be inserted into the cytoplasmic membrane, secreted across it into the growth medium or can be attached to the cell wall by ionic and covalent linkages. Gram-negative bacteria have a more complex arrangement. The cytoplasmic membrane is encapsulated by a thinner layer of peptidoglycan that is further surrounded by an outer membrane. In this case non-cytoplasmic proteins maybe inserted into the cytoplasmic membrane or translocated across it to the periplasm. Some proteins maybe further inserted into the outer membrane or secreted from the cell by specialised secretion systems. Other secretion systems have evolved that secrete proteins in a single process across both membranes (Saier, 2006). A diagram showing the cell walls of both types of bacteria is shown in Figure 1.1.

In bacteria up to 20% of all of the proteins synthesised in the cytoplasm are destined for translocation across the cytoplasmic membrane. Most translocated proteins are transported via the Sec (General secretory) pathway (Pugsley, 1993), but a small number of substrates use the Tat pathway. This thesis focuses on the translocation of proteins by the Tat pathway and this will be discussed in detail.

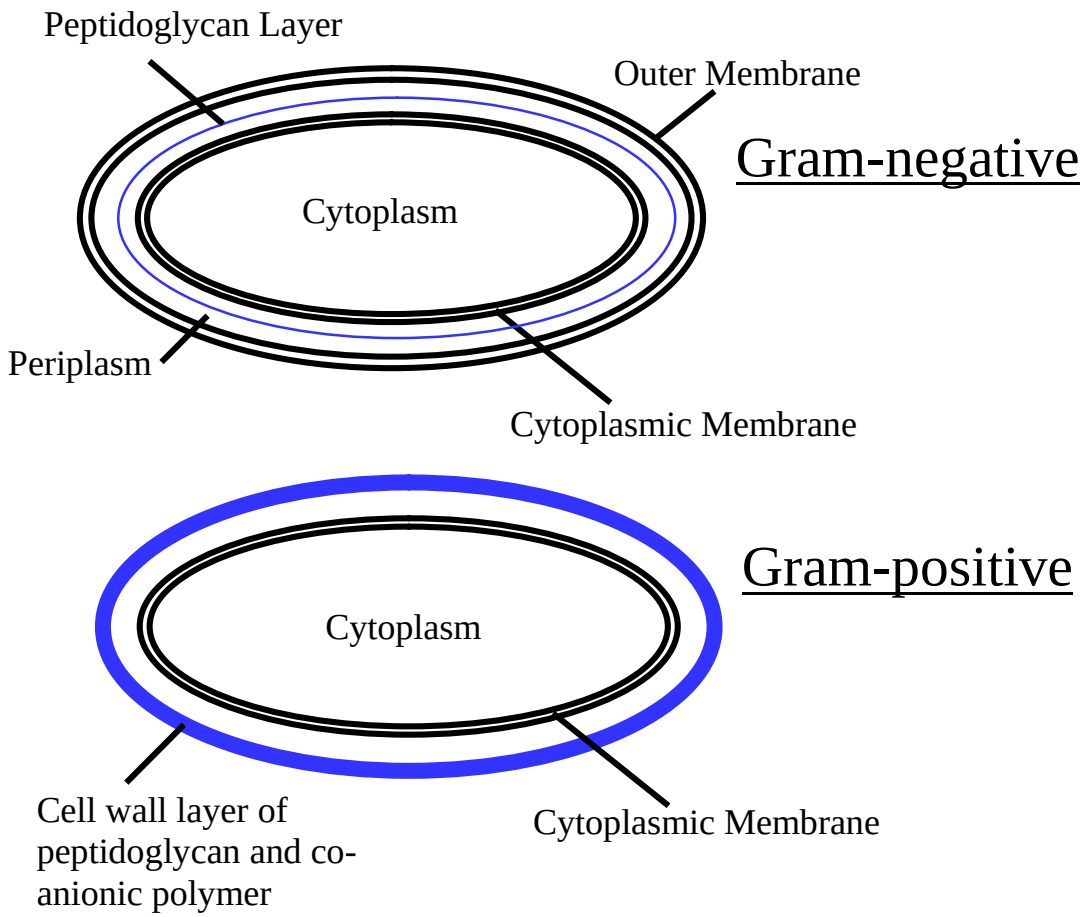

Figure 1.1 Bacterial cell walls.
Schematic representation of the bacterial cell wall, both types of bacteria are shown. The Gram-negative cell wall is composed of a cytoplasmic inner membrane, thin peptidoglycan layer and a further outer membrane. Gram-positive bacteria have a single membrane surrounded by a much thicker cell wall layer of peptidoglycan and co-anionic polymer.

1.2 The General Secretory (Sec) pathway

Most translocated proteins in bacteria use the well characterised General secretory or Sec pathway (Pugsley, 1993). This pathway translocates proteins in an unfolded conformation through the heterotrimeric SecYEG pore within the membrane. In *E. coli* SecY is a 48 kDa protein with 10 transmembrane spans (Akiyama and Ito, 1987), whilst the SecE and SecG proteins are ~ 15 kDa and have 3 and 2 transmembrane spans respectively (Schatz *et al.*, 1989; Nishiyama *et al*., 1994). Within each Sec YEG complex, SecY and SecE are both strictly essential and are tightly bound to one another (Brundage *et al*., 1990), whilst SecG is located peripherally in the complex (Hanada *et al*., 1994; Nishiyama *et al*., 1994). Another heterotrimeric complex, the SecDFYajC complex, associates with SecYEG but is not essential for translocation; although cells lacking SecDF exhibit a reduced level of translocation activity (Duong and Wickner, 1997). The proposed translocation channel is formed by a SecYEG dimer and has the overall shape of an hourglass that is ~ 4 Å at it most constricted point and ~ 20-25 Å at its widest (Breyton *et al*., 2002; Mitra *et al*., 2005; Van den Berg *et al*., 2004). The channel is closed by a periplasmic loop of the SecY protein that forms a plug. The SecY protein is likely to undergo a conformational change during the translocation process leading to displacement of the channel plug and opening of the pore (Li *et al*., 2007; Maillard *et al*., 2007; Tam *et al*., 2005).

Some substrates that are translocated by the Sec pathway are bound by general cytosolic chaperones such as GroEL immediately after synthesis. These chaperones maintain the substrate in a largely unfolded and translocation competent state for translocation through the SecYEG channel (Kumamoto, 1991). Other substrates are bound to the chaperone SecB after protein synthesis (Kumamoto and Francetic, 1993). SecB is a chaperone that is specific for translocation, targeting substrates to the membrane by interactions with the SecA protein (Hartl *et al*., 1990). ATP binding to SecA is the main driving force of translocation but the proton motive force is also important (Driessen, 1992). SecA is a 102 kDa hydrophilic protein and is found both within the cytosol and in a membrane bound state where it is peripherally associated with SecYEG (Cabelli *et al*., 1991; Chun and Randall, 1994). The SecA ATPase binds with high affinity to SecB and to substrate proteins (Hartl, *et al*., 1990), and drives the

polypeptide chain through the translocation channel in repeated cycles of ATP binding and subsequent release of the substrate upon ATP hydrolysis (Driessen, 1992). Figure 1.2 shows the current model of Sec-dependent translocation in *E. coli.*

The Sec pathway also operates in eukaryotes but this will not be discussed here. For a review of the Sec pathway in both prokaryotes and eukaryotes see Stephenson, 2005.

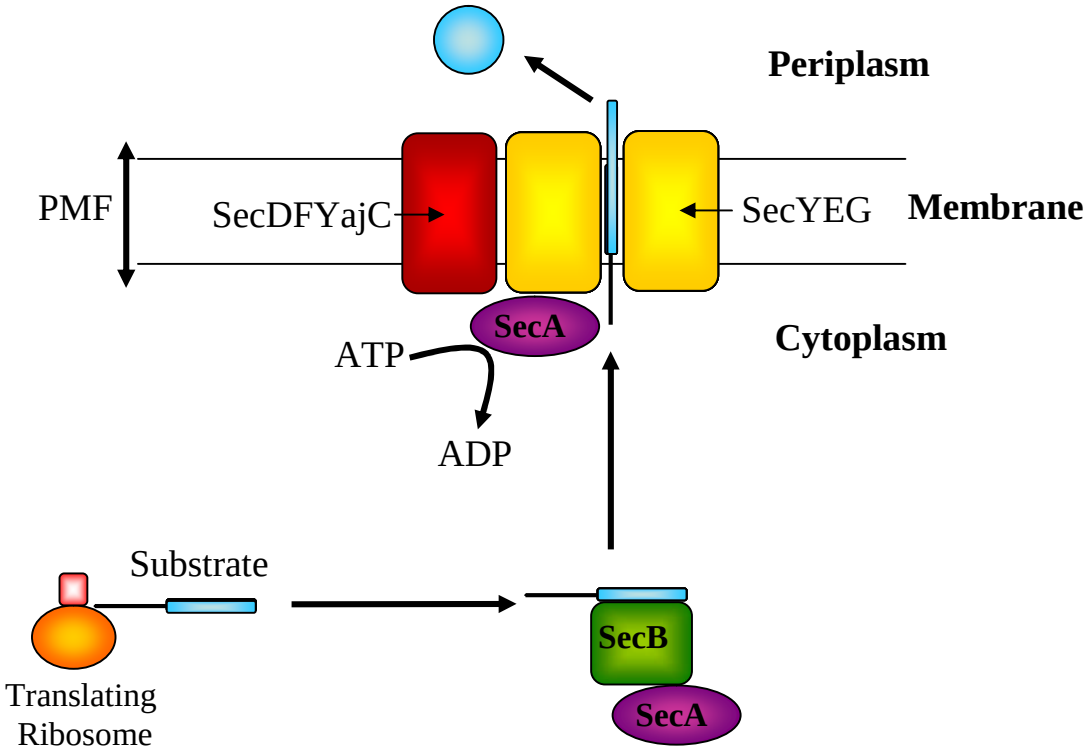

Figure 1.2 Overview of protein translocation by the *E. coli* Sec pathway
Schematic representation of the bacterial Sec pathway: Following protein synthesis, substrate proteins are bound by the SecB chaperone. The substrate is targeted to SecYEG through the interactions of SecB with the SecYEG associated SecA protein. The signal peptide of the substrate binds to SecA triggering the binding of ATP to SecA and the release of SecB. The substrate is then translocated through the SecYEG pore in a threading mechanism that is driven by ATP binding to SecA and then subsequent ATP hydrolysis leading to release of the substrate. The PMF force is also important for driving translocation as are the accessory proteins SecDFYajC.

1.3 The Signal Recognition Particle (SRP)

Proteins that are inserted into the bacterial cytoplasmic membrane use the Signal Recognition Particle (SRP) to target proteins to the Sec pathway. SRP is also present in eukaryotes, for a review of the SRP in both prokaryotes and eukaryotes see Pool, 2005.

The bacterial SRP meets the Sec pathway at the SecYEG pore in the membrane. The SRP is composed of 4.5S RNA and Ffh, a 48 kDa GTPase (Phillips and Silhavy, 1992) that interacts with the signal peptides (Luirink *et al.*, 1992) and transmembrane spanning domains of substrate proteins (Valent *et al.*, 1995). In eukaryotes SRP binds to substrates as they emerge from the ribosome resulting in translation arrest, but in bacteria translation arrest has not been observed. The Ffh component of SRP only binds to substrates that are still bound to the ribosome, (Luirink *et al.*, 1992). In bacteria the SRP/ribosome/substrate complex is targeted to the FtsY protein in a process that is dependent on GTP (Gill and Salmond, 1990; Miller *et al.*, 1994) . The FtsY protein is found bound to the anionic phospholipids of the membrane and also to SecYEG (Luirink *et al.*, 1994). The substrate protein enters the SecYEG pore during translation at the ribosome. It is thought that the SecYEG channel has a gate that allows membrane proteins to insert laterally into the lipid bilayer directly from the translocation channel (Duong and Wickner, 1998). The *in vitro* membrane insertion of FtsQ into SecYEG proteoliposomes requires the SRP, SecYEG, SecA and a membrane electrical potential minimally (Van der Laan *et al*., 2004). The bacterial SRP targeting pathway is shown in Figure 1.3.

An additional mechanism has recently been discovered that allows membrane protein insertion to occur in a process dependent on the protein YidC (Samuelson *et al.*, 2000). YidC is able to act in concert with SecYEG (Scotti *et al.*, 2000) or act independently as a membrane protein insertase (Samuelson *et al.*, 2001; Serek *et al*, 2004). YidC itself has a membrane localisation. For a review of YidC dependent membrane protein insertion see Kol *et al*., 2008.

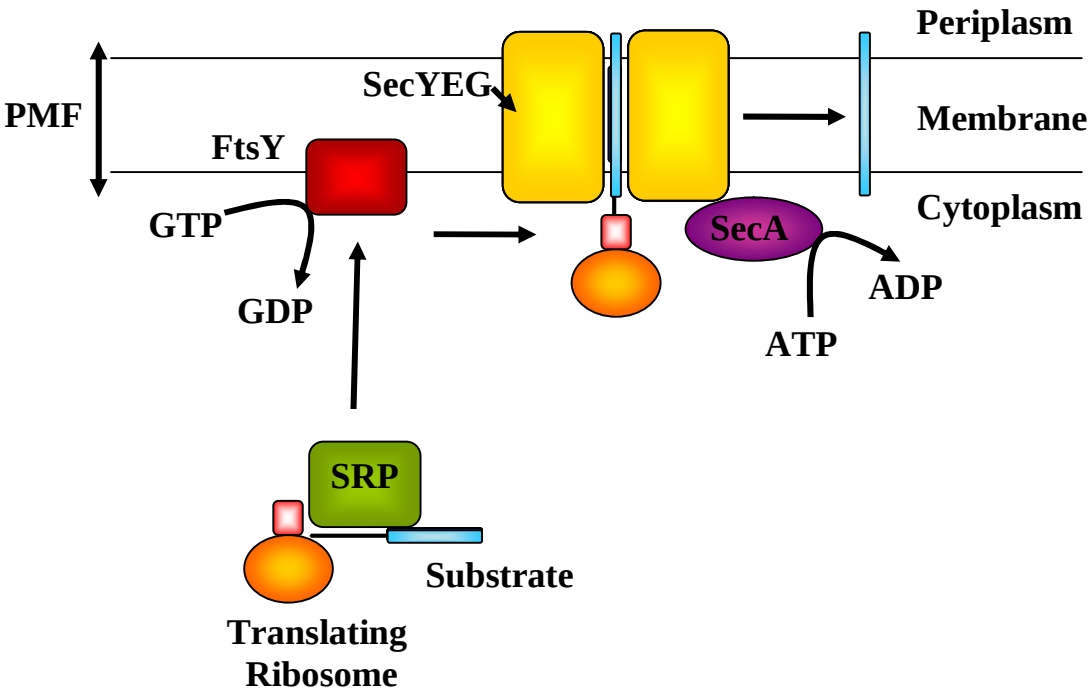

Figure 1.3 Overview of membrane protein insertion directed by bacterial SRP
Schematic representation of the bacterial SRP pathway: Proteins bind to SRP as they exit the translating ribosome. Ribosome/substrate/SRP complexes dock with SecYEG associated FtsY proteins. Substrates pass into the SecYEG pore co-translationally before inserting laterally into the lipid bilayer.

Operating alongside the Sec pathway is the more recently discovered Tat, or Twin-Arginine Translocation pathway. It is this pathway that is the focus of this thesis and is discussed in detail below. For reviews see Lee *et al*., 2006; Muller and Klosgen, 2005; Robinson and Bolhuis, 2004.

1.4 The Twin-Arginine translocation pathway.

1.4.1 Introduction

The Tat, or Twin-Arginine Translocation pathway was discovered in chloroplasts towards the beginning of the 1990s. It was discovered that a number of polypeptides were translocated across thylakoid membranes without any requirement for ATP (Cline *et al*., 1992; Mould and Robinson, 1991). Translocation was supported solely by the proton motive force and reflecting this, the pathway was originally called the ΔpH-dependent pathway. It is now called the chloroplast Tat pathway (cpTat). The cpTat pathway was later found to support the transport of pre-folded proteins across thylakoid membranes and into the lumen (Creighton *et al*., 1995). The chloroplast Tat pathway requires three proteins, these are Tha4 that is also called TatA (Mori *et al*., 1999; Walker *et al*., 1999), Hcf106 that is also called TatB (Settles *et al*., 1997), and cpTatC (Cline and Mori, 2001). For a review of the chloroplast Tat pathway see Muller and Klosgen, 2005.

Homologues of each of these proteins are also found in bacteria and are called TatA, TatB and TatC respectively (Bogsch *et al*., 1998; Sargent *et al*., 1998; Sargent *et al.*, 1999) . Gram-negative bacteria have been found to contain all three of these proteins, while all Gram-positive bacteria except for *Streptomyces* species contain only TatA and TatC (Yen *et al*., 2002).

The most widely studied Tat pathway is that of the model organism *Escherichia coli*. The three *tat* genes of *E. coli* that are required for translocation, *tatA*, *tatB*, and *tatC* are co-expressed alongside the *tatD* gene in an operon. The *tatD* gene encodes a protein with DNase activity and was originally thought not to function in the Tat pathway (Wexler *et al*., 2000). However recent research has uncovered the involvement of the TatD protein in the quality-control of Tat substrates (Matos *et al*., 2009). The *tat* operon is constitutively expressed in *E. coli* but is only essential for anaerobic growth on minimal media (Santini *et al*., 1998; Sargent *et al*., 1998, Weiner *et al*., 1998). Another *tat* gene, *tatE*, is also present in *E. coli* and is expressed elsewhere in the genome. The *tatE* gene is monocistronic and is thought to be a gene

duplication of *tatA* but is not thought to have any significant role in translocation. TatE is present at significantly lower levels than the TatA protein and is not required for Tat function. It can however partially complement *E. coli ΔtatA* cells (Sargent *et al*., 1998; Jack *et al*., 2001). The organisation of the *tat* genes of *E. coli* is shown schematically in Figure 1.4.1

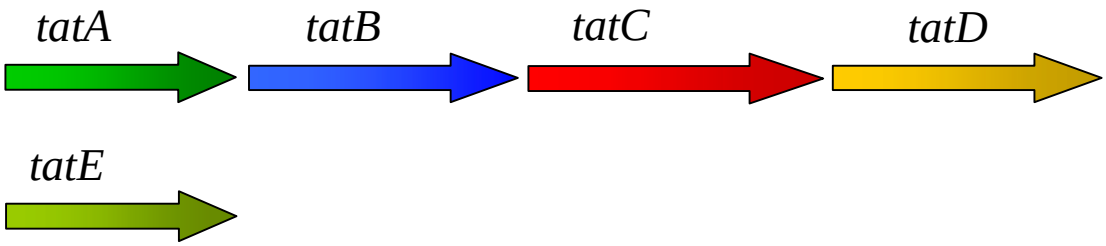

Figure 1.4.1 The *tat* genes of *E. coli*
The 3 *tat* genes of *E. coli* that are required for translocation are constitutively expressed alongside the *tatD* gene in an operon. The *tatD* gene is involved in the quality-control of Tat substrates. A fifth *tat* gene, *tatE* is a gene duplication of *tatA* that is expressed elsewhere in the genome.

1.4.2. The TatABC proteins

The *tatA* gene encodes an 82 amino-acid integral membrane protein of ~9.5 kDa with its N-terminal end protruding into the periplasm and its C-terminal end in the cytosol. It has a single N-terminal transmembrane spanning domain linked to an amphipathic helix that lies along the inner face of the membrane surface. The two helices are connected by a well conserved but short hinge. A short and largely unstructured C-terminal tail follows the amphipathic helix (Settles *et al.*, 1997; Sargent *et al.*, 1998; Lee *et al*., 2002). This topology of TatA across the membrane has been questioned and a dual topology has been proposed (Chan *et al*., 2007; Gouffi *et al.*, 2004; Porcelli *et al.*, 2002), suggesting that the C-terminal amphipathic domain of TatA may insert into the membrane bilayer during translocation.

TatA is found at ~20 times the level of TatB (Sargent *et al.*, 2001), and appears to be a major constituent of the translocation channel (Gohlke *et al*., 2005). The localisation of TatA was studied using a fusion of TatA and YFP. The TatA protein has an even

distribution around the periphery of the cell (Berthelmann and Bruser, 2004; Leake *et al*., 2008; Ray *et al*., 2005). TatA has also been found to have a cytosolic as well as a membrane localisation in several bacteria including *E. coli* (Berthelmann *et al*., 2008; De Keersmaeker *et al*., 2005; Pop *et al*., 2003). More recently a soluble population of the plant homologue of TatA, Tha4 was found alongside its thylakoid membrane localisation in the chloroplast stroma (Frielingsdorf *et al*., 2008). The role that cytosolic TatA plays in the translocation process is ambiguous and further work is needed to examine its role if any. Several mutagenesis studies have been performed on the *E. coli* TatA protein to identify amino-acid residues critical for Tat-dependent translocation. Most amino-acid substitutions that severely affect translocation activity, are localised to the hinge region and to the amphipathic helix (Barrett *et al*., 2003; Greene *et al*., 2007; Hicks *et al*., 2003; Lee *et al*., 2002).

The *tatB* gene encodes a protein with homology to TatA. It has a similar secondary structure and membrane topology to TatA, although it is larger. TatB is ~18.5 kDa and is composed of 171 amino acids. Like TatA it has a transmembrane domain with its N-terminus protruding into the periplasm and it's C-terminus in the cytoplasm (Bolhuis *et al*., 2001). Following the transmembrane span is a small hinge region and amphipathic helix that aligns along the inside surface of the membrane (De Leeuw *et al*., 2001; Settles *et al*., 1997; Sargent *et al*., 1998). TatB has a much larger C-terminal tail extension than TatA. This C-terminal tail is largely unstructured and truncation analysis has found that it is not required for translocation activity (Lee *et al*., 2002). Further mutagenesis studies found that like TatA the hinge region and amphipathic helix are critical for function with single amino acid substitutions in these regions having dramatic effects on translocation activity (Barrett *et al*., 2003; Hicks *et al*., 2003; Lee *et al*., 2006). The localisation of TatB in the plasma membrane is somewhat ambiguous with two independent studies using a TatB-GFP fusion drawing different conclusions. In one study the TatB protein had a uniform distribution around the periphery of the cell (Ray *et al*., 2005), whilst another study found TatB to localise to the cell poles (Berthelmann and Bruser, 2004). In *E. coli* TatB has a strict membrane localisation, but in one Gram-positive bacterium, *Streptomyces lividans*, TatB has also been found in a cytosolic localisation (De Keersmaeker *et al*., 2005). The functional significance that cytosolic TatB has remains to be determined. Whilst the presence of TatB is a prerequisite for the translocation of native *E. coli* Tat substrates, Colicin V

was translocated in the complete absence of TatB in *E. coli* (Ize *et al*., 2002b). More recently the translocation of a reporter protein that consisted of a fusion of the signal peptide of TMAO reductase (TorA), (an *E. coli* Tat substrate) with MalE was observed in the absence of TatB (Blaudeck *et al*., 2005). Single amino acid substitutions to the N-terminal periplasmic domain of TatA resulted in significant increases in translocation by *E. coli* TatAC. These data suggest TatB is not required for transport of all substrates. It also points to an important role for the extreme N-terminal periplasmic domain of TatB for function.

TatC, the largest of the three Tat proteins required for translocation, is also the most highly conserved. TatC is ~ 32 kDa and is 258 amino acids in length. It has 6 transmembrane alpha-helical domains and has its N and C-termini protruding into the cytosol (Behrendt *et al*., 2004). The cytosolic loops connecting the transmembrane domains are particularly important for function. Several mutagenesis studies have found that single amino acid substitutions within these cytosolic loops can have a drastic effect on translocation activity (Allen *et al*., 2002; Buchanan *et al*., 2002, Punginelli *et al*., 2007). Similar to TatB, the localisation of TatC within the plasma membrane is debated with two independent studies using TatC-GFP fusions showing a polar localisation (Berthelmann and Bruser, 2004), and a uniform distribution around the plasma membrane (Ray *et al*., 2005). The overall membrane topologies and secondary structures of the 3 required Tat proteins of *E. coli* are shown in Figure 1.4.2.

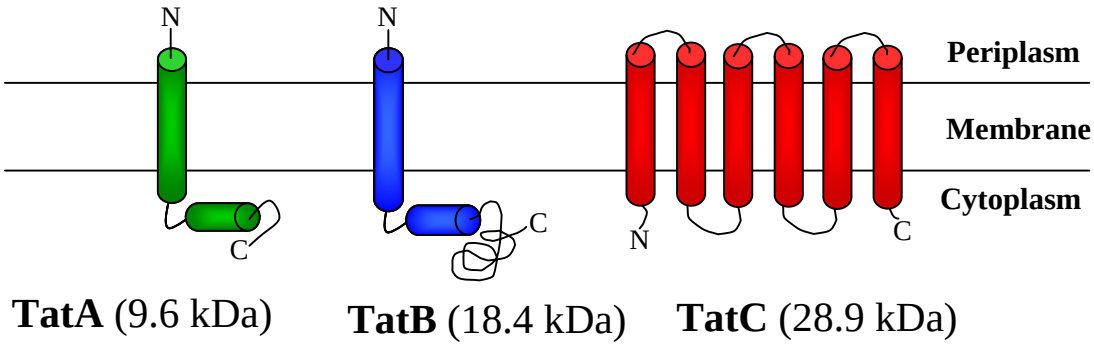

Figure 1.4.2 Topology of the 3 Tat proteins of *E. coli* required for translocation in the plasma membrane
A schematic representation of the topologies of the 3 Tat proteins of *E. coli* required for translocation within the plasma membrane: TatA and TatB have a single transmembrane spanning domain connected to a small hinge region linking the amphipathic helix that lies along the inner surface of the plasma membrane. Following the amphipathic helix is a C-terminal extension with TatB having a much larger extension than TatA. TatC has 6 transmembrane spans with both N and C-termini at the cytosolic face of the membrane.

1.4.3 Tat protein complexes

The organisation of the 3 Tat proteins required for translocation into complexes within the plasma membrane has been widely investigated. A TatABC containing complex was purified from *E. coli* membranes using affinity chromatography (utilising an affinity-tag on the TatC proteins C-terminus). Within this complex the TatB and the TatC subunits exist in equimolar stochiometry whilst the amount of TatA present varies suggesting a looser association within this complex (Bolhuis *et al*., 2001). In the plant thylakoid membrane the TatA homologue Tha4 is not found in a complex with hcf106 and cpTatC (TatBC), and these two proteins form a stable 700 kDa hcf106-cpTatC complex (Cline and Mori, 2001).

The size of the *E. coli* TatABC complex was estimated by gel filtration chromatography in the detergent digitonin and found to be around 600 kDa (Bolhuis *et al*., 2001). Clearly multiple copies of TatABC are present within this complex. A more accurate determination of the TatABC complex size was obtained using blue-native PAGE where the TatABC complexes run as a discrete band of 370 kDa (Oates *et al*., 2005). Single particle analysis of purified TatABC complexes by electron microscopy

using negative staining found the TatABC complex to have an overall asymmetric oval shape with 6 or 7 stain excluding domains (that may be single TatABC units), and a central pool of stain linking to the exterior of the complex (Oates *et al*., 2003).

It was reported in the literature that within the *E. coli* TatABC complex, the TatA protein is essential for stability (Mangels *et al*., 2005), however a more recent report has found that TatA has an effect on neither the formation nor stability of the TatBC complex (Orriss *et al*., 2007). In the same report TatB and TatC were found to assemble into homo-multimeric complexes in the absence of each other and these multimers may represent structural subcomplexes that assemble to form the TatBC containing complex. A separate study found that TatB without TatC formed complexes that varied in size from 100 – 880 kDa and that this multimerization of TatB was suppressed by TatC (Behrendt *et al*., 2007). In the same study the TatC protein when expressed on its own was found to form 250 kDa complexes; it was suggested that this could form a scaffold onto which TatB assembles to form the TatBC complex (Behrendt *et al*., 2007).

The arrangement of the Tat proteins within the TatABC complex remains to be determined unambiguously. The availability of highly purified Tat complexes should be exploited and used for further structural analysis that may help to resolve this question.

The TatABC complexes from several other Gram-negative bacteria including *Salmonella typhimurium*, and *Agrobacterium tumefaciens* have been analysed in a similar way to the *E. coli* Tat complexes; essentially similar findings were obtained indicating a degree of conservation in terms of both complex organisation and structure (Oates *et al*., 2003).

The vast majority of *E. coli* TatA is not found within the TatABC complex but forms separate homo-oligomeric complexes within the membrane. The TatA complexes vary enormously in size and form a ladder of bands on BN-gels running from below 100 kDa to over 500 kDa (Oates *et al*., 2005). Electron microscopy found that these complexes form channels of variable diameter (Gohlke *et al*., 2005). In the plant Tat system, Tha4 has a different arrangement and is found to form discrete homo-

oligomeric complexes of 400 kDa (Cline and Mori, 2001). The stochiometry of *E. coli* TatA complexes was further probed using *in vivo* imaging of TatA-YFP at native levels of expression in *E. coli*. The TatA protein was found to have a variable stochiometry as previously described but on average comprised 25 TatA molecules. Furthermore the TatA protein was found to be organised into approximately 15 mobile complexes within the membrane with a separate pool of more disperse TatA molecules also present (Leake *et al*., 2008).

Although it is now widely accepted that two major membrane localised Tat complexes are present, TatABC and separate TatA, other studies have found a rather different organisation. Two independent studies isolated a complex that contained essentially all of the TatA protein contained within the cell membrane with just a small amount of the total TatB protein present (Bolhuis *et al*., 2001; De Leeuw *et al*., 2001). These isolated TatAB complexes were analysed by electron microscopy and found to have a ring shaped structure organised in two layers (Sargent *et al*., 2001). Another study found that TatA rather than forming homo-oligomeric complexes that vary in size, actually forms a discrete complex of ~ 460 kDa (Porcelli *et al*., 2002).

Most of the studies mentioned above have examined the Tat complexes formed during over expression of the proteins in *E. coli*. One study has examined Tat complex formation with native levels of expression and found TatB and TatC form a complex of 400 - 500 kDa (judged by gel filtration chromatography) and that all of the TatA forms separate homo-oligomeric complexes of variable size (McDevitt *et al*., 2006). This suggests that perhaps like in the cpTat pathway, *E. coli* TatBC are present in a complex separate from any TatA and that over expression results in TatA association with TatBC.

1.4.4 Tat substrates

It was discovered that the Tat pathway translocates a small set of cofactor containing redox enzymes in *E. coli* (Berks, 1996; Weiner *et al*., 1998). These substrates require the insertion of metal ion cofactors within the cytosol prior to translocation, explaining the need for a pathway capable of transporting folded proteins. Examples include trimethyl *N*-oxide reductase (TorA), and dimethyl sulfoxide reductase (DmsA) that are used in anaerobic respiration (Mejean *et al*., 1994; Weiner *et al*., 1988). A functioning Tat pathway is essential for anaerobic growth (Jack *et al*., 2001). Since then several Tat substrates have been identified that do not have a cofactor and it seems likely that these are translocated *via* Tat because of the rapid folding kinetics of these particular proteins. The Tat pathway is required for cell wall biogenesis. Mis-localisation of the two *E. coli* Tat substrates AmiA and AmiC in *tat* null mutants, results in a cell division phenotype with cells growing as long filamentous chains (Ize *et al*., 2003; Bernhardt and de Boer, 2003). These filamentous cells have an increased sensitivity to the detergent SDS and SDS sensitivity has been used to assay for a functional Tat pathway; neither AmiA nor AmiC possesses a cofactor.

Another hypothesis is that some substrates are unable to attain their biologically active state once translocated to the periplasm. For example, GFP is transported by the *E. coli* Tat and Sec translocases, however it is found in its active fluorescent state only when translocated in a Tat-dependant manner (Feilmeier *et al*., 2000; Thomas *et al*., 2001).

Some organisms favour the Tat pathway due to their harsh external environments. *Halophilic archaea* are thought to use the Tat pathway as the high salt concentrations in the external environment would cause aggregation of unfolded proteins (Rose *et al*., 2002).

In summary then, the Tat pathway exists to allow the translocation of proteins requiring a certain degree of folding prior to transport.

The extent to which different bacterial species utilise the Tat pathway varies considerably (Dilks *et al*., 2003), presumably due to differences in their requirements

for folding of substrates prior to transport, the reasons for which are outlined above. The bacterium *Streptomyces coelicolor* has 25 identified Tat substrates making it an important translocation pathway in this bacterium (Widdick *et al*., 2006), and *E. coli* has ~ 30 Tat substrates (Dilks *et al*., 2003). In contrast some bacteria make little use of the Tat pathway. The Gram-positive bacterium *B. subtilis* has just 4 confirmed Tat substrates (Widdick *et al*., 2008). Other bacteria such as *Lactococcus lactis* do not possess any Tat protein homologues (Dilks *et al*., 2003).

The virulence of several pathogenic bacteria also relies heavily on the Tat pathway. Examples include, *Pseudomanas aeruginosa* (Ochsner *et al*., 2002), *Yersinia pseudotuberculosis,* (Lavander *et al*., 2006) as well as some strains of *E. coli.* The secretion of virulence factors in *P. aeruginosa* relies on the Tat pathway, with virulence abolished in *tat* null mutants. As discussed above the *E. coli* Tat pathway is important for anaerobic growth as well as for membrane biogenesis and cell division. The two cell wall amidases of *E. coli*, AmiA and AmiC are mislocalised in *tat* mutants leading to an increased susceptibility to lysis and sensitivity to compounds such as the detergent SDS (Ize *et al*., 2003; Bernhardt and de Boer, 2003). Such defeats in the *E. coli* cell will only serve to hinder the ability of *E. coli* to infect host organisms. The absence of any Tat homologues in mammalian cells makes the Tat pathway of human pathogens a potential target for the development of novel antimicrobial drugs. For a review of the requirement of the Tat pathway in bacterial virulence see De Buck *et al*., 2008.

The Tat pathway is of importance in plant pathogens too, and was found to have a role in establishment of plant infections by *Agrobacterium tumefacians* (Ding and Christie, 2003).

As well as serving to translocate proteins to the periplasm over the bacterial plasma membrane, the *E. coli* Tat pathway is also able to mediate integral membrane protein insertion in a number of cases (Hatzixanthis *et al*., 2003; Summer *et al*., 2000), in a mechanism that is independent of both YidC and SecYEG (Hatzixanthis *et al*., 2003). Examples have also been found in other organisms with the Rieske Fe/S proteins of *Legionella pneumophila* and *Paracoccus dentrificans* inserted into the plasma membrane via the Tat pathway (Bachmann *et al*., 2006; De Buck *et al*., 2007). A

remaining question is whether integral membrane proteins are inserted directly from the Tat translocase or whether they are inserted by some other mechanism from the periplasm following translocation. Since the ability of Tat to mediate membrane protein insertion was first discovered little progress has been made in elucidating the mechanism of insertion and this warrants further attention.

The potential exploitation of the Tat pathway for the development of novel antimicrobials has been discussed above, but the Tat pathway is also attractive to biotechnological exploitation and offers an alternative route in the production of commercially important protein products. For a review see Bruser, 2007. The Sec pathway has been widely used to export proteins of interest to the external growth medium from which they can be purified; however many proteins that are of commercial interest are not compatible with the Sec pathway. A good example of this, GFP, has already been mentioned above. When GFP is translocated by the Sec pathway it is unable to fold correctly and reach its active fluorescent state (Feilmeier *et al*., 2000). When translocated by the Tat pathway the protein reaches its active state before it is exported (Thomas *et al*., 2001).

1.4.5 The folded state of Tat substrates and quality-control mechanisms

Several pieces of evidence showing the Tat pathway is able to translocate fully folded proteins have been presented. In one such study on the thylakoid Tat pathway dihydrofolate reductase (DHFR) was successfully translocated across the thylakoid membrane into the lumen by the Tat pathway in the presence of methotrexate, (methotrexate causes tight folding of DHFR) (Hynds *et al*., 1998).

For the bacterial Tat pathway most evidence presented is indirect. The bacterial Tat pathway is responsible for the translocation of cofactor-containing redox enzymes. These substrates must acquire their cofactors in the cytosol before transport so folding must take place before translocation (Berks, 1996; Ilbert *et al*., 2003; Santini *et al*., 1998). Cytosolic chaperones have been identified in *E. coli* that interact with the N-terminal signal peptides of Tat substrates. These serve to prevent premature interactions with the Tat machinery before cofactor assembly and protein folding is complete. TorD and DmsD have both been identified as such quality-control

chaperones in *E. coli* binding to the signal peptides of TorA and DmsA respectively (Genest *et al*., 2006; Hatzixanthis *et al*., 2005a; Jack *et al*., 2004; Ray *et al*., 2003). For a review on the translocation of metal-ion cofactor requiring redox enzymes by the Tat pathway see Palmer *et al*., 2005. One report provided more direct evidence of quality-control in *E. coli*. Two *E. coli* Tat substrates that contain FeS centres, NrfC and NapG were mutated to prevent correct insertion and assembly of the FeS clusters. These mutant versions of the proteins were not only rejected by the Tat machinery for translocation but were directed for degradation by the Tat system itself (Matos *et al*., 2008). The TatD protein that was originally thought not to have a functional role in the Tat pathway (Wexler *et al*., 2000) has a central role in this quality-control function (Matos *et al*., 2009).

A further piece of evidence has been mentioned above already. GFP can be targeted for translocation to either the Sec or the Tat pathway, but only when it is translocated by Tat is it found in an active fluorescent state (presumably because it is prefolded before export) (Thomas *et al*., 2001; Feilmeier *et al*., 2000). More recently recombinant GFP that was fully folded was imported into *E. coli* inner membrane vesicles in a Tat-dependant manner, confirming that GFP is indeed translocated in a folded state (Bageshwar and Musser, 2007).

1.4.6 Tat signal peptides

Proteins that are destined for translocation over the bacterial plasma membrane by either the Sec or Tat pathways are targeted by short polypeptide chains at the N-terminus referred to as signal peptides. These peptides are similar for both Tat and Sec substrates and are divided into distinct regions; A positively charged region (N) at the N-terminal end, a central region that is largely hydrophobic (H), and a C-terminal region (C) that is polar. At the C-terminal end of these peptides is an Ala-Xaa-Ala motif that is required for removal of the signal peptide by signal peptidase following translocation (von Heijne, 1995). Tat signal peptides contain a highly conserved sequence of amino acids (S/TRRXFLK), (X in this case can any residue), between the N and H regions (Crsitobal *et al*., 1999; Berks, 1996). An example of a signal peptide of one *E. coli* Tat targeted substrate, (TorA), is shown in Figure 1.4.6. The two

arginine residues are almost completely conserved within the consensus motif and conservative substitution of both residues with Lysine causes a complete block in translocation activity (Buchanan *et al*., 2001; De Lisa *et al*., 2002; Ize *et al*., 2002a; Mendel *et al*., 2008, Stanley *et al*., 2000). It is these two conserved arginine residues that lend the Tat pathway its name. Substitution of just a single arginine within the RR pair is tolerated although in some cases a reduction in translocation activity has been observed (Buchanan *et al*., 2001; De Lisa *et al*., 2002; Ize *et al*., 2002a; Mendel *et al*., 2008, Stanley *et al*., 2000). Some naturally occurring variants of the consensus motif also occur. The signal peptide of TtrB (a confirmed Tat substrate in *Salmonella enterica*) has a KR rather than an RR pair (Hinsley *et al*., 2001) and *E. coli* penicillin amidase has a RNR motif (Ignatova *et al*., 2002). One more recent study has found mutations within the first and second cytoplasmic loops of *E. coli* TatC that allow translocation of TorA carrying a twin-Lysine rather than a twin-Arginine pair (Strauch and Georgiou, 2007), and a further study found that mutations in the N-terminus of TatB and first cytosolic loop of TatC allowed export of TorA-MalE carrying LQ in place of the RR pair (Kreutzenbeck *et al*., 2007).

Other determinants within the consensus motif have also been found to be important for translocation. The Serine residue immediately before the RR-pair when mutated to Alanine in the signal peptides of *E. coli* TorA and DmsA caused a dramatic reduction in translocation activity (Mendel *et al*., 2008). Interestingly another study that made the same S to A substitution in the N-terminal signal peptide from a different *E. coli* Tat substrate, SufI, found that this residue was not important for export (Stanley *et al*., 2000). It would seem the importance of the Serine residue within the consensus motif can vary between substrates.

The residue 2 places in front of the RR pair, is usually either a Phenylalanine or a Leucine. One study using the model *E. coli* Tat substrate TorA-GFP found that substitution of this residue with either Alanine or Serine had no effect on translocation, whilst substitution by Aspartic acid caused a complete block in transport (Mendel *et al*., 2008). The same study also looked at the effects on translocation of mutations in the DmsA signal peptide. DmsA has a Leucine residue 2 positions in front of the twin-Arginine pair. Substitution of this Leucine with either Alanine or Aspartic acid caused a complete block in transport (Mendel *et al*., 2008). Cleary the

importance of the residue at this +2 position varies between substrates but an acidic residue at this position cannot be tolerated. Separately it was found that mutation of the conserved Phenylalanine 2 positions forward of the Arginine pair in the SufI signal peptide to Leucine, Alanine, or Tyrosine had no effect on export (Stanley *et al*., 2000).

The Tat systems of Gram-negative and Gram-positive bacteria both appear to recognise the same targeting determinants within Tat signal peptides (Mendel *et al*., 2008).

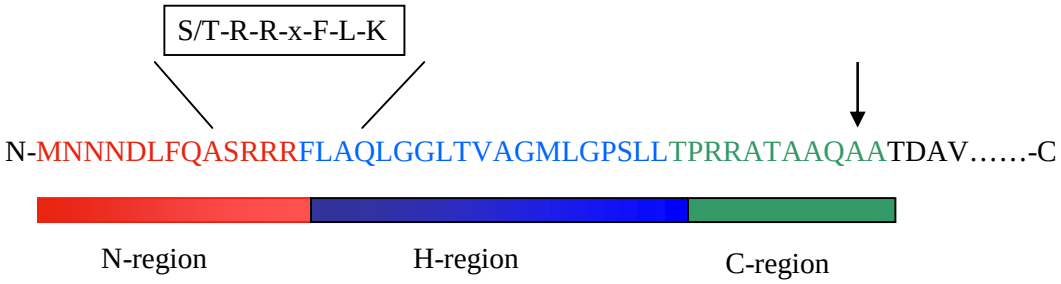

Figure 1.4.6. An example of an *E. coli* Tat signal peptide.
The N-terminal Tat targeting signal peptide of *E. coli* TMAO reductase is shown, having the typical three domain arrangement; N-terminal positively charged region, hydrophobic central region, and C-terminal polar region. The Tat consensus motif (S/TRRxFLK) is highlighted and the point of cleavage by signal peptidase at the Ala-Xaa-Ala motif shown with an arrow.

Other residues separate from the consensus motif have been found to be important for translocation activity, including basic residues within the C-terminal region (Ize *et al*., 20002a; Bogsch *et al*., 1997), and a Proline residue towards the C-terminal end of the H-region (Cristobal *et al*., 1999).

A further difference between Tat and Sec signal peptides concerns the overall hydrophobicity, with Sec signal peptides being more hydrophobic than Tat signal peptides. The signal peptide of *E. coli* TorA was transformed from a Tat-targeting signal peptide to a Sec-targeting signal peptide by an increase in its overall hydrophobicity (Cristobal *et al*., 1999; Ize *et al*., 2002a). The N-terminal signal peptides of Tat substrates are also generally longer than those of Sec substrates with

an average length of 38 residues compared to just 24 in Sec signal peptides (Cristobal *et al*., 1999).

The signal peptides of many Tat substrates are not just required for an interaction with the Tat machinery but they also bind to cytosolic chaperones. The signal peptide of TMAO reductase was found to bind the substrate specific chaperone TorD (Hatzixanthis *et al*., 2005a; Genest *et al*., 2006). One residue within the TorA signal peptide has been identified that is critical for this interaction. Substitution of Leucine at position 31 (at the end of the H-region) with Glutamate prevented TorA-TorD interaction (Buchanan *et al*., 2008).

Some Tat substrates lack a signal peptide altogether, such as *E. coli* DmsB. These substrates are translocated in a hitch-hiker mechanism by interactions with Tat substrates that do have a signal peptide. In the case of DmsB translocation occurs by hitch-hiking with DmsA (Sambasivarao *et al*., 2000).

Determinants for translocation by the Tat pathway do not just reside within the signal peptide and are also present in the passenger protein itself. The presence of N-terminal charged residues can abolish Sec-dependent translocation but Tat substrates often have charged residues within the N-terminal end of the substrate (Blaudeck *et al*., 2003; Cristobal *et al*., 1999; Tullman-Ercek *et al*., 2007). It was suggested, in addition to the reasons outlined above, that some proteins have evolved to use the Tat pathway rather than the Sec pathway due to a requirement for charged residues at the N-terminus.

1.4.7 Tat pathway Mechanism

The mechanism by which Tat substrates are translocated across the plasma membrane remains poorly understood. It is thought that in its resting state the Tat system consists of separate TatABC and TatA complexes (Bolhuis *et al*., 2001; Oates *et al*., 2003; Oates *et al*., 2005) and that during the translocation cycle these complexes come together and form an active translocon (Mori and Cline, 2002). It seems likely that the major component of the translocation channel is the TatA protein and different sized TatA complexes have been identified that could accommodate folded substrates that vary in size and shape (Gohlke *et al*., 2005; Oates *et al*., 2005). Some evidence for a dual topology of TatA exists and it was suggested that the amphipathic helix could insert into the lipid bilayer to form a hydrophillically lined channel (Gouffi *et al*., 2003). Tat substrates appear to bind first to the TatABC complex within the membrane and this substrate binding is likely to trigger the recruitment of separate TatA complexes (Alami *et al*., 2002; Alami *et al*., 2003). Within the TatABC complex it is the TatC and TatB components that are critical for this interaction with the signal peptide initially interacting with TatC via the Twin-arginine motif and then more extensive contacts being made with TatB (Alami *et al*., 2002; Alami *et al*., 2003; Mori and Cline, 2001). TatB appears to modulate the recruitment of TatA complexes and the passage of substrate from TatC to TatA. Following translocation the system is reset and the TatA and TatABC complexes dissociate ready for another round of translocation. A model of Tat dependent translocation in *E. coli* is presented in Figure 1.4.7.

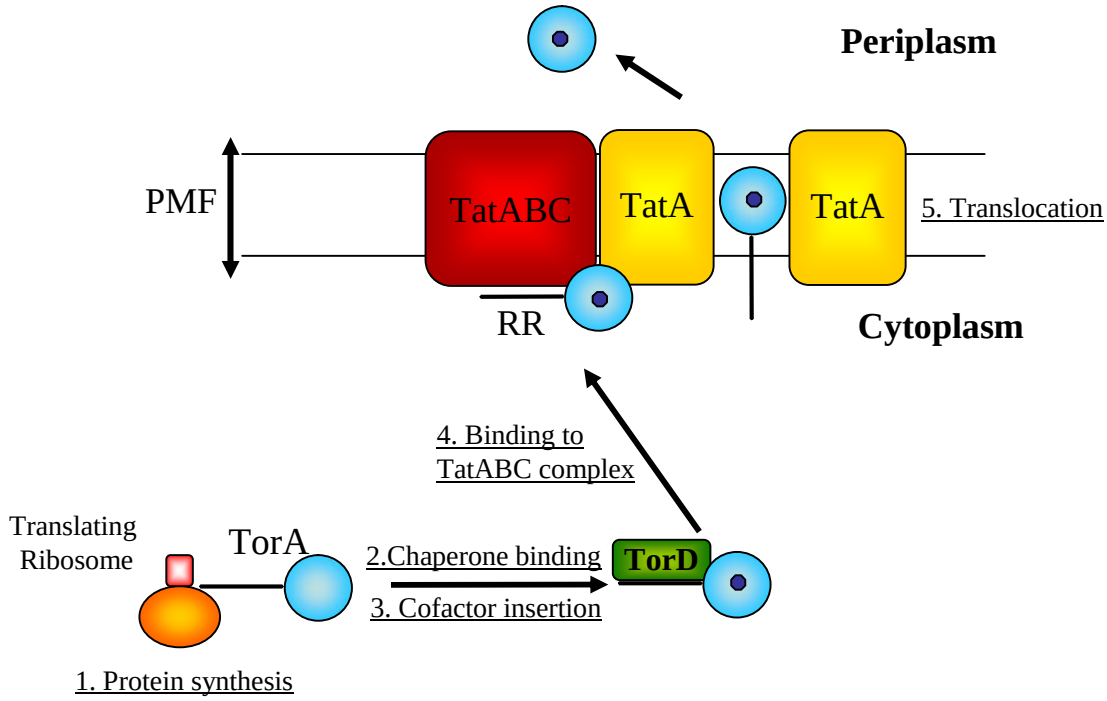

Figure 1.4.7 Model of the mechanism of Tat translocation in *E. coli*
1. The Tat substrate (in this case TorA), is translated at the ribosome. 2. The substrate specific chaperone, TorD, binds to the signal peptide of TorA. 3. TorD prevents premature interaction of TorA with the Tat machinery before cofactor insertion and correct protein folding has occurred. 4. The Tat substrate interacts with membrane TatABC via its signal peptide and in the presence of the proton motive force triggers recruitment of free TatA. 5. The recruitment of TatA results in the formation or opening of a channel or pore through which translocation occurs.

Unlike the Sec pathway that utilizes ATP hydrolysis to drive translocation, the Tat pathway uses the proton motive force to drive transport. The translocation of Tat substrate proteins into *E. coli* membrane vesicles has no requirement for ATP but is blocked if a proton motive force is not present (Alami *et al*., 2002; Alami *et al*., 2003; Yahr and Wickner, 2001). One report found that *E. coli* SufI could be imported into IMVs in the absence of a ΔpH and demonstrated that transport required two distinct electrical-potential dependent steps (Bageshwar and Musser, 2007).

1.4.8 The Tat pathway in Gram-positive bacteria.

Our current understanding of how the Tat pathway is operating in bacteria comes from studies using the Tat system of the Gram-negative bacterium *E. coli* as a model. *E. coli* has proven to be a good model as it appears to be representative of other Gram-negative Tat systems (Oates *et al*., 2003).

The Tat pathway in Gram-positive bacteria differs in an important respect to the pathway in Gram-negative bacteria. Whilst Gram-negative Tat systems consist minimally of a TatA, TatB, and TatC protein that each plays a distinct role, Gram-positive Tat systems are comprised of just a single TatA and TatC component (Dilks *et al*., 2003; Yen *et al*., 2002). Some Gram-positive bacteria also have more than one Tat pathway that operates in parallel. *Bacillus subtilis* is used as a model organism to study the Tat pathway of Gram-positive bacteria. It has two TatAC-type pathways that operate in parallel with different substrate specificities (Jongbloed *et al*., 2004). One pathway denoted the TatAdCd pathway is encoded by the *tatAd* and *tatCd* genes that are coexpressed with the Tat substrate PhoD in an operon. PhoD is the only identified substrate of the TatAdCd pathway (Pop *et al*., 2002). The *phoD* operon forms part of the *pho* regulon and is expressed in response to phosphate limitation. PhoD has phosphodiesterase and alkaline phosphatase activity and is required for producing additional inorganic phosphate at the cell wall (Eder *et al*., 1996). Once translocated across the plasma membrane the protein is inefficiently processed resulting in a cell wall association (Muller and Wagner, 1999).

The second minimal Tat system of *B. subtilis* is encoded by the *tatAy* and *tatCy* genes that are constitutively expressed in an operon. Again just a single substrate has been identified that is translocated by the TatAyCy pathway, YwbN, a DyP-dependent peroxidase (Jongbloed *et al*., 2004). Two novel Tat substrates have recently been identified in *B. subtilis*, QcrA and YkuE, but it remains to be determined whether they are translocated by the TatAdCd, TatAyCy or both pathways (Widdick *et al*., 2008). The organisation of the *B. subtilis tat* genes is shown in Figure 1.4.8.

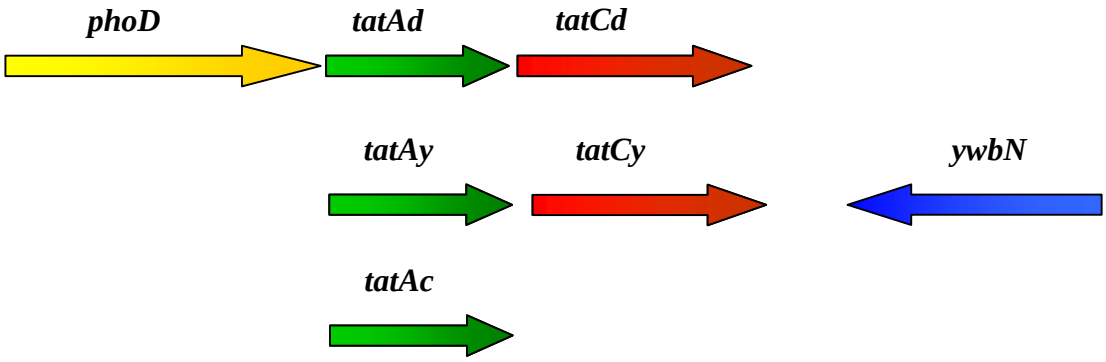

Figure 1.4.8 Organisation of *B. subtilis tat* genes.
Bacillus subtilis has two operons encoding two autonomous Tat pathways. The first is comprised of the *tatAd* and *tatCd* genes that are coexpressed with the gene for the Tat substrate PhoD. This operon is only expressed under phosphate depleted conditions. The other minimal Tat system is encoded by the *tatAy* and *tatCy* genes that are also coexpressed in an operon. The only identified substrate of the TatAyCy pathway is expressed elsewhere in the genome and is YwbN. A third *tatA* gene, *tatAc* is also found in *B. subtilis* but this is not expressed with any other *tat* genes and is not thought to be involved in the Tat pathway.

Despite the strict substrate specificity between the TatAdCd and TatAyCy pathways it was recently found that TatAd when over expressed could substitute for TatAy in the secretion of YwbN (Eijlander *et al.*, 2009). The TatAdCd pathway when over expressed is also able to translocate a number of other Tat substrate proteins tested in contrast to TatAyCy. The substrate specificity of the TatAdCd and TatAyCy pathways was further investigated in chapter 5.

The TatAd protein has been found alongside its membrane localisation in a soluble form in the cytosol (Pop *et al.*, 2003) where it is forms ~ 250 kDa complexes with the TatAd molecules apparently arranged in micelle type structures (Westermann *et al.*, 2006). This soluble population of TatAd was found to have affinity for the Tat substrate PhoD (Pop *et al.*, 2003) and for membrane localised TatCd (Schreiber *et al.*, 2006), leading to the suggestion of a completely different model of Tat dependent translocation to the current *E. coli* model. This model involves soluble TatAd acting as the initial receptor for Tat substrates and is discussed in detail in chapter 4.

The absence of a TatB component in Gram-positive bacteria also led to the idea that the TatA proteins may be bifunctional and fulfil both TatA and TatB roles (Jongbloed

et al., 2004; Jongbloed *et al*., 2006). The bifunctional nature of the TatAd protein is explored in Chapter 6.

The absence of a TatB component also suggests a difference in Tat complex organisation between Gram-negative and Gram-positive bacteria and this is investigated in chapters 3 and 5.

1.5 Aims and Objectives of this study

The overall aim of this study was to investigate and characterise the Tat pathway of a Gram-positive bacterium in detail, in order to identify any differences to Gram-negative systems; the work centred on answering the following questions.

(*Bacillus subtilis* was the model organism chosen for this work as previous studies on Gram-positive Tat systems have focused on this bacterium).

1. The absence of a TatB component in Gram-positive bacteria led to the suggestion that TatA in these bacteria may be bifunctional. Are the TatA proteins of Gram-positive bacteria bifunctional with both TatA and TatB roles? If so what regions of the bifunctional TatA protein are important for TatA and TatB functions?

2. The absence of a TatB component in Gram-positive bacteria suggests differences in Tat complex organisation. How are the TatA and TatC proteins of Gram-positive Tat systems organised into complexes within the membrane?

3. The TatAd protein of *B. subtilis* has a dual localisation and is found in both membrane and cytosolic compartments. Does cytosolic TatAd play a role in translocation?

4. *B. subtilis* has two independent Tat pathways each responsible for the translocation of its own specific substrate. Why does *B. subtilis* have two separate Tat pathways and how substrate specific are they?

5. Do the Tat pathways of Gram-positive bacteria differ fundamentally in terms of translocation mechanism to the Tat pathways of Gram-negative bacteria?

Chapter 2

Materials and Methods

2.1 Suppliers of chemicals

Chemicals were obtained from the companies indicated below.

Acros (UK): Methyl viologen and Trimethylamine *N*-oxide.

Amersham Pharmacia Biotech (UK): ECL™ detection reagents; Native protein markers for gel electrophoresis and gel filtration chromatography; Hybond™-P PVDF membrane, Q-sepharose anion exchange resin, and Superose-6 pre-packed gel filtration columns.

Applied Biosystems (USA): Big Dye™ v 3.1 terminators.

BD Clontech (USA): Talon™ affinity chromatography resin.

Calbiochem (Germany): Digitonin; *n*-Dodecyl-*ß*-D-maltoside, and *n*-Octylglucoside.

Fisher Scientific (UK): Acetic acid (glacial); Acetone; Ethanol; Formaldehyde; Glycerol; Glycine; Hydrochloric acid; Magnesium sulphate; Methanol; Sodium chloride; sodium dodecyl sulphate; Sucrose, and Tris.

Fuji (Japan): Super RX film.

IBA (Germany): Buffer E; Strep-tactin™ HRP-conjugate, and Strep-tactin™ affinity chromatography resin.

Invitrogen (USA): Anti-GFP monoclonal antibody and Anti-His (C-terminal) antibody.

New England Biolabs (USA): Pre-stained broad range protein markers.

Pierce (USA): BCA linked protein determination kit.

Premier International Foods (UK): Marvel milk powder.

Promega (UK) Anti-rabbit-HRP and anti-mouse-HRP conjugates

Qiagen (Germany): QIAprep miniprep kit.

Roche applied science (UK): Complete^{TM} protease inhibitor cocktail tablets.

Serva (Germany): Serva G Coomassie blue and Isopropyl-*ß*-D-thiogalactoside.

Sigma (UK): Aminocaproic acid; Ampicillin; L-arabinose; Avidin; Bis-Tris; *ß*-mercaptoethanol; Bovine serum albumin; Imidazole; Kanamycin; Lysozyme; Silver nitrate; Sodium carbonate; Sodium dithionite; Sodium thiosulphate; Sodium molybdate; TEMED; Tricine; Triton X-114, and Trizma.

Stratagene (USA): *Pfu* DNA polymerase, dNTPs, *DpnI* restriction enzyme.

Stratech (UK): Instant Blue stain.

VHBio (UK): Custom DNA primers.

VWR (UK): 40% Acrylamide solution; Ammonium persulphate; Bromophenol blue; Calcium chloride; Disodium hydrogen phosphate; EDTA; Glucose; Magnesium chloride; Potassium chloride; Sodium dihydrogen phosphate; Sodium hydroxide pellets; Trichloroacetic acid and Tween 20..

Whatmann (UK): 3mm filter paper.

2.2 Growth and storage of *E. coli* cultures

2.2.1 Strains of *E. coli* used

All strains of *E. coli* used are given below in table 2.2.1.

Strain	Properties	Reference
MC1061	*F-, araD139, Δ*(*ara-leu*)7696; *Δ*(*lac*)X74, *galU*, *galK*, *hsdR*2, *mcrA*, *mcrB*1, *rspL*	Wertman *et al*., 1986
MC4100	*F- ΔlacU169, araD139, rpsL150, relA1, ptsF, rbs, flbBS301*	Casadaban and Cohen, 1980
ΔtatABCDE	MC4100 *ΔtatABCDE, Ara*^{r}	Sargent *et al*., 1988
ΔtatA/E	MC4100 *ΔtatA/E, Ara*^{r}	Sargent *et al*., 1988
ΔtatB	MC4100 *ΔtatB, Ara*^{r}	Sargent *et al*., 1988
DH5α	*supE44, ΔlacU169(80lacZΔM15), hsdR17, recA1, endA1, gyrA96, thi-1, relA1*	Sambrook *et al*., 1989

Table 2.2.1 Strains of *E. coli* used in this work

2.2.2 Standard growth conditions

E. coli were cultured using liquid Luria-Bertani (LB) media (10 g/l NaCl; 10 g/l bacto-tryptone; and 5 g/l yeast extract). Media was pre-warmed to 37 °C before inoculation with a single bacterial colony taken from an agar plate. Unless otherwise stated liquid cultures were grown at 37 °C in a shaking incubator at 200 rpm overnight (~16 hours).

E. coli cells were cultured on solid media (LB + 16 g/l bacto-agar) by streaking 5 µl of liquid culture over a fresh agar plate, followed by incubation at 37 °C overnight (~16 hours). *E. coli* cultures were stored on LB-agar plates at 4 °C for a maximum of 6 weeks.

2.2.3 Antibiotic supplements

Ampicillin (100 µg/ml), and Kanamycin (50 µg/ml) were used in cultures carrying pBAD24 and pEXT plasmids respectively.

2.2.4 Storage of *E. coli* cells

Glycerol stocks of *E. coli* cultures were prepared for long-term storage by mixing 2 parts of liquid culture with 1 part of 50% (v/v) glycerol. Cultures were frozen on dry-ice and then stored -70 °C.

2.3 Preparation and transformation of competent *E. coli* cells

2.3.1 Preparation of competent cells

A 5 mL culture of *E. coli* cells was grown overnight as described (2.2.2) and 100 µl diluted in 9.9 ml of fresh LB. The culture was grown until it reached an OD_{600} of ~0.3-0.4. Harvested cells re-suspended in 10 ml of 0.1 M $MgCl_2$ were incubated in a bucket of ice for exactly 5 minutes. Cells were collected a second time and re-suspended in 1.0 ml of 0.1 M $CaCl_2$. The cells were incubated on ice overnight before use.

2.3.2 Preparation of plasmid DNA from *E. coli* cells

A 5 ml culture of *E. coli* cells was grown overnight as described (2.2.2). Plasmid DNA was extracted from the culture using a 'Mini-prep' kit (Qiagen, Germany). The preparation was carried out exactly as instructed by the manufacturer.

2.3.3 Transformation of competent *E. coli* cells with plasmid DNA.

2 µl of plasmid DNA prepared as described (2.3.2) was incubated with 150 µl of competent cells (2.3.1). Cells were incubated in a bucket of ice for half an hour before being heated to 42 °C for 1½ minutes. Cells were then put back on ice for approximately 2 minutes. The transformed cells were diluted with 500 µl of fresh LB

and cells subsequently cultured at 37 °C with agitation at 200 rpm for exactly 1 hour. The culture was then grown on LB-agar plates (2.2.2), and transformants selected for with appropriate antibiotics (2.2.3).

2.3.4 Bacterial plasmids used in this work

Bacterial plasmids used in this work are given below in table 2.3.4.

Plasmid	Properties	Reference	Source
pBAdCds	pBAD24 + *B. subtilis tatAdCd-strep*	Barnett *et al*., 2008	Robyn Eijlander (University of Groningen)
pEXT-AdCd	pEXT22 + *B. subtilis tatAdCd*	Barnett *et al*., 2008	Robyn Eijlander (University of Groningen)
pBAdh	pBAD24 + *B. subtilis tatAd-his*	Barnett *et al*., 2008	Robyn Eijlander (University of Groningen)
pBAyCys	pBAD24 + *B. subtilis tatAyCy-strep*	Barnett *et al*., 2009	Robyn Eijlander (University of Groningen)
pEXT-AyCy	pEXT22 + *B. subtilis tatAyCy*	Barnett *et al*., 2009	Robyn Eijlander (University of Groningen)
pBAD-ABCs	pBAD24 + *E. coli tatABC-strep*	Bolhuis *et al*., 2001	Albert Bolhuis (University of Warwick)
pEXT-ABC	pEXT22 + *E. coli tatABC*	Barrett *et al*., 2003	Claire Barrett (University of Warwick)
pJDT1	pBAD24 + *torA-gfp*	Thomas *et al*., 2001	Joanne Thomas (University of Warwick)
pBAD-MdoD-GFP	pBAD24 + *mdoD-gfp*	Barnett *et al*., 2009	Anja Nenninger (University of Warwick)
pBAD-AmiA-GFP	pBAD24 + *amiA-gfp*	Barnett *et al*., 2009	Anja Nenninger (University of Warwick
pBAD-DmsA-GFP	pBAD24 + *dmsA-gfp*	Ray *et al*., 2003	Nicola Ray (University of Warwick)

Table 2.3.4. List of plasmids used in this study.

2.3.5 Affinity tags used

To facilitate protein detection and purification C-terminal tags were used where stated. The 10 amino acid *Strep*-tag II (IBA, Germany) was present on *E. coli* TatC and *B. subtilis* TatCd and TatCy proteins (denoted by *–strep* or simply s). *B. subtilis* TatAd was tagged with a hexa-histidine tag (denoted by *–his* or simply h) where stated.

2.4 DNA site-specific mutagenesis and constructs generated

2.4.1 Site-directed *in vitro* mutagenesis of plasmid DNA

Point mutations were introduced into *E. coli* plasmid DNA using the QuikChange™ site-specific mutagenesis system (Stratagene, USA), following the manufacturers instructions. PCR reactions were performed using a Biometra T3 thermocycler. The PCR product was used to transform *E. coli* DH5α competent cells as described (2.3.3).

2.4.2 Primers used for the mutagenesis of *tatAd* and constructs generated

Table 2.4.2 lists all primers used for the site directed mutagenesis of TatAd.

Constructs Generated	Name of primers	Primer sequence (5' to 3')
TatAdCd-S3A	S3AF	ggaggaattcaccatgtttgccaacattggaataccggg
TatAd-S3A	S3AR	cccggtattccaatgttggcaaacatggtgaattcctcc
TatAdCd-N4A	N4AF	ggaattcaccatgttttcagccattggaataccgggc
TatAd-N4A	N4AR	gcccggtattccaatggctgaaaacatggtgaattcc
TatAdCd-I5A	I5AF	ccatgttttcaaacgccggaataccgggcttgattctcatcttcg
TatAd-I5A	I5AR	cgaagatgagaatcaagcccggtattccggcgtttgaaaacatgg

Constructs Generated	**Name of primers**	**Primer sequence (5' to 3')**
TatAdCd-G6A	G6AF	ccatgttttcaaacattgccataccgggcttgattctc
TatAd-G6A	G6AR	gagaatcaagcccggtatggcaatgtttgaaaacatgg
TatAdCd-P8A	P8AF	ggaatagccggcttgattctcatcttcgtcatcgcc
TatAd-P8A	P8AR	ggcgatgacgaagatgagaatcaagccggctattcc
TatAdCd-G9A	G9AF	cattggaataccggccttgattctcatcttcg
TatAd-G9A	G9AR	cgaagatgagaatcaaggccggtattccaatg
TatAdCd-L10A	L10AF	cgaataccgggcgcgattctcatcttcgtcatcgcc
TatAd-L10A	L10AR	ggcgatgacgaagatgagaatcgcgcccggtattcg
TatAdCd-I11A	I11AF	cgaataccgggcttggccctcatcttcgtcatcg
TatAd-I11A	I11AR	cgatgacgaagatgagggccaagcccggtattcg
TatAdCd-L12A	L12AF	ccgggcttgattgccatcttctcacgccc
TatAd-L12A	L12AR	gggcgtgagaagatggcaatcaagcccgg
TatAdCd-F14A	F14AF	gggcttgattctcatcgccgtcatcgccctc
	F14AR	gagggcgatgacggcgatgagaatcaagccc
TatAdCd-V15A	V15AF	ctcatcttcgccatcgccctcattatttttggccc
TatAd-V15A	V15AR	gggccaaaataatgagggcgatggcgaagatgag
TatAdCd-I16A	I16AF	ctcatcttcgtcgccgccctcattatttttggccc
TatAd-I16A	I16AR	gggccaaaataatgagggcggcgacgaagatgag
TatAdCd-I18A	I18AF	ggtcatcgccgccatattttggcccttcc
TatAd-I18A	I18AR	ggaagggccaaaaatatggcggcgatgacc
TatAdCd-I19A	I19AF	Cgtcatcgccctccgccatttttggcccttccaagc
TatAd-I19A	I19AR	gcttggaagggccaaaaatggcggagggcgatgacg
TatAdCd-F21A	F21AF	cgtcatcgccctcattattgctggcccttccaagc
TatAd-F21A	F21AR	gcttggaagggccagcaataatgagggcgatgacg
TatAdCd-G22A	G22AF	cgccctcattattttgccccttccaagctgcc
TatAd-G22A	G22AR	ggcagcttggaaggggcaaaaataatgagggcg
TatAdCd-P23A	P23AF	ccctcattattttggcgcttccaagctgccg
TatAd-P23A	P23AR	cggcagcttggaagcgccaaaaataatgaggg

Constructs Generated	Name of primers	Primer sequence (5' to 3')
TatAdCd-K25A	K25AF	ggcccttccgcgctgccggaaatcgcc
TatAd-K25A	K25AR	ggcgatttccggcagcgcggaagggcc
TatAdCd-L26A	L26AF	ggcccttccaaggcgccggaaatcgggcg
	L26AR	cgcccgatttccggcgccttggaagggcc
TatAdCd-P27A	P27AF	cctttccaagctggcggaaatcgggcg
TatAd-P27A	P27AR	cgcccgatttccgccagcttggaaagg
TatAdCd-G30A	G30AF	gggcgtgccgccgcacggacactgctgg
TatAd-G30A	G30AR	ccagcagtgtccgtgcggcggcacgccc

Table 2.4.2 List of DNA primers used for site-directed mutagenesis of TatAd.

2.4.3 DNA sequencing

All DNA sequencing was conducted in house using the University of Warwick molecular biology service with Applied Biosystems Big Dye v3.1 and an ABI 3100 genetic analyser^{TM}. For sequencing of the pBAD24 plasmid the following primer was used: BADSEQ (5' tatttgcacggcgtcaca 3'). Chromas software was used to analyse DNA sequences.

2.4.4 Induction of plasmids

Typically, induction of pBAD24 and pEXT22 plasmids was achieved by the addition of 200-500 µM arabinose and 5 mM IPTG to the growth medium respectively. Under standard conditions plasmid induction was allowed to proceed until the culture reached mid-exponential growth phase (~3 hours).

Where cells carried pBAD24 and pEXT22 plasmids (for example, in GFP export assays), the pBAD24 plasmid was induced first for ~ 2 hours before removal of arabinose from the growth medium and subsequent induction of the pEXT22 plasmid for ~2 hours.

2.5 Preparation of *E. coli* cell fractions

2.5.1 Fractionation of *E. coli* cells

E. coli cells were separated into periplasm, cytoplasm, and membrane samples using the previously described lysozyme/cold osmotic shock method (Randall and Hardy, 1986). Briefly, the cells from a 10 ml culture of *E. coli* were pelleted down by centrifugation before being resuspended in 0.5 ml of pre-chilled buffer 1 (100 mM tris-acetate pH 8.2, 500mM sucrose and 5 mM EDTA). 0.5 ml of H_2O and 20 µl of a 4 mg/ml stock of lysozyme was added simultaneously to the cell suspension. Samples were incubated in an ice bucket for 5 to 10 minutes. The resulting spheroplasts were treated with 20 µl of 1.0 M $MgSO_4$ and pelleted by centrifugation. The supernatant (the periplasmic fraction) was collected. Spheroplasts were washed using 1 ml buffer 3 (50 mM tris-acetate pH 8.2, and 2.5 mM EDTA) that had been pre-cooled, and briefly sonicated (30 seconds at ~12 microns) to break the membranes. The membrane and cytoplasmic compartments were separated by ultracentrifugation at 250000 *g* for 25-30 minutes (using a Beckman TL100.3 rotor that had been pre-cooled to 4 °C). Membranes were solubilised in 1.0 ml buffer 3 containing 1 % (w/v) SDS unless otherwise stated.

2.5.2 Isolation and solubilisation of *E. coli* membranes for protein purification and gel filtration chromatography

For purification of proteins from the membrane fraction, membranes were prepared from a 500 ml culture of *E. coli* as described above (2.5.1) but using 50 times the volume of the buffer or reagent stated (complete protease inhibitor tablets were added to buffers 1 and 3). Membranes were solubilised in 8.0 ml of buffer (20 mM Tris-HCl pH 8.0, 150 mM NaCl), supplemented with detergent overnight. Detergents used for solubilisation were: digitonin, 2 % (w/v), *n*-dodecyl-ß-D-maltoside 1 % (w/v) and *n*-octyl glucoside 25 mM.

2.6 Protein chromatography methods

2.6.1 Q-Sepharose anion exchange chromatography

E. coli membranes were prepared from 500 ml cultures as described (2.5.2) and solubilised in buffer containing the stated detergent (usually digitonin). Membranes were run directly through a 10 ml anion exchange column (Q-Sepharose) that had been pre-washed with equilibration buffer (20 mM Tris-HCl pH 8.0 and 0.1 % digitonin). The column was subjected to washing with 20 ml of equilibration buffer plus 100 mM NaCl to remove weakly bound proteins from the column. For elution of strongly bound proteins from the column 20 ml of buffer with 300 mM NaCl was used. The eluted fraction was diluted in equilibration buffer (without salt) to reduce the NaCl concentration to 150 mM.

2.6.2 Streptactin™-Sepharose affinity chromatography

Streptactin™ affinity chromatography was performed with solubilised membranes (prepared as described in 2.5.2 using the detergent digitonin) and with membrane proteins that had already been partially purified by anion exchange chromatography (2.6.1). Generally and unless stated otherwise a 4 ml Streptactin™ affinity column was used. Columns were pre-equilibrated in buffer (20 mM Tris-HCl pH8.0, 150 mM NaCl, and 0.1 % digitonin) prior to use. Before application to the column samples were incubated with 1 µM avidin for 30 minutes in an ice bucket to prevent the non-specific binding of biotinylated proteins to the streptactin™ resin. Following sample application the column was washed with equilibration buffer (typically using fractions of 6 x 4 ml) before elution with 6 x 2 ml of buffer E plus detergent (20 mM Tris-HCl, 150 mM NaCl, 0.1 % digitonin, and 3 mM desthiobiotin).

2.6.3 Talon™ metal affinity chromatography

Talon™ affinity chromatography was performed with solubilised membranes prepared as described in 2.5.2 but with the omission of EDTA from all buffers. Typically and unless stated otherwise a 4 ml Talon™ affinity column was used. The column was

pre-equilibrated using 10 ml of buffer (20 mM Tris-HCl pH 8.0, 150 mM NaCl, and 0.1 % digitonin) before applying membranes directly to the column. After addition of sample the column was subjected to washing using equilibration buffer (20 ml) that contained 25 mM imidazole to remove weakly bound proteins. Strongly bound proteins were then eluted with 5 x 2 ml fractions of the equilibration buffer containing 150 mM imidazole.

Talon^{TM} affinity chromatography was also used for purification of protein from the soluble fraction of *E. coli*. The soluble (cytosolic) fraction of *E. coli* was prepared as described (2.5.1) but using a 500 ml culture instead. To account for the larger sized cultures all buffer volumes were increased 50 times and buffers 1 and 3 were supplemented with complete protease inhibitor cocktail. EDTA was omitted from all buffers used. The purification was performed exactly as described for membrane proteins above but in the absence of any detergent.

2.6.4 Superose-6 gel filtration chromatography

Size exclusion chromatography was used as both an analytical tool to estimate the masses of protein complexes and as a final clean-up step in protein purification.

For protein purification the elution samples from a Streptactin^{TM} affinity column (2.6.2) were pooled before being concentrated with Vivaspin centrifugal concentrators (Millipore). The selected concentrators had a 10 kDa molecular weight limit. 240 µl of the sample was injected onto a Superose-6 column attached to an AKTA purifier FPLC system (Amersham bioscience UK). The column was pre-equilibrated with buffer (20 mM Trizma-HCl, 150 mM NaCl, and 0.1 % (w/v) digitonin). Following sample application the protein was eluted from the column using a single column volume of the equilibration buffer. The eluted sample was collected in 0.6 ml fractions.

For analytical studies the protocol used was the same as above except detergent solubilised membranes were applied directly to the Superose-6 column. Membranes were prepared as described in 2.5.2.

2.6.5 Size exclusion chromatography: Estimation of mass of protein complexes

In order to estimate the mass of protein complexes the Superose-6 gel filtration column was calibrated. To achieve this, four protein standards of known molecular mass were run through the column 2 at a time. These were catalase 232 kDa, and thyroglobin 669 kDa; and aldolase 158 kDa and ferritin 440 kDa. Elution volumes of these standards were used to prepare a calibration curve to allow the estimation of the mass of a protein complex of unknown size from its peak elution volume.

2.6.6 Determining the concentration of purified protein

The concentration of purified proteins was determined using a BCA linked protein determination kit (Pierce UK). The method used was exactly as recommended by the manufacturer.

2.7 Protein electrophoresis

2.7.1 SDS gel electrophoresis (SDS-PAGE)

All gel electrophoresis of proteins was performed using the C.B.S. (USA) vertical gel system as instructed by the manufacturer. The method of electrophoresis used was based on that described in a paper by Laemmli, 1970. A 17.5 % resolving gel was used (17.5 % acrylogel; 375 mM Tris-HCl pH 8.8; 0.1 % APS, and 0.06 % TEMED). A stacking gel of 4 % was used over the resolving gel (4 % acrylogel; 125 mM Tris-HCl pH 6.8; 0.1 % SDS; 0.6 % APS, and 0.06 % TEMED).

Samples for SDS-PAGE were prepared by mixing 1:1 in loading buffer (125 mM Tris-HCl pH 6.8; 20 % glycerol; 4 % SDS; 0.02 % bromophenol blue and 5 % ß-mercaptoethanol), and were heated to 50 °C for 5 minutes for membrane proteins, and 100 °C for 5 minutes for soluble proteins.

Electrophoresis was performed with a uniform running buffer (25 mM tris, 250 mM glycine, and 0.1 % SDS), at 30 mA for 3 hours.

2.7.2 Native gel electrophoresis (N-PAGE)

All native gel electrophoresis was performed using the C.B.S. (USA) vertical gel system as instructed by the manufacturer. A 10 % resolving gel was used (10 % acrylogel; 375 mM Tris-HCl pH 8.8; 0.1 % APS, and 0.06 % TEMED). A 5 % stacking gel was used over the resolving gel (5 % acrylogel; 125 mM Tris-HCl pH 6.8; 0.6 % APS, and 0.06 % TEMED).

Samples were prepared by mixing 1:1 with native sample loading buffer (125 mM Tris-HCl pH 6.8, 20 % glycerol, and 0.02 % bromophenol blue).

Electrophoresis was performed using a uniform buffer (25 mM tris and 250 mM glycine), and gels were run overnight for ~16 hours at 10 mA.

2.7.3 Blue native gel electrophoresis (BN-PAGE)

All electrophoresis using blue-native gels was performed using the C.B.S. (USA) vertical gel system as instructed by the manufacturer. The method used was based on one originally described by Schagger and von Jagow (1991). A resolving gel was prepared with a continuous acrylamide gradient of 5-13%. The gel was prepared in a gradient maker using the following two solutions.

Reagent	Solution 1	Solution 2
Acrylogel	5 %	13 %
Bis-Tris-HCl pH 7.0	50 mM	50 mM
Aminocaproic acid	0.5 mM	0.5 mM
Glycerol	0.76 %	5 %
APS	0.36 %	0.36 %
TEMED	0.365 %	0.365%

A stacking gel of 4 % was used over the resolving gel (4 % acrylogel; 50 mM Bis-Tris-HCl pH 7.0; 0.5 mM aminocaproic acid; 0.7 % APS, and 0.07 % TEMED).

Samples for electrophoresis were prepared by mixing 10 µl of solubilised membranes or purified protein with 1 µl of sample loading buffer (5 % coomassie and 750 mM aminocaproic acid).

Electrophoresis was performed overnight in a cold room (4 °C) at 60 V using a buffer consisting of 50 mM tricine, 15 mM Bis-Tris, and 0.02 % Coomassie at the cathode. A buffer consisting of 50 mM Bis-Tris-HCl pH 7.0 was used for the anode. Once the Coomassie blue had ran two thirds of the way down the gel, the cathode buffer was changed for fresh buffer, this time without Coommassie blue dye. The gel was then allowed to run until all of the coomassie dye had run off the bottom of the gel.

2.8 Detection of proteins

2.8.1 Protein detection by Western blotting

Western blotting was used to transfer protein from SDS-PAGE gels onto PVDF membranes and was performed using semi-dry western blotting apparatus, (Sigma, UK). The apparatus was used exactly as instructed by the manufacturer. A uniform Towbin transfer buffer was used (25 mM Tris, 192 mM glycine, and 20 % methanol) (Towbin *et al*., 1979). Briefly, two sheets of Whatman paper soaked in transfer buffer were placed onto the positive electrode. PVDF membrane pre-soaked in methanol was placed over the Whatman paper and the gel placed on top. Finally a top layer of two sheets of Whatman paper soaked in transfer buffer was placed over the gel. The transfer of proteins was achieved using ~ 200 mA of current over a two hour period.

For transfer of proteins from BN-gels, a different buffer was used, (50 mM Tricine pH 7.0, 15 mM Bis-Tris-HCl pH 7.0 and 0.05 % SDS). The PVDF membrane was prepared by soaking in methanol, followed by water and then the BN transfer buffer. Following the transfer of proteins from a BN gel, the PVDF membrane was de-stained for 1 hour using 25 % methanol and 10 % acetic acid, before finally being washed with PBS-T (137 mM NaCl, 2.7 mM KCl, 10 mM Na_2PO_4 and 0.01 % Tween 20).

2.8.2 Detection of proteins by immunoblotting

After the transfer of proteins from acrylamide gels to PVDF membranes as detailed above (2.8.1), the membranes were blocked to prevent non-specific binding of antibodies using 5 % (w/v) dried milk that was dissolved in PBS-T. Blocking was performed for at least 1 hour but preferably overnight. The PVDF sheets were subsequently placed into a fresh container containing 20 ml of diluted primary antibody (diluted in PBS-T as indicated below in table 2.8.2). After 1 hour the membrane was washed for at least 4 x 10 minutes in PBS-T. Once washed, a secondary antibody conjugated to horse radish peroxidise (HRP) was used, again as detailed in table 2.8.2 for 1 hour. Finally the membrane was washed for a second time for at least 5 x 10 minutes in PBS-T. The detection of proteins was performed using ECL^{TM} detection reagents exactly as recommended by the manufacturer. X-ray films were developed using an AGFA Curix 60 automatic developer as directed by the manufacturer's instructions. Antibodies used for immunodetection are listed in table 2.8.2 below.

Antibody	Dilution	Source
Rabbit anti-TatA	3 in 20000	Laboratory stock
Rabbit anti-TatB	3 in 20000	Laboratory stock
Rabbit anti-TatAd	1 in 10000	Jorg Muller (University of Jena)
Rabbit anti-TatAy	1 in 10000	Jan Maarten van Dijl (University of Groningen)
Rabbit anti-SufI	3 in 20000	Tracy Palmer (University of Dundee)
Rabbit anti-GFP	3 in 20000	Invitrogen, USA
Mouse anti-*His* (C-terminal)	3 in 20000	Invitrogen, USA
Mouse anti-*strep*-tag II HRP conjugate	1 in 10000	IBA, Germany
Anti-rabbit IgG HRP conjugate	1 in 10000	Promega, USA
Anti-mouse IgG HRP conjugate	1 in 10000	Promega, USA

Table 2.8.2. Antibodies used for immunoblotting

2.8.3 Silver staining

Following SDS-PAGE (2.7.1), gels were placed in fixer (50 % acetone, 1.25 % TCA, and 0.015 % formaldehyde) and incubated for 15 minutes. Fixer was washed from the gel with H_2O and the gel incubated with 50 % acetone for 5 minutes followed by 1 minute in sodium thiosulphate solution (0.02 % (w/v)). Gels were washed with H_2O before incubation in staining solution (0.4 % formaldehyde and 0.25 % (w/v) silver nitrate). After 8 minutes the staining solution was washed from the gel with H_2O before incubation with developer solution (0.2 mM sodium carbonate, 0.004 % (w/v) sodium thiosulphate, and 0.015 % formaldehyde). Once protein bands became apparent the staining was stopped. This was achieved by incubating the gel with 1 % acetic acid. The gel was finally washed in H_2O and then dried.

2.8.4 Coomassie staining

Following SDS-PAGE (2.7.1) gels were stained with Instant Blue™ Coomassie stain according to the manufacturer's instructions.

2.8.5 TMAO reductase activity assays

This assay was adapted from that described by Silvestro *et al.,* (1989). *E. coli* cell fractions were prepared as described (2.5.1) and proteins separated by native-PAGE (2.7.2). Immediately after electrophoresis the gel was submerged in 100 mM phosphate buffer pH 6.5 that contained 0.25 % (w/v) methyl viologen. Buffer was completely saturated with N_2 before use. The gel was then stained blue by 0.1 % (w/v) sodium dithionite (that was pre-dissolved in 0.1 M NaOH). The gel was allowed to stain for around 15 minutes before being transferred into fresh phosphate buffer (completely saturated with N_2) supplemented with 40 mM TMAO until white bands were visualised. The gels were then scanned as they developed.

2.9 Confocal microscopy

Confocal microscopy was performed with Dr. Anja Nenninger. The microscope used was a Leica DMRE microscope. For image acquisition the laser was set to 488 nm and standard Leica confocal software was used to record the images. A 63 x oil immersion lens was used. The images generated were averaged using at least four separate scans.

2.10 Triton X-114 to separate membrane and soluble proteins

The separation of proteins into aqueous and detergent fractions was performed as described previously in a paper by Bordier, (1981) using the detergent Triton X-114. *E. coli* cell fractions were prepared (2.5.1) and both the membrane and cytosolic fractions supplemented with 1 % Triton X-114. Samples were mixed well and incubated in an ice bucket for 30 minutes. The detergent solution was allowed to undergo a phase separation into detergent and aqueous phases by incubating the samples at 30 °C for 5 minutes. The samples were spun in a bench top centrifuge at

300 x *g* for 3 minutes to separate the two phases. The aqueous phase was collected and fresh Triton X-114 was added (to 1 %) before repeating the above procedure. The detergent phase was collected and re-suspended in buffer 3 (2.5.1) and the above procedure again repeated. The aqueous phase was finally collected and the detergent phase collected and re-suspended in buffer 3. As well as using cell fractions, purified proteins prepared in buffer supplemented with 1 % Triton X-114 were also used.

2.11 Circular Dichroism (CD) spectroscopy

Circular Dichroism spectrophotometry of purified protein samples was performed using a Jasco J-815 spectrophotometer exactly as instructed by the manufacturer. Scans were taken across a wavelength range of 200-260 nm at a constant temperature of 20 °C. All spectra shown were averaged from 8 successive scans.

Chapter 3

The Bacillus subtilis TatAdCd pathway: Identification of novel features

3.1 Introduction

The *E. coli* Tat pathway requires a *tatA*, *tatB*, and a *tatC* gene (Bogsch *et al*., 1998; Sargent *et al*., 1998; Sargent *et al.*, 1999), that encode integral membrane proteins of ~ 9.6 kDa (TatA), ~ 18 kDa (TatB), and ~ 28 kDa (TatC). These three proteins are organised into two main types of complex within the membrane, a TatABC complex of around 370 kDa and separate complexes of TatA of ~100 kDa -500 kDa (Oates *et al.*, 2005). Within the TatABC complex the TatB and TatC proteins have equimolar stochiometry and form a "structural and functional unit" (Bolhuis *et al.*, 2001). TatA binds only weakly to the TatBC unit and is found within the TatABC complex in varying amounts (Bolhuis *et al*., 2001). The TatABC complex is believed to act as the initial receptor for Tat substrate proteins (Alami *et al*., 2003). Upon interaction of substrate with TatABC complexes separate TatA complexes dock onto the TatABC complex in a mechanism that requires the proton motive force (Mori and Cline, 2002). This transient association of TatA and TatABC complexes results in the formation of a pore or channel through which Tat substrates are translocated. The variation in the sizes of the TatA complexes has been linked to the translocation of substrates of different sizes (Gohlke *et al*., 2005), and helps to explain how different sized folded proteins can be accommodated without compromising the integrity of the membrane. The *E. coli* Tat pathway has proven to be a good model to study as it is representative of the Tat pathway in most other Gram-negative bacteria studied to date (Oates *et al*., 2003).

In contrast the Tat pathways of Gram-positive bacteria differ in key respects. The most notable difference is the absence of a TatB component, with the only exception being *Streptomyces* species (Dilks *et al.*, 2003; Yen *et al*., 2002). In Gram-positive bacteria the minimal Tat pathway is comprised of TatA and TatC. This led to the suggestion that the TatA protein in these bacteria is bifunctional, with both TatA and TatB roles (Jongbloed *et al*., 2006). Gram-positive bacteria like *B. subtilis* often contain more then one Tat pathway that operates in parallel. *B. subtilis* contains two Tat pathways (Jongbloed *et al*., 2004). One is encoded by the *tatAd* and *tatCd* genes that are co expressed along with a gene encoding the Tat substrate PhoD (Pop *et al*., 2002). This operon forms part of the *pho* regulon and is only expressed under

conditions of phosphate limitation. PhoD is to date the only identified substrate of the TatAdCd pathway. It has both phoshodiesterase and alkaline phosphatase activity and is required for the release of inorganic phosphate from cell wall turnover products (Jongbloed *et al*., 2000). The second minimal Tat pathway of *B. subtilis* is encoded by the *tatAy* and *tatCy* genes *(*Jongbloed *et al.*, 2004). These genes are constitutively expressed in an operon. Again, to date just a single substrate has been identified that is translocated by the TatAyCy pathway, YwbN a DyP-dependent peroxidase (Jongbloed *et al*., 2004). The absence of a TatB component in Gram-positive bacteria could have implications in terms of complex organisation and/or translocation mechanism, but almost nothing was known about the Tat complexes of Gram-positive bacteria at the start of this work.

In this chapter the TatAdCd pathway of *B. subtilis* was characterised in some detail in an attempt identify any differences, particularly mechanistic differences between the Tat pathways of Gram-positive and Gran-negative bacteria.

3.2 Results

3.2.1 Translocation of TMAO reductase by the TatAdCd pathway

In order to use a single defined background for comparing Tat systems from Gram-negative and Gram-positive bacteria, the ability of the TatAdCd system of *B. subtilis* to form an active translocation pathway when expressed in *E. coli* was tested. To do this the *B. subtilis tatAdCd* genes were expressed using the pBAdCds plasmid in *E. coli tat* mutant cells (*ΔtatABCDE*), and the ability of the TatAdCd proteins to support translocation of trimethylamine-*N*-oxide (TMAO) reductase tested. TMAO reductase (TorA) is the largest Tat substrate identified in *E. coli* at ~90 kDa. It contains a molybdopterin cofactor that it aquires in the cytoplasm before translocation by the Tat pathway to the periplasm (Silvestro *et al.*, 1989; Czjzek *et al.*, 1998). A cytoplasmic chaperone, TorD, has been identified that binds to the signal peptide of TorA to prevent premature interaction with the Tat machinery before cofactor insertion and correct protein folding has occurred (Jack *et al*., 2004; Genest *et al*., 2006). TorA acts as a final electron acceptor of the respiratory chain during anaerobic growth of *E. coli* on TMAO medium.

A well established gel based activity assay exists that allows us to test for translocation of TorA to the *E. coli* periplasm (Barrett *et al*., 2003a; Hicks *et al*., 2003). The TatAdCd proteins were expressed in *E. coli ΔtatABCDE* cells and periplasmic (P), cytoplasmic (C), and membrane (M) fractions prepared. Samples of each were run on a native-PAGE gel that was stained blue with reduced methyl viologen. Upon addition of the substrate (TMAO), the methyl viologen became oxidised where TMAO reductase was present. This is visualised by a clearing of the gel turbidity and the appearance of a white band. Figure 3.2.1 shows that the TatAdCd pathway is indeed active in *E. coli.* A white band is clearly visible in the lane corresponding to the periplasmic sample prepared from *ΔtatABCDE* cells expressing TatAdCd. As a positive control samples prepared from wild-type *E. coli* cells (strains MC4100 and MC1061) were also run on the gel. As expected a clear white band is present in the periplasmic lanes of both samples indicating efficient translocation of TorA. Low levels of activity are also observed in the cytoplasmic and membrane samples and this has been observed before (Barrett *et al.*, 2003a; Hicks *et al*., 2003). A

third positive control was also tested. Here cell fractions from *E. coli ΔtatABCDE* cells expressing the *E. coli* TatABC proteins (from plasmid pBAD-ABCs) were used. Again as expected, the activity of the TorA enzyme is detected in the periplasmic sample as shown by a white band in the periplasmic lane. Finally as a negative control, *E. coli ΔtatABCDE* cells that were not carrying any plasmid were tested. This time all of the TorA activity is localised to the cytoplasmic fraction with no activity detectable in the periplasm. Clearly TatAdCd of *B. subtilis* is able to form an active translocation pathway in the *E. coli ΔtatABCDE* strain.

This is the first demonstration that a TatAC-type system from a Gram-positive bacterium can function in a Gram-negative background and translocate endogenous Tat substrates. The data also indicates that there are no factors present in *B. subtilis* that are absent in *E. coli* that are required for translocation by the TatAdCd pathway. Finally, as TatA and TatB in *E. coli* are both essential for transport of TorA, the fact that the TatAdCd system can support TorA transport suggests that the TatAd protein of *B. subtilis* is bifunctional with both TatA and TatB activities.

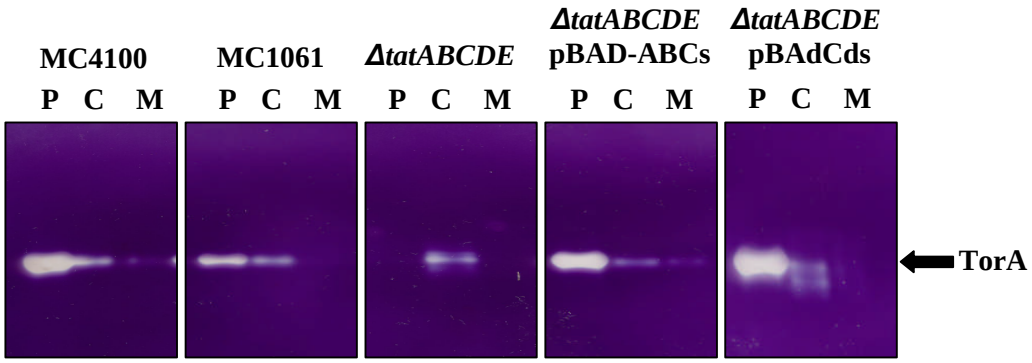

Figure 3.2.1 Translocation of TMAO reductase by TatAdCd
E. coli MC4100, MC1061, *ΔtatABCDE* and *ΔtatABCDE* cells expressing TatABC or TatAdCd (from the pBAD24 plasmid) were grown. Periplasm (P), Cytoplasm (C), and Membrane (M) fractions were prepared. Samples were subjected to native-PAGE and the gel assayed for TorA activity. The position of active TorA is indicated on the right of the figure with an arrow.

3.2.2 Translocation of TorA-GFP by the TatAdCd pathway

As well as testing the capability of the TatAdCd pathway to translocate TorA in *E. coli*, its ability to support the translocation of other substrates was tested. First a substrate comprised of the signal peptide of TorA linked to GFP was used. It has been shown previously that this substrate is translocated in a strictly Tat dependent manner when tested in *E. coli* (Thomas *et al*., 2001; Barrett *et al*., 2003b). The TorA-GFP protein was expressed using pJDT1 plasmids. Where co-expression of *E. coli* TatABC or *B. subtilis* TatAdCd was required the compatible plasmids pEXT-ABC and pEXT-AdCd were used. Following protein expression, *E. coli* cells were fractionated into periplasm (P), cytoplasm (C), and membrane (M) samples and proteins analysed by SDS-PAGE and subsequent immunoblotting with antibodies raised against GFP. Figure 3.2.2 shows a mature sized GFP band present in the periplasmic lane from *ΔtatABCDE* cells expressing TatAdCd, indicating translocation of GFP by the TatAdCd pathway to the periplasm. A mature size band is also detectable in the cytosolic and membrane fractions as has been observed before (Barrett *et al*., 2003b), and is most likely due to non-specific clipping of the precursor form of the protein. As a negative control samples from *E. coli ΔtatABCDE* cells that were carrying only the pJDT1 plasmid were also ran. As expected, GFP is located exclusively in the cytoplasmic sample. Again as described above, some clipping of the precursor protein to mature size is also seen. Finally as two positive controls wild-type *E. coli* cells carrying the pJDT1 plasmid and *E. coli ΔtatABCDE* cells carrying both pJDT1 and pEXT-ABC plasmids were used. The figure shows that in both cases GFP is efficiently translocated into the periplasmic compartment as shown by mature size bands in these lanes. Non-specific clipping of the precursor protein to mature size is again observed in the cytoplasmic fractions.

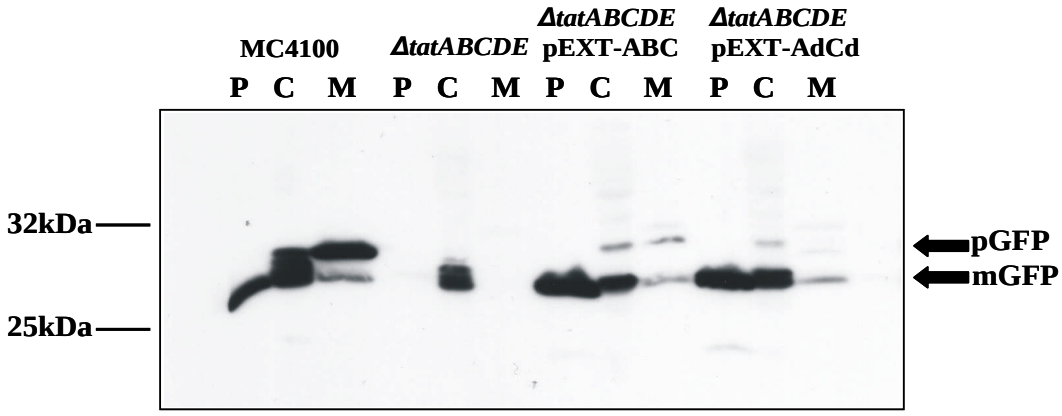

Figure 3.2.2 Translocation of TorA-GFP by TatAdCd
Plasmid pJDT1 expressing TorA-GFP was expressed in MC4100 and *ΔtatABCDE* cells, and co-expressed in *ΔtatABCDE* cells with TatABC and TatAdCd (from the pEXT22 plasmid). Cells were fractionated into periplasm (P), cytoplasm (C), and membrane (M) samples and samples ran on an SDS-PAGE gel before immunoblotting with antibodies to GFP. Molecular weight markers are presented to the left. Positions of the precursor (p) and mature (m) forms of the TorA-GFP substrate are marked on the right.

The translocation of TorA-GFP to the *E. coli* periplasm was confirmed by confocal microscopy (Figure 3.2.3). Clear halos of GFP fluorescence are seen around the periplasm of *E. coli* MC4100 cells expressing protein from plasmid pJDT1 and *E. coli ΔtatABCDE* cells expressing protein from both pJDT1 and either pEXT-ABC or pEXT-AdCd plasmids. Some variation between cells is observed with some cells displaying greater levels of GFP fluorescence than others. Those cells with the highest levels of GFP fluorescence have a more uniform flouresence perhaps due to saturation of the Tat system leading to a cytosolic as well as a periplasmic localisation. GFP fluorescence in *E. coli ΔtatABCDE* cells is located throughout the cytosol. The important point here is that the translocated GFP is fluorescent and must therefore have been correctly folded before translocation. This is in contrast to another study investigating the secretion of TorA-GFP by the TatAdCd pathway in *B. subtilis* itself. That study found that whilst the GFP protein was exported in a Tat-dependent manner the GFP was found in an inactive form (Meissner *et al*., 2007).

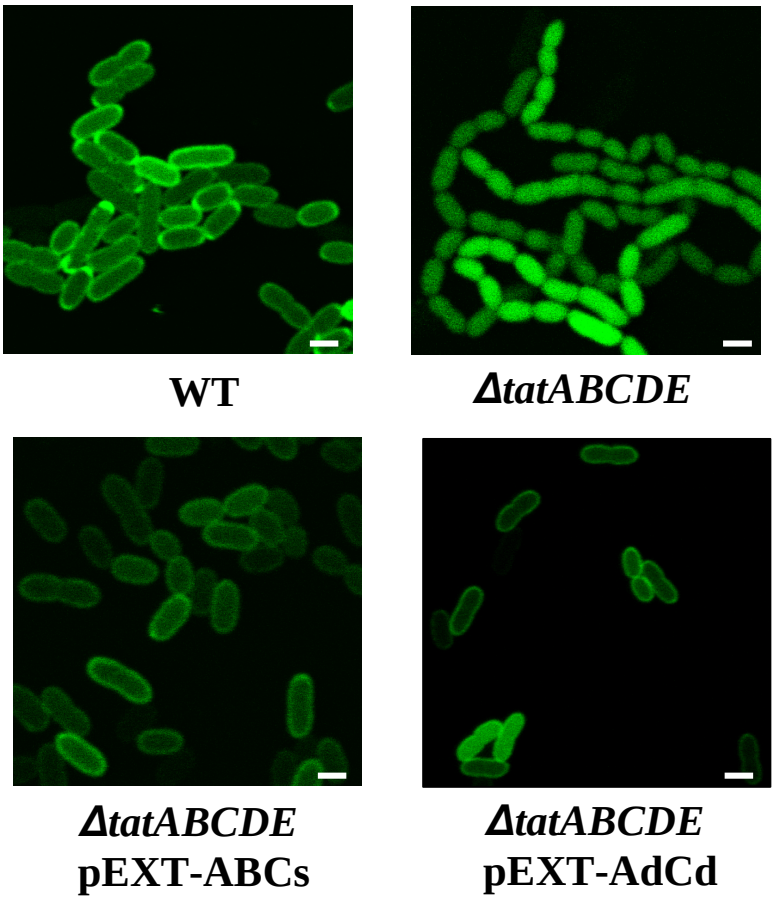

Figure 3.2.3 Translocation of active GFP by the TatAdCd pathway
Plasmid pJDT1 expressing TorA-GFP was expressed in MC4100 cells, *ΔtatABCDE* cells and *ΔtatABCDE* cells expressing TatAdCd or TatABC (from compatible pEXT22 plasmids). Cells were analysed by confocal microscopy using the 488 nm laser line. The scale bars represent 1µm. All experiments were performed in duplicate and a reprentative sample is shown.

3.2.3 Translocation of the cell wall amidases, AmiA and AmiC by TatAdCd

E. coli amidases AmiA and AmiC are periplasmic proteins that are translocated by the Tat pathway (Ize *et al*., 2003; Bernhardt and de Boer, 2003). They are both required for the final stages of cell division. *E. coli tat* null mutant strains show a filamentous phenotype caused by these two amidase proteins being unable to get across the membrane to the periplasm. We can therefore say something about the ability of the TatAdCd pathway to support translocation of these two Tat substrates from the confocal microscopy data shown above (Figure 3.2.3). Wild-type *E. coli* cells can be clearly seen as single or dividing cells whilst the *ΔtatABCDE* cells are seen as long

chain like filaments exactly as expected. Expression of *E. coli* TatABC or more importantly *B. subtilis* TatAdCd in *ΔtatABCDE* cells can complement for the mutant phenotype and cells are able to divide normally. Although indirect this observation implies that the TatAdCd pathway can translocate *E. coli* AmiA and AmiC.

In this experiment the TatAdCd proteins were expressed from the low copy number plasmid pEXT22. In a further experiment, the ability of TatAdCd to complement the mutant phenotype of *E. coli ΔtatABCDE* cells was investigated by expressing the TatAdCd proteins at a much higher level, using the pBAD24 plasmid (Figure 3.2.4). As described above wild-type *E. coli* (MC4100) cells are seen as single or dividing cells whilst *ΔtatABCDE* cells show a filamentous phenotype as expected. As an additional positive control TatABC was expressed from the pBAD-ABCs plasmid in the *E. coli ΔtatABCDE* strain and was found to complement the mutant phenotype. Surprisingly then, expression of TatAdCd from plasmid pBAdCd in the *ΔtatABCDE* strain did not complement the mutant phenotype and cells are seen in long chains. The expression levels of the Tat proteins may therefore affect the ability of the *tatAdCd* genes to complement the mutant phenotype of *ΔtatABCDE* cells. Another study investigating the Tat pathway of *Vibrio cholerae* also found that high levels of expression of the *tatABC* genes in *E. coli Δtat* cells abolished complementation (Xiong *et al*., 2007). The expression of membrane proteins in *E. coli* can result in a filamentous phenotype (Wagner *et al*., 2007), and this may also explain why a high level of TatAdCd expression seems unable to complement the mutant phenotype.

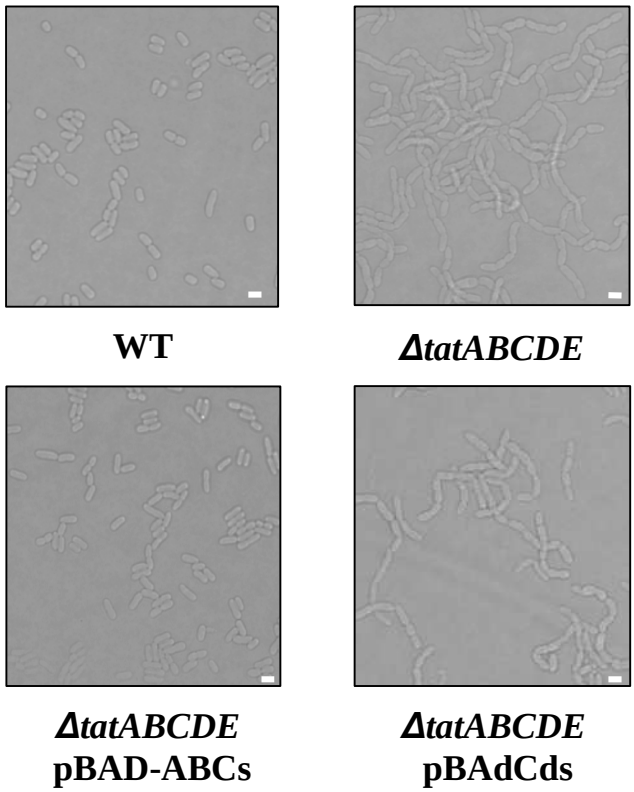

Figure 3.2.4 High level TatAdCd expression cannot complement for the mutant phenotype of *E. coli ΔtatABCDE* cells.
Confocal microscope images of wild-type (WT) *E. coli* MC4100 cells, *E. coli ΔtatABCDE* cells, and *E. coli ΔtatABCDE* cells expressing either TatABC or TatAdCd from the pBAD24 plasmid. The scale bar represents 1µm.

3.2.4 Affinity chromatography of TatAdCd and TatAd complexes

In *E. coli* and similarly in many other Gram-negative bacteria that have been studied, two major membrane localised Tat complexes have been isolated (Oates *et al*., 2003). A TatABC containing complex that is the initial receptor for Tat substrates (Alami *et al*., 2003), and separate TatA complexes that are thought to be recruited to the TatABC complex to form a complete translocation channel (Oates *et al*., 2005; Gohlke *et al*., 2005). Affinity chromatography was used to determine whether the TatAd and TatCd proteins were organised in a similar way into separate TatAdCd and TatAd complexes within the plasma membrane. The *tatAdCd* genes were expressed in *E. coli ΔtatABCDE* cells from plasmid pBAdCds and membranes isolated and solubilised in the detergent digitonin (2.5.2). Digitonin is a mild non-ionic detergent that is effective in solubilising membrane protein complexes. The digitonin solubilised membranes

were applied to an equilibrated 4 ml Streptactin™ affinity column. The TatCd protein was tagged with a C-terminal *strep*-tag II that binds specifically to the Streptactin™ resin. After sample application the column was subjected to washing with 8 x 4 ml of equilibration buffer before tightly bound proteins were finally eluted with 6 x 2 ml of buffer supplemented with desthiobiotin (a biotin derivative that completes for binding to the Streptactin chromatography media). All column wash and elution fractions were resolved on SDS-PAGE gels and subsequently immunoblotted using antibodies against the *strep*-tag II on TatCd and against TatAd (Figure 3.2.5). The figure shows that essentially all of the TatCd-*strep* protein had bound to the column as very little is observed in the wash fractions. The TatCd protein eluted from the column across elution fractions 2-4 with a peak in fraction 3. A small amount of the TatAd protein co-eluted with the TatCd protein indicating the presence of a TatAdCd containing complex. Most of the TatAd protein however was not bound to the TatCd protein and was found in the first few column wash fractions, strongly suggesting the presence of a separate TatAd complex within the membrane. This organisation into two main types of complex, TatABC and TatA or TatAdCd and TatAd is therefore a common feature of all Tat systems analysed in this way to date.

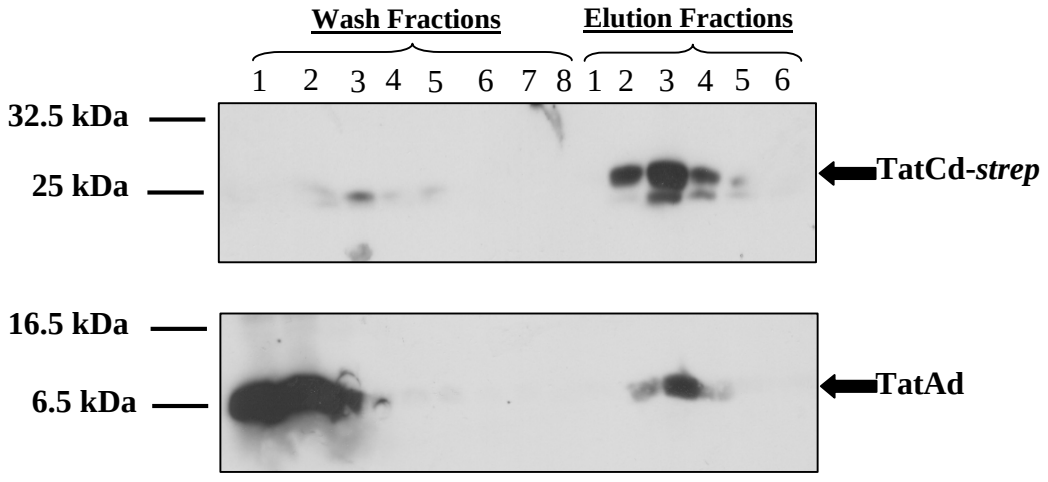

Figure 3.2.5 Affinity chromatography of TatAdCds
E. coli membranes from *ΔtatABCDE* cells expressing *B. subtilis* TatAdCd from plasmid pBAdCds were prepared and solubilised in digitonin. Membranes were subjected to Streptactin™ affinity chromatography as described above. The column wash fractions (Wash 1-8) and elution fractions (Elution 1-6) were immunoblotted using antibodies directed against the *strep*-tag II on TatCd and against TatAd. Positions of TatCd and TatAd are presented on the right of the figure and molecular weight markers are shown on the left.

The purity of the TatAdCd protein from the 3 peak elution fractions from the Streptactin™ affinity column was assessed by silver staining. The silver stain (Figure 3.2.6) shows that the TatAd and TatCd proteins are the major species present but higher molecular weight contaminating bands are also observed. A major aim of this project was to produce highly purified protein for structural analysis by electron microscopy. Further purification of the TatAdCd protein was therefore needed to generate samples of a high enough quality.

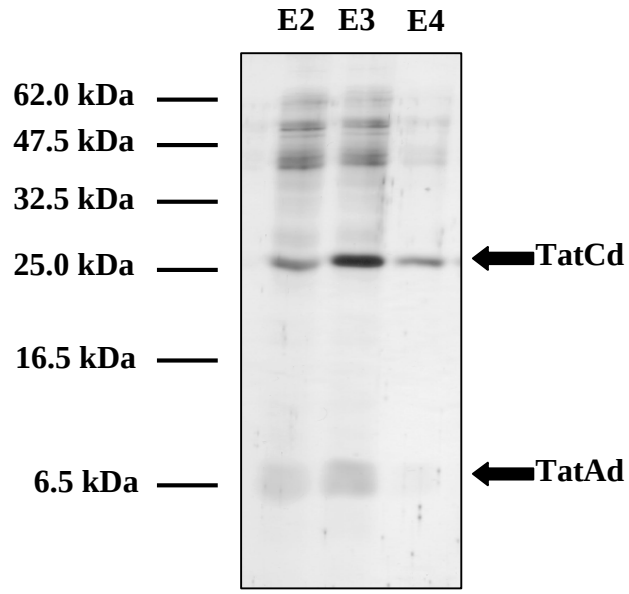

Figure 3.2.6 Silver stain of purified TatAdCd complex after a single Streptactin™ affinity column.
The 3 peak elution fractions (E2 – E4) from the Streptactin™ affinity column (above) were stained with silver to assess protein purity. Mobility's of the TatCd and TatAd proteins are shown on the right and molecular weight markers indicated on the left.

3.2.5 Complete purification of the TatAdCd complex for structural analysis

In order to produce highly purified protein that was suitable for analysis by electron microscopy, additional chromatography steps were used. *E. coli* membranes were prepared from a 500 ml culture of *ΔtatABCDE* cells expressing plasmid pBAdCds and solubilised with the detergent digitonin. This detergent was chosen as it had been used previously for purification of *E. coli* TatABC complexes for analysis by electron microscopy (Oates *et al*., 2003). Membranes were applied first to an anion exchange resin (Q-Sepharose), and the eluted samples further purified using a Streptactin™ affinity column, and finally a size exclusion column (Superose-6) as detailed in chapter 2. Figure 3.2.7A shows a silver stain of the purified TatAdCd protein after elution from each column. The figure shows only the TatCd protein present in the final elution but the presence of TatAd was confirmed by immunoblotting with anti-TatAd antibodies (Fig. 3.2.7B). The very small amount of TatAd present in the TatAdCd complex was difficult to visualise by silver staining. The data clearly shows that the TatAdCd complex has been purified to homogeneity.

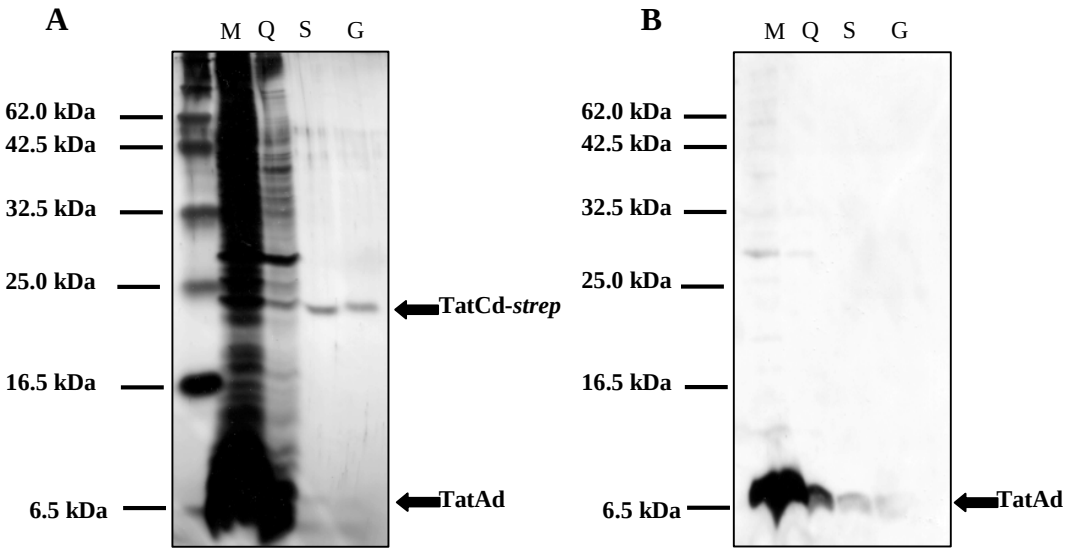

Figure 3.2.7 Complete purification of TatAdCd
Digitonin solubilised membranes were produced from *ΔtatABCDE* cells expressing TatAdCd from plasmid pBAdCds. Protein was purified using Q-Sepharose (Q), Streptactin™ (S), and Superose-6 (G) chromatography columns. A, The peak elution fraction from each column was analysed on a silver stained gel to assess purity. B, The presence of TatAd at each stage of the purification procedure was confirmed by immunoblotting with anti-TatAd antibodies. Positions of TatCd and TatAd are indicated on the right of the gels and molecular weight markers are shown on the left.

3.2.6 Protein yields from TatAdCd purifications

Several purifications of the TatAdCd complex were performed and samples sent to Dr. Kirstin Model at the Max-Planck Institute, Frankfurt for analysis by electron microscopy. The total yield of protein obtained from various purifications was determined using the BCA method as outlined in chapter 2. Figure 3.2.8A shows a standard curve of protein concentration plotted against absorbance. This standard curve was used to determine the concentrations of samples of purified TatAdCd protein taken from the peak elution fraction of the final gel filtration column (Figure 3.2.8B). The average yield of protein from the peak elution fraction of the gel filtration column was 160 µg.

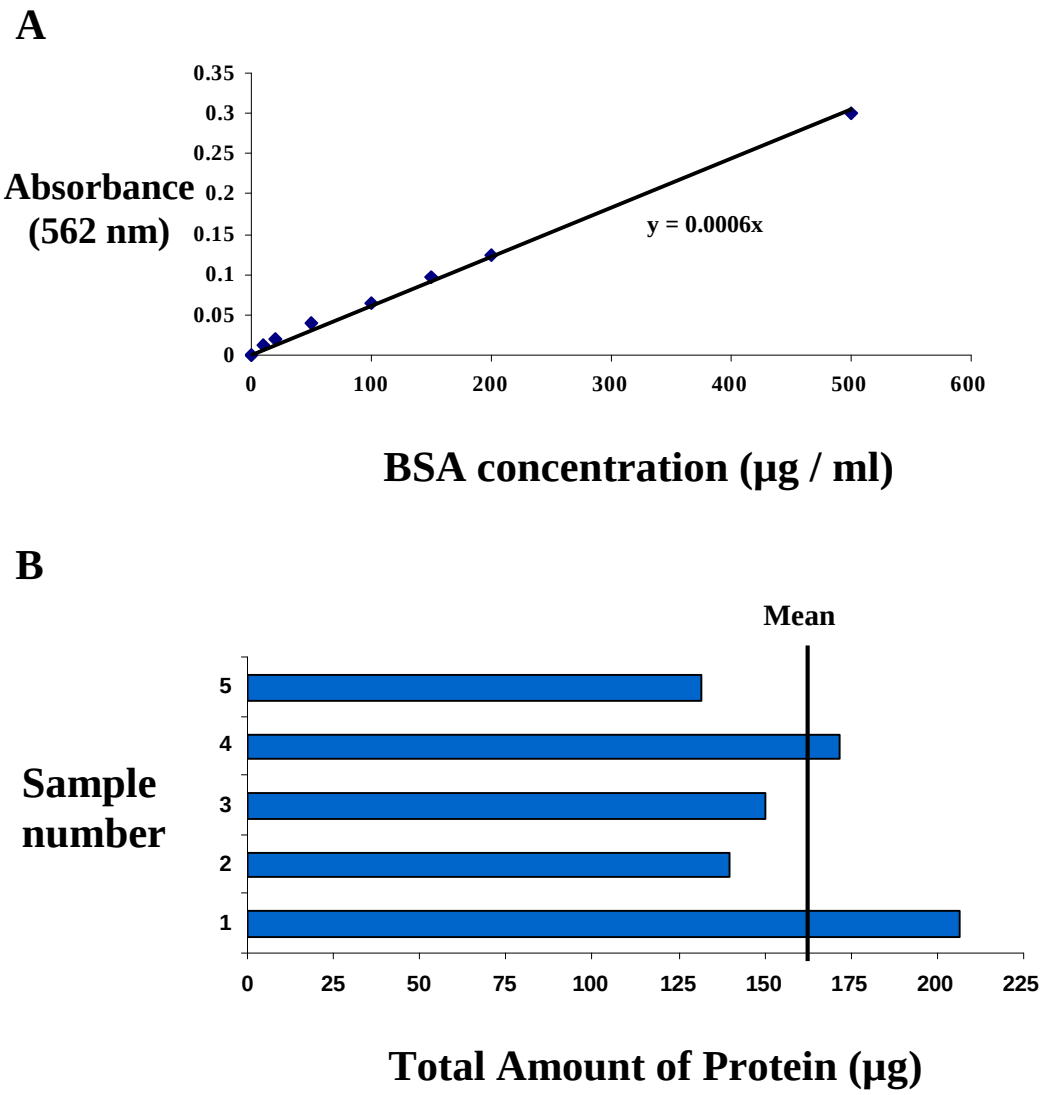

Figure 3.2.8 Determination of protein concentration by the BCA method.
A, 50 µl samples of BSA solutions of different concentration were prepared and mixed with 1 ml of BCA reagent. Absorbance was measured at 562 nm and plotted against protein concentration to generate a calibration curve. B, 5 purifications of TatAdCd: The final yield of protein taken from the peak elution fraction from the Superose-6 column was determined using the BCA method. The average yield is shown.

3.2.7 Gel filtration chromatography of TatAdCd and TatAd complexes

Gel filtration chromatography was used to provide an estimate of the TatAdCd and TatAd complex sizes. *E. coli* membranes were prepared from *ΔtatABCDE* cells expressing TatAdCd from the pBAdCds plasmid. Membranes were solubilised in buffer containing digitonin (2.5.2) and applied directly to an equilibrated Superose-6 (gel filtration) column. The sample was eluted from the column in 0.6 ml fractions with a single column volume of equilibration buffer. All eluted fractions were analysed by SDS-PAGE and the gels subjected to immunoblotting with *strep*-II tag antibodies and with specific anti-TatAd antibodies (Figure 3.2.9). The figure shows TatCd eluting across fractions 20 – 27 with a peak in fraction 23 and is presumably the TatAdCd complex that was identified earlier by affinity chromatography. The TatAd protein elutes over fractions 20 – 26 with a peak in fraction 24. As most of the TatAd protein is not found in a complex with TatCd this is likely to be the separate TatAd complex. In addition TatAdCd protein that had been purified by anion exchange and affinity chromatography in the detergent digitonin was also analysed by gel filtration chromatography in the same way, and protein present in elution fractions resolved on an SDS-PAGE gel before immunoblotting using antibodies against the *strep*-II tag on TatCd (Figure 3.2.9). The purified protein is eluting over fractions 20 -27 with a peak in fraction 23, the same as observed when digitonin-solubilised membranes were analysed. This shows the composition of TatAdCd complexes is not affected by the purification procedure employed.

To estimate the sizes of TatAdCd and TatAd complexes the Superose-6 gel filtration column was calibrated using four protein standards of known molecular weight. These were aldolase (158 kDa), catalase (232 kDa), ferritin (440 kDa), and thyroglobin (669 kDa). The elution volume of each of these standards was plotted against the Log of molecular weight to produce a calibration curve (Figure 3.2.10). The TatAdCd complex eluted from the column with a peak in fraction 23 or 13.3 ml. This gives a size estimate of 350 kDa. This is considerably smaller than the *E. coli* TatABC complex that when analysed in the same way gave a size estimate of ~ 600 kDa (Bolhuis *et al.*, 2001). This difference in mass could reflect the absence of a TatB component but could also have important implications in translocation mechanism if the complex is composed of a different number of TatAdCd subunits compared to *E.*

coli TatABC. The TatAd complex eluted slightly later from the Superose-6 column in fraction 24 or 14.4 ml. This results in a size estimate of 270 kDa.

The immunoblots of the TatAdCd and TatAd complexes from solubilised membranes were further analysed by densitometry, and the intensity of the signal of each band plotted against fraction number (Figure 3.2.9). The graph shows the TatAd complex is eluting as a relatively sharp peak. When analysed in the same way, the *E. coli* TatA protein has a much broader elution profile and is present in a bigger range of fractions, reflecting the enormous variation in TatA complex size (Oates *et al*., 2005). The narrow elution range of the TatAd protein points to a much more restricted size range, and this difference in the heterogeneity of the TatA complex implies a translocation mechanism involving a single defined translocon, rather than a spectrum of size variants. This is despite the TatAdCd pathway being able to translocate a number of different substrates that vary in both size and shape, from GFP (~27 kDa), to PhoD (~60 kDa), to TorA (~90 kDa), and therefore casts doubt on the functional significance of the size variation of the *E. coli* TatA complex.

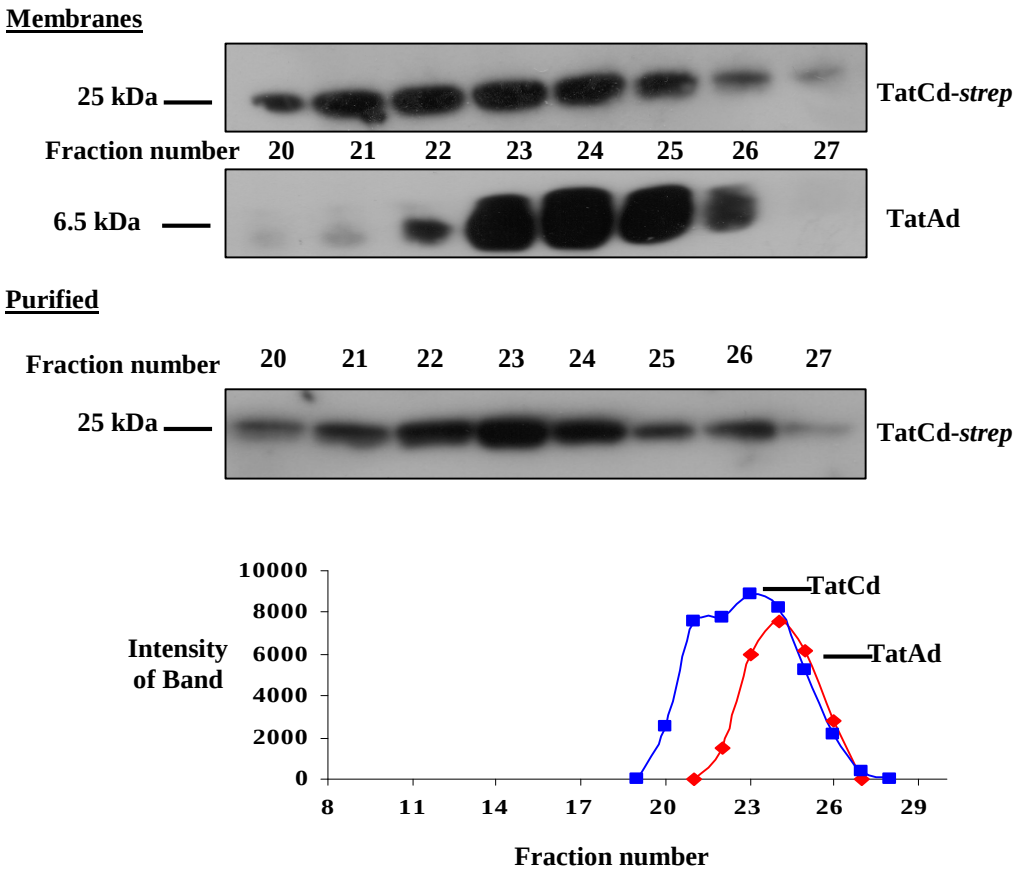

Figure 3.2.9 Gel filtration chromatography of TatAdCd and TatAd complexes. Digitonin-solubilised membranes from *ΔtatABCDE* cells expressing TatAdCd from pBAdCds plasmids, or purified TatAdCds, were applied to a calibrated gel filtration column (Superose-6). Elution fractions were resolved by SDS-PAGE and subjected to immunoblotting with anti-*strep*-tag II antibodies or anti-TatAd antibodies as indicated. Molecular weight markers are shown on the left. Immunoblots of membrane samples were analysed by densitometry and intensities of the bands plotted against fraction number. The elution profile of TatCd is shown in blue and TatAd in red.

Protein standard	Molecular weight (Daltons)	Log molecular weight	Volume eluted (ml)
Thyroglobin	**669,000**	**5.825426118**	**11.88**
Ferritin	**440,000**	**5.643452676**	**13.8**
Catalase	**232,000**	**5.365487985**	**14.98**
Aldolase	**158,000**	**5.198657087**	**15.27**

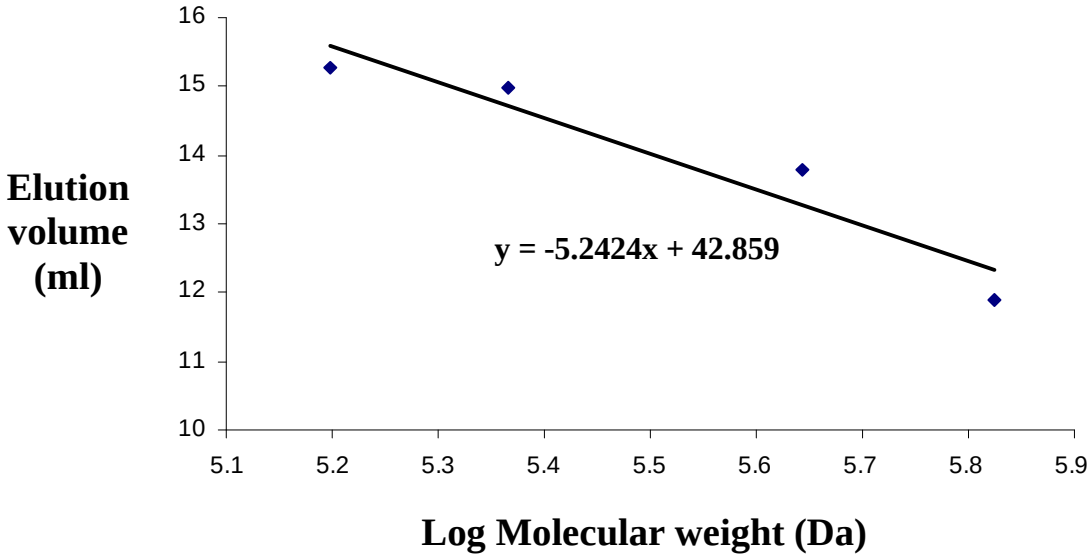

Figure 3.2.10 Calibration curve for the Superose-6 gel filtration column
The superose-6 gel filtration column was calibrated using protein standards of known molecular weight. The standards used were aldolase (158 kDa), catalase (232 kDa), ferritin (440 kDa), and thyroglobin (669 kDa). The elution volumes of each of the protein standards was plotted against Log molecular weight to generate a calibration curve. The equation of the line is shown.

3.2.8 Blue-Native PAGE of the TatAdCd complex.

The TatAdCd complex was further analysed using Blue-Native PAGE. Whilst gel filtration chromatography can give a reasonable estimate of complex size, this estimate is heavily influenced by the size of the detergent micelle. BN-PAGE effectively removes this bias and thus gives a more accurate estimate of molecular mass. Membranes were obtained from *E. coli ΔtatABCDE* cells expressing TatAdCd from pBAdCds (Bs), or *E. coli* TatABC from plasmid pBAD-ABCs (Ec) and solubilised in digitonin. Purified TatAdCd (AdCd) was also prepared for analysis. Samples were run on blue-native gels that were subsequently immunoblotted using anti-*strep*-tag II antibodies and with antibodies raised against TatA and TatAd. The results are shown in Figure 3.2.11. Reproducing earlier findings where the TatABC complex was found to run at 370 kDa on BN-gels, the TatABC complex (lane Ec) is seen migrating to just below the 440 kDa marker (detected using anti-*strep*-tag II antibodies). Also reproducing earlier findings, the anti *E. coli* TatA immunoblot shows a ladder of bands indicating the different sized *E. coli* TatA complexes that are present in the membrane (lane Ec). Looking at the purified TatAdCds complex (lane AdCd), the anti-*strep*-tag II immunoblot shows a band around the 232 kDa marker and a corresponding band with the same migration is found in the anti-TatAd immunoblot giving us a size estimate of ~230 kDa for the TatAdCd complex. This matches well with the estimate obtained by gel filtration where the detergent micelle can add up to a third of the mass estimate. A band of ~230 kDa is also seen in the anti-TatAd immunoblot in the lane where digitonin-solubilised membranes expressing TatAdCd were loaded (Bs), indicating the same size complex is present within detergent solubilised membranes, although in this case the TatCd-*strep* was difficult to observe in the anti-*strep*-tag II immunoblot. Unfortunately despite repeated efforts the TatAd complex could not be clearly resolved using this gel system, perhaps due to the small size of the complex.

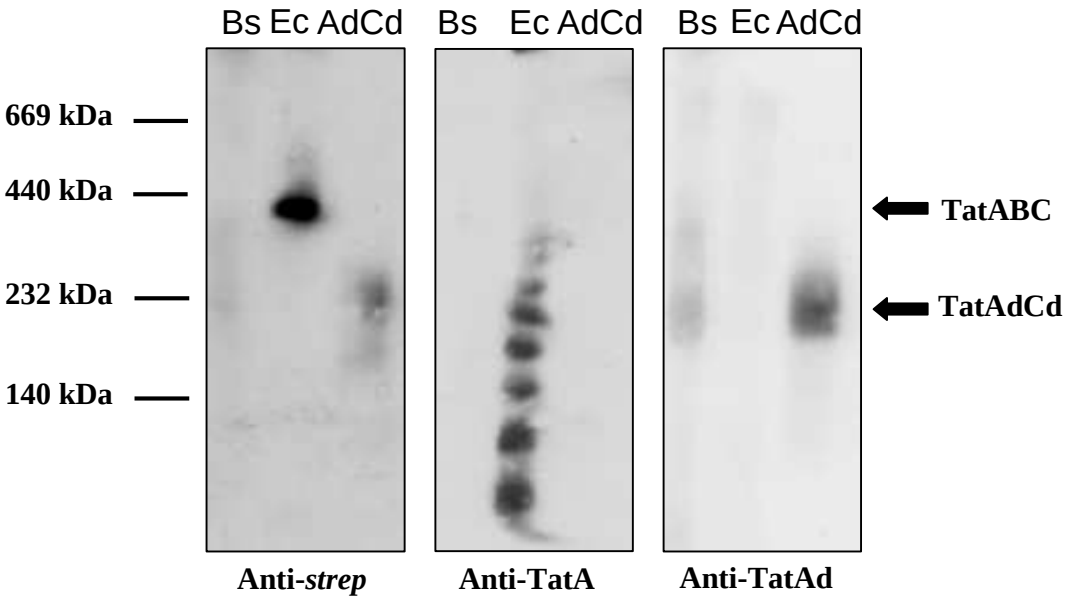

Figure 3.2.11 Blue-Native PAGE of TatAdCd complexes
Membranes were extracted from *E. coli ΔtatABCDE* cells expressing TatAdCds from pBAdCds (Bs), or *E. coli* TatABCs from pBAD-ABCs (Ec) and solubilised in digitonin. Membranes were run on blue-native gels alongside purified TatAdCds (AdCd). Immunodetection of complexes was achieved using antibodies to the *strep*-tag II on the C-terminus of TatCd and TatC, and to TatA, and TatAd as indicated below the blots. Positions of the TatABC and TatAdCd complexes are presented to the right. Molecular weight markers are shown to the left.

3.2.9 Further analysis of the TatAd complex by gel filtration chromatography

As the TatAd complex could not be resolved using Blue-Native gel electrophoresis it was further analysed by gel filtration chromatography. Digitonin forms large micelles so by using detergents with smaller micelle sizes such as octyl glucoside and dodecyl maltoside a more accurate estimate of molecular mass can be made. Also, whilst digitonin is a relatively mild detergent that is widely regarded as being suitable for solubilising membrane protein complexes, it is essential to examine whether the homogeneous nature of the TatAd complex compared to the highly heterogeneous nature of the *E. coli* TatA complexes may result from the effects of the detergent on the protein complex. *E. coli* membranes were extracted from *ΔtatABCDE* cells expressing TatAd-*his* using the plasmid pBAdh. Membranes were solubilised using digitonin, octyl glucoside, or dodecyl maltoside and applied to an equilibrated Superose-6 gel filtration column. The sample was eluted with a single column volume of buffer and the eluted sample collected in 0.6 ml fractions. All fractions were

resolved on SDS-PAGE gels and immunoblotted using anti-TatAd antibodies and immunoblots further analysed by densitometry (Figure 3.2.12). As expected the TatAd complex in digitonin eluted from the column with a peak in fraction 24 confirming the findings detailed above (3.2.7). The TatAd complex in the detergents octyl glucoside (OG) and dodecyl maltoside (DDM) actually eluted later with a peak in fraction 26. Using the calibration curve prepared earlier (Fig 3.2.10); the mass of the TatAd complex can be estimated to be ~160 kDa in this fraction. The smaller size is due to the much smaller detergent micelle sizes of octyl glucoside and dodecyl maltoside. However the complex is likely to be even smaller with these detergents still accounting for some of this size estimate. The most important point from this experiment is that even in these other detergents, the TatAd complex is eluting as a relatively homogenous species compared to the *E. coli* TatA complex.

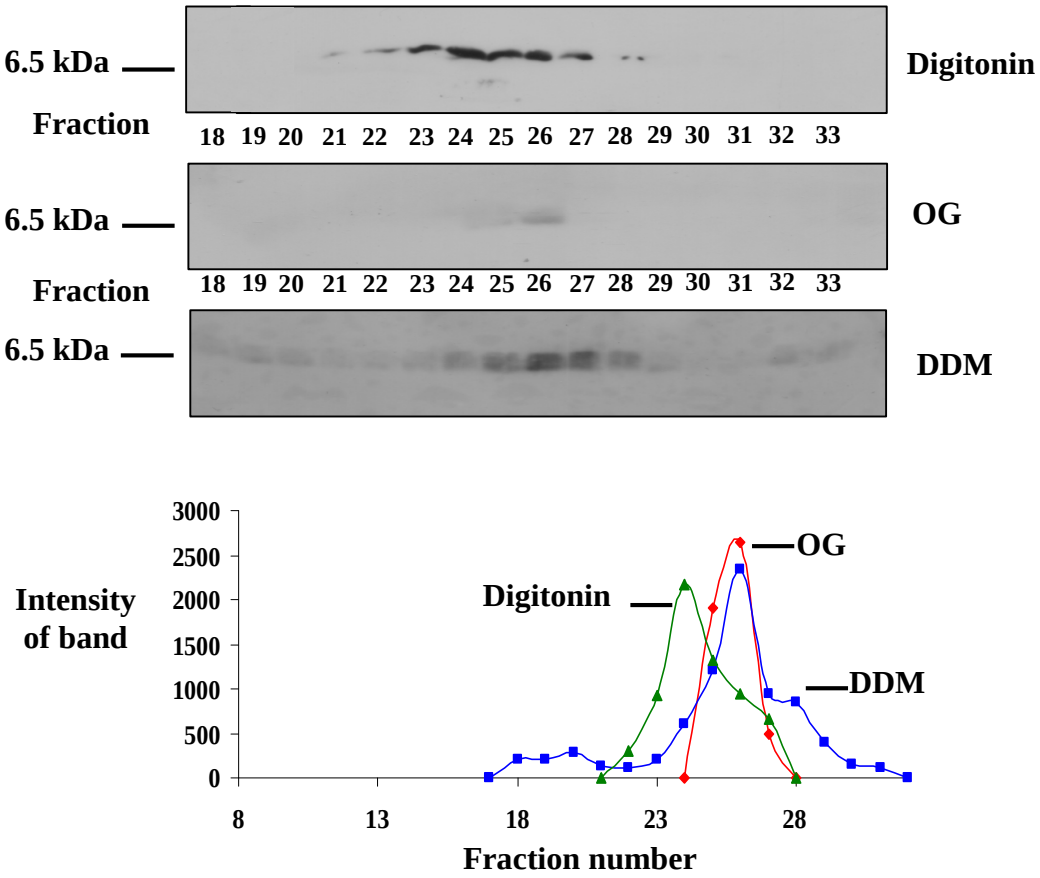

Figure 3.2.12 Gel filtration chromatography of TatAd complexes.
E. coli membranes were isolated from *ΔtatABCDE* cells expressing TatAd-*his* from plasmid pBAdh. Membranes were solubilised in 2% digitonin, 1% octyl glucoside (OG), or 1% dodecyl maltoside (DDM), and subjected to gel filtration chromatography using the same detergent. Elution fractions were immunoblotted with specific anti-TatAd antibodies. Molecular weight markers are shown towards the left of the blots. Immunoblots were further analysed by densitometry and intensity of the bands plotted against fraction number for each of the detergents used. The elution profile of digitonin is shown in green, octyl glucoside (OG) in red, and dodecyl maltoside (DDM) in blue.

3.2.10 Gel filtration chromatography of *E. coli* TatA

The above experiments repeatedly refer to the heterogeneity of the *E. coli* TatA complex. Therefore as a control the *E. coli* TatA complex was subjected to gel filtration chromatography under exactly the same conditions used to analyse the *B. subtilis* TatAd complex. The *E. coli* membrane fraction was isolated from *Δtat* cells expressing TatABCs from the plasmid pBAD-ABCs. The isolated membranes were solubilised in the detergent digitonin before being applied to an equilibrated gel filtration column. Just as in the previous experiments protein was eluted using a single column volume of equilibration buffer in 0.6 ml fractions. Proteins present in elution fractions were resolved on SDS-PAGE gels that were immunoblotted using specific antibodies against TatA (Figure 3.2.13). The figure shows the TatA protein eluting from the column over a broad range of fractions, from fraction 10 to fraction 40. Using the standard curve in Figure 3.2.10 gives a size range of 10 MDa – 4 kDa over these fractions, confirming the heterogeneous nature of the TatA complexes. It should be noted that whilst the standard curve gives a mass estimate of 10 MDa for protein eluting in fraction 10, the maximum size resolution of the Superose-6 column used is 5 MDa. Although *E. coli* TatA monomers are less than 10 kDa in size the protein runs aberrantly on SDS-gels and is seen migrating with the 16.5 kDa marker in the immunoblot.

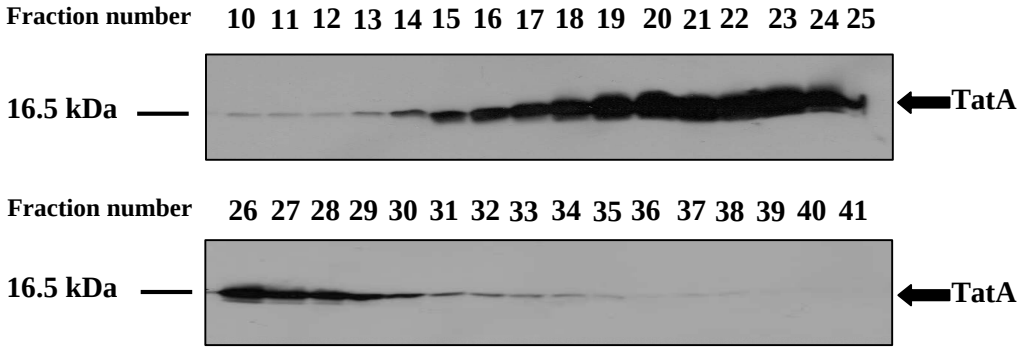

Figure 3.2.13 Gel filtration of *E. coli* TatA complexes
E. coli membranes were isolated from *ΔtatABCDE* cells that were expressing TatABCs from plasmid pBAD-ABCs and solubilised in 2% digitonin. Membranes were applied directly to a gel filtration column and protein eluted in 0.6 ml fractions with a single column volume of buffer. Proteins in elution fractions were resolved by SDS-PAGE and immunoblotted with anti-TatA antibodies. Molecular weight markers are presented to the left of the figure and the position of TatA indicated on the right.

3.2.11 Purification of *E. coli* TatABC complexes.

The *E. coli* TatABCs complex was purified by affinity chromatography for subsequent analysis by circular dichroism spectroscopy. Briefly, the membrane fraction was isolated from *E. coli ΔtatABCDE* cells expressing TatABC-*strep* from pBAD-ABCs plasmids and solubilised in buffer containing digitonin. Solubilised membranes were applied to an equilibrated 4 ml Streptactin™ affinity column that binds the *strep*-tag II on TatC. The column was washed with 4 x 4 ml of buffer and protein subsequently eluted with 6 x 2 ml of buffer supplemented with 3 mM desthiobiotin. Protein present in all column fractions was resolved on an SDS-PAGE gel and the gel immunoblotted with anti-*strep*-tag II antibodies and with antibodies against TatA and TatB (Figure 3.2.14). The anti *strep*-tag II immunoblot shows that not all of the TatC bound to the column and protein was detected in the column wash fractions. However the TatC-*strep* protein that did bind specifically eluted from the column with a clear peak across fractions 2-4. Higher molecular weight bands are also present (indicated by *) and this has been seen before (Bolhuis *et al*., 2001). A slightly faster migrating band is also present on the immunoblot and could be a result of a small amount of proteolytic clipping of the protein. As expected both *E. coli* TatA and TatB co-eluted from the column with the TatC protein. Again other bands that are faster migrating than the TatB and TatA proteins are present and these could also be due to non-specific clipping of the Tat proteins.

The TatABC complexes were analysed by SDS-PAGE and silver staining to determine the proteins purity. The peak elution fractions from the streptactin™ affinity column were tested. The fourth elution fraction (E4) was the purest fraction and this was used for subsequent experiments. A silver stain showing the purity of this fraction is seen in Figure 3.2.15. Other bands are present on the silver stain but these have not been assigned.

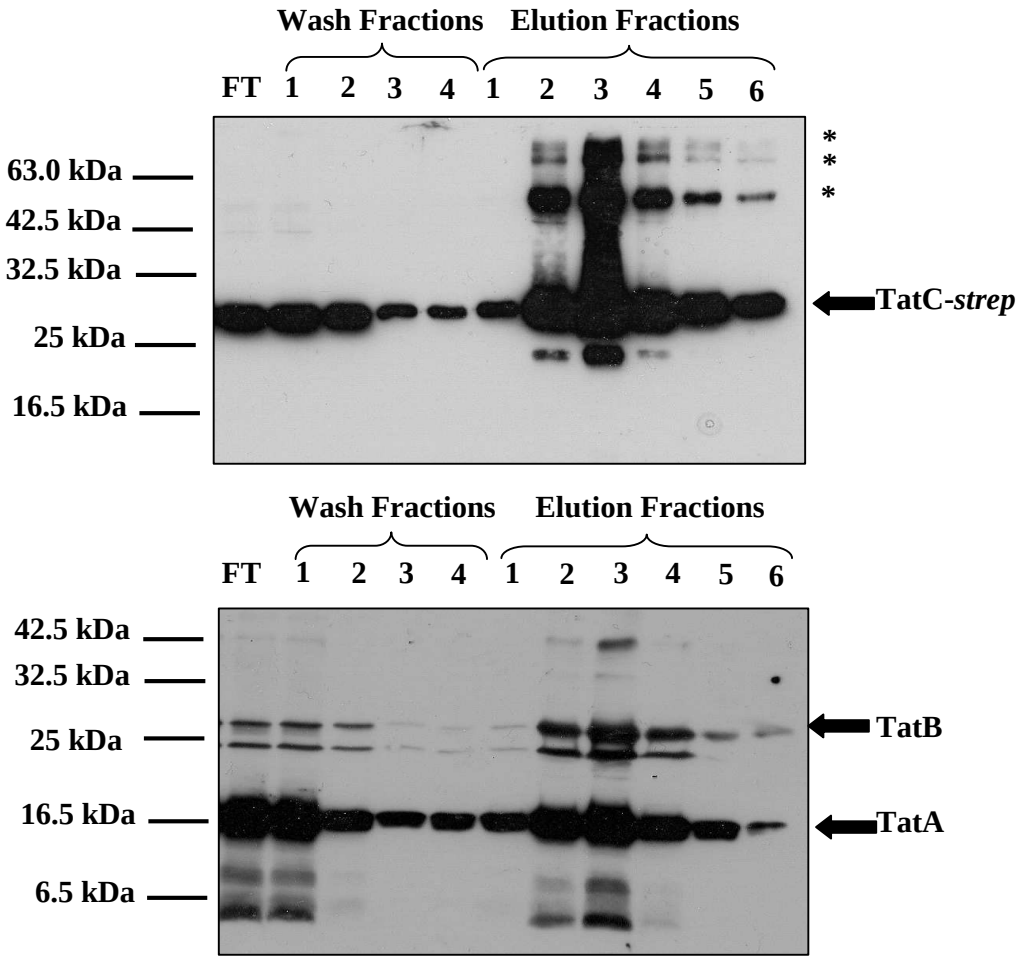

Figure 3.2.14 Affinity purification of *E. coli* TatABCs
Membranes extracted from *ΔtatABCDE* cells expressing TatABCs from plasmid pBAD-ABCs were solubilised in digitonin and used for Streptactin™ affinity chromatography. Column flow-through (FT), wash, and elution fractions were resolved by SDS-PAGE and immunoblotted with antibodies against the *strep*-tag II on TatC (top panel), and against TatA and TatB (bottom panel). Positions of the Tat proteins are indicated on the right, as are slower migrating forms of TatC (indicated by *). Molecular weight markers are shown on the left.

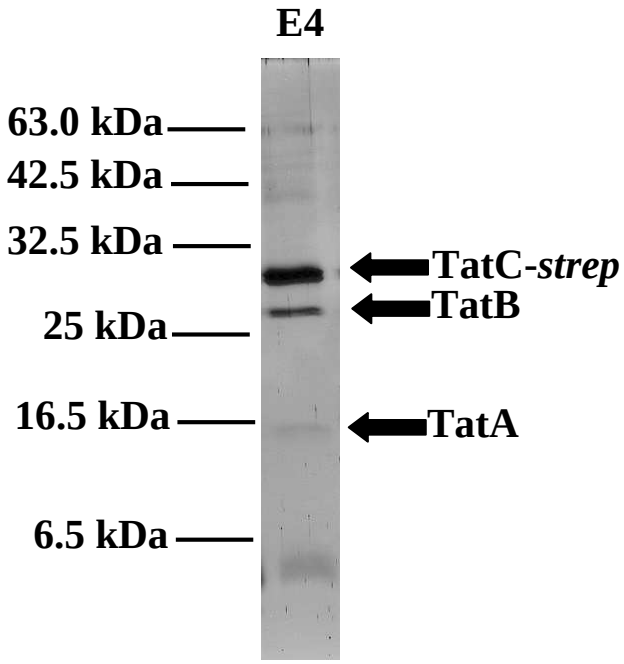

Figure 3.2.15 Silver stain of affinity purified *E. coli* TatABC
The fourth elution fraction from the Streptactin™ affinity column above was stained with silver to determine purity. The positions of the Tat proteins are indicated on the right whilst molecular weight markers are given to the left of the figure.

3.2.12 Secondary structure determination of the TatAdCd complex.

Circular dichroism spectroscopy (CD) provides a relatively straight forward way of determining the secondary structure of a protein. CD measures the difference between the absorbance of right circularly polarised light and left circularly polarised light over wavelengths of typically between 260 nm to 180 nm. The spectra generated allow us to distinguish between the main secondary structural elements of proteins, including alpha-helix and beta-sheet. Here CD spectra were exploited to compare the secondary structural features of *E. coli* TatABC complexes and *B. subtilis* TatAdCd complexes to see just how similar the two complexes are in terms of structure. CD was performed with samples of purified *E. coli* TatABCs and *B. subtilis* TatAdCds (both in the detergent digitonin). The results are shown in Figure 3.2.16. For both proteins CD spectra is obtained with clear minima at 208 nm and 222 nm. This is characteristic of proteins that are rich in alpha-helix.

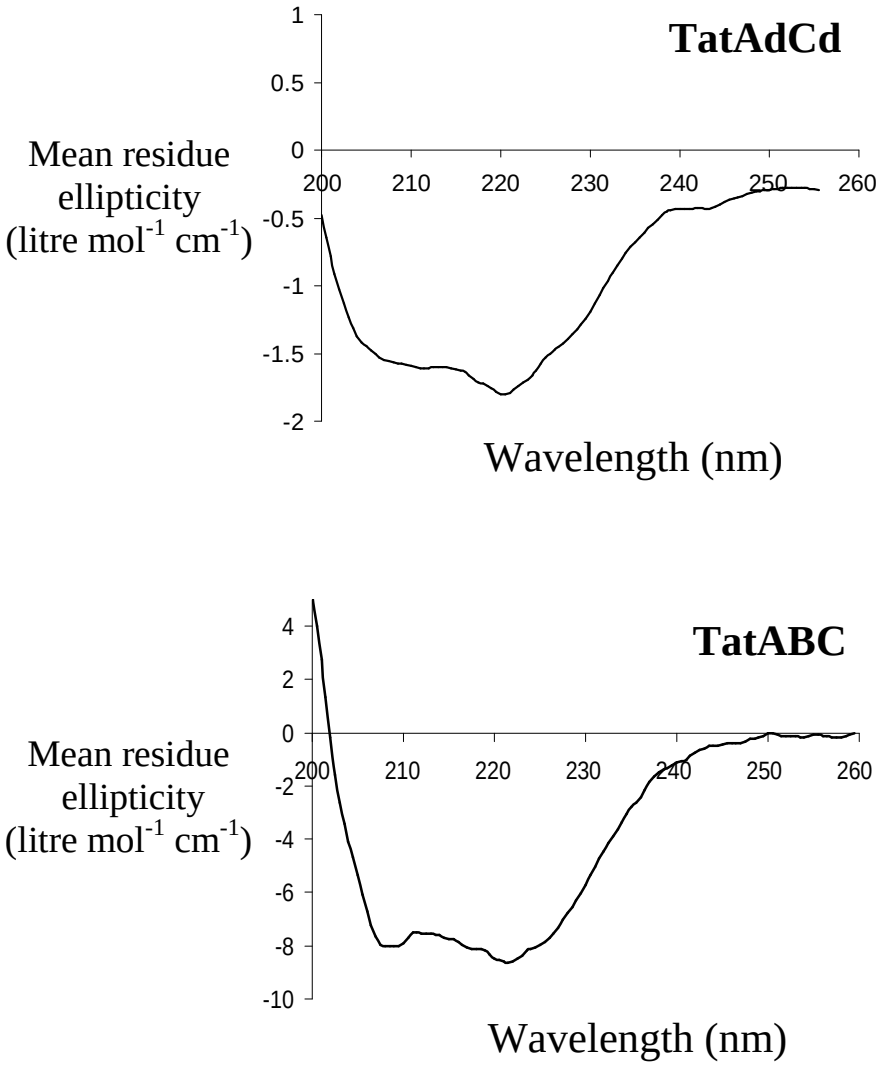

Figure 3.2.16 Circular Dichroism spectra of purified *E. coli* TatABCs and *B. subtilis* TatAdCds
Purified *E. coli* TatABCs and *B. subtilis* TatAdCds was used to obtain CD spectra over 200-260 nm using a Jasco J-815 spectrophotometer as described in Chapter 2 (2.11). The spectra shown is an average taken from 8 consecutive scans.

3.3 Discussion

In this Chapter the Tat complexes of the *B. subtilis* TatAdCd pathway have been studied in detail. The absence of a TatB component in Gram-positive bacteria suggested that the Tat systems of these bacteria differ significantly from the Tat systems of Gram-negative bacteria.

In *E. coli* a 370 kDa membrane localised TatABC complex has been isolated (Oates *et al*., 2005) that is thought to act as the initial receptor for Tat substrates (Alami *et al*., 2003). Cross-linking studies indicate that the TatC and TatB components play a critical role in this substrate binding (Alami *et al*., 2003; Holzapfel *et al*., 2007).
Whilst the TatA protein appears to only be loosely associated with TatBC in the TatABC complex, TatB and TatC form a tight association. A translational fusion of TatB-TatC of *E. coli* has been found to be active (Bolhuis *et al*., 2001).

Most of the TatA protein found within the membrane forms separate homo-oligomeric complexes of variable mass (100 kDa -500 kDa) (Oates *et al*., 2005). Data from the thylakoidal Tat pathway point to a model that upon interaction of substrate proteins with the TatABC complexes, free TatA complexes are recruited (Dabney-Smith *et al*., 2006). Electron microscopy data show the *E. coli* TatA complexes form pore-like structures with central cavities of variable diameter (Gohlke *et al*., 2005) and taken together these data point to TatA as being the most likely candidate for the formation of a channel through which substrates can cross the membrane.

A major aim of this work was to identify any differences, particularly differences in translocation mechanism between the Tat pathways of Gram-negative and Gram-positive bacteria using the TatAdCd system as a model. The TatAdCd pathway was found to support translocation of the *E. coli* Tat substrate TorA when the *tatAdCd* genes were expressed in an *E. coli* background. Furthermore, TorA was not the only substrate that the TatAdCd pathway could translocate. Efficient translocation of a fusion of the TorA signal peptide and GFP was observed in addition to the *tatAdCd* genes ability to complement *E. coli ΔtatABCD* cells for their filamentous phenotype, indicating translocation of AmiA and AmiC. This clearly demonstrates that the Tat system from a Gram-positive bacterium can function in a Gram-negative background

and shows that there are no factors that are essential for translocation in *B. subtilis* that are absent in *E. coli.* This focuses attention on the TatAd and TatCd proteins as being the critical components of this pathway.

The absence of a TatB component in *B. subtilis* led to the suggestion that the TatAd protein may be bifunctional and perform the roles of both *E. coli* TatA and TatB (Jongbloed *et al*., 2006). The fact the TatAdCd pathway can translocate the *E. coli* Tat substrate TorA for which TatA and TatB have been shown to have distinct and essential roles, strongly suggests that the TatAd protein is indeed bifunctional. The bifunctional nature of the TatAd protein is studied in more detail in chapter 6.

The Tat complexes of *B. subtilis* show both similarities to and differences from the *E. coli* Tat complexes. Expression of *tatAdCd* in *E. coli* and subsequent affinity chromatography of the TatCd protein allowed the isolation of both a TatAdCd containing complex and TatAd complex. This organisation into two types of complex is common to the Tat pathways of a number of Gram-negative bacteria studied in the same way (Oates *et al*., 2003), and taken together with the ability of the TatAdCd pathway to translocate different *E. coli* Tat substrates, points to a similar mode of action.

The TatAdCd and TatAd complexes however, also exhibit striking differences to their *E. coli* counterparts. Firstly the TatAdCd complex is significantly smaller than the *E. coil* TatABC complex (~230 kDa for TatAdCd and ~370 kDa for TatABC). This difference might be attributed to the absence of a TatB component. Just one TatAdCd unit with equimolar stochiometry (as seen with *E. coli* TatBC) has a mass of ~35 kDa compared to *E. coli* TatABC that is 56 kDa. It may also be possible however that the TatAdCd complex is composed of a different number of TatAdCd domains and this point is currently being addressed by electron microscopy.

The second difference concerns the TatAd complex. Whilst the *E. coli* TatA complex is highly heterogeneous in nature and forms a wide range of complex sizes (100 kDa to 500 kDa) (Oates *et al*., 2005), the TatAd complex appears to have a much more restricted size range. The TatAd complex was found to elute from the gel filtration column as a single homogenous species compared to *E. coli* TatA that eluted over a

very broad range of fractions. It was suggested that the variation in TatA complex size is linked to its ability to translocate substrates that vary in size and shape (Oates *et al*., 2005; Gohlke *et al.*, 2005). This made sense as it provided a way that the cell could move different sized proteins across the membrane without compromising its integrity. The more restricted size variation of the TatAd complex points to a mechanism involving a single defined translocon rather than a spectrum of size variants. Despite this the TatAdCd pathway can still translocate a number of substrates that vary considerably in size, from GFP (27 kDa), to PhoD (62.5 kDa), to TorA (85 kDa). Not only does the restricted size of the TatAd complex raise questions about the functional significance of the size variation of the *E. coli* TatA complexes, but it also raises questions about the nature of the translocation channel. The TatAd complex is fairly small. Estimated to be just 160 kDa by gel filtration chromatography, and since the detergent micelle accounts for a proportion of this estimate it is likely to be even smaller. It is difficult to see how the coalescence of a single TatAdCd (~270 kDa) and TatAd (~160 kDa) complex could result in the formation of a channel capable of accommodating the largest Tat substrates such as TorA. It is possible that the translocation mechanism is more complex than previously thought and perhaps involves the recruitment of several TatAd complexes.

In addition to identifying novel features of the TatAdCd and TatAd complexes this work has provided a solid foundation for future structural analysis.

Chapter 4

A role for soluble TatA in translocation?

4.1 Introduction

Two main models have been presented for the transport of proteins by the TatAdCd pathway of *B. subtilis*. The first is the same as the proposed mechanism of the *E. coli* Tat pathway. In the *E. coli* model Tat substrates are thought to bind initially to a membrane localised TatABC receptor complex, with TatB and TatC being critical for this interaction (Alami *et al*., 2003). Upon binding of substrate to the 'core' TatABC complex, separate TatA complexes are recruited to form some kind of channel or pore through which substrates can cross the membrane (Dabney-Smith *et al*., 2006; Mori and Cline, 2002). Following translocation the Tat machinery is reset for another round of transport. The data presented in chapter 3 support the hypothesis that the TatAdCd pathway in operating in a broadly similar manner to the *E. coli* Tat pathway, not least because it can translocate a number of *E. coli* Tat substrates tested.

However an alternative model of TatAdCd mediated translocation has been presented in the literature. In this model a soluble population of the TatAd protein, that has been found to form 150-250 kDa homo-oligomeric complexes in the cytosol (Westermann *et al.*, 2006), acts as the initial receptor for Tat substrate proteins. PhoD, the only identified substrate of the TatAdCd pathway has affinity for and binds to this soluble population of TatAd (Pop *et al.*, 2003). This led to the suggestion that the soluble TatAd complexes bind substrate and act as a guidance factor targeting substrate to membrane localised TatCd (Schreiber *et al.*, 2006). The PhoD-TatAd complex would presumably insert into the membrane upon binding TatCd and the PhoD substrate released from the cell. Both models are outlined in Figure 4.1.

A great deal of interest has been generated by the identification of a soluble population of TatAd in *B. subtilis*, and since then soluble populations of TatA have been identified in other organisms too. In the Gram-positive bacterium S*treptomyces lividans* both TatA and TatB proteins are present in the cytosol (De Keersmaeker *et al*., 2005). More recently and despite the suggestion that the Tat pathways of Gram-positive and Gram-negative bacteria may operate in a fundamentally different way, a soluble population of TatA has been identified in *E. coli* and was found to form large tube-like structures (Berthelmann *et al*., 2008). Within the plant chloroplast the TatA

homologue Tha4 has been found to have a dual localisation with stromal Tha4 found to improve the efficiency of Tat-dependent translocation across the thylakoid membrane (Frielingsdorf *et al*., 2008). In that particular study it was suggested that rather than acting as a receptor for Tat substrates, the soluble Tha4 provides an additional pool of protein that probably inserts into the membrane where it exerts its function.

The precise role of soluble TatA in translocation remains to be determined but the recent identification of this dual localisation in a number of organisms perhaps suggests that the Tat pathway mechanism is more widely conserved than previously suggested. In this chapter the dual localisation of TatAd is confirmed and evidence is presented that suggests that the cytosolic pool of TatAd may be mis-localised.

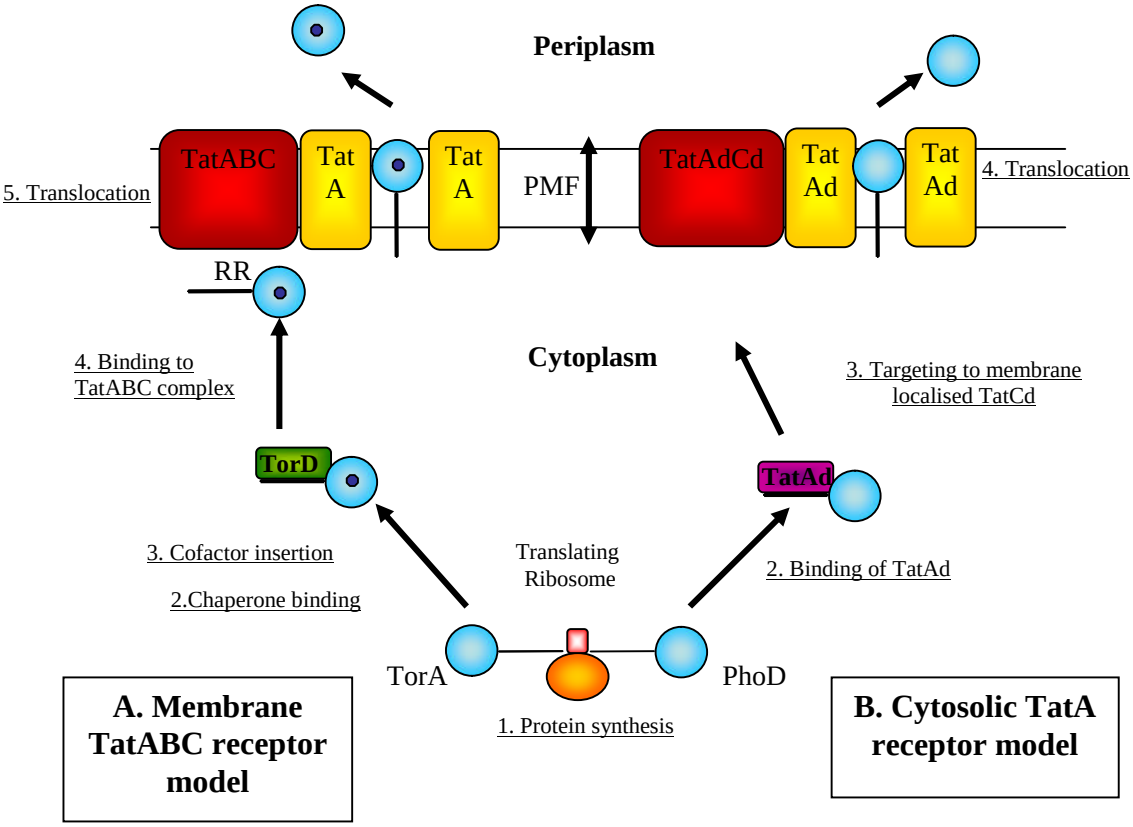

Figure 4.1 Two models of Tat-dependent translocation in bacteria.

A. Membrane TatABC receptor model. 1. The Tat substrate TorA is synthesised in the cytoplasm. 2. The TorA specific chaperone TorD binds to TorA. 3. TorD facilitates cofactor insertion and prevents premature interaction of substrate with the Tat machinery. 4. The Tat substrate binds to the TatABC receptor complex in the membrane via the twin-arginine motif. 5. Upon substrate binding to the TatBC receptor complex, TatA complexes are recruited to form a channel through which the substrate is translocated.
B. Cytosolic TatA receptor model. 1. The Tat substrate PhoD is synthesised in the cytoplasm. 2. Soluble TatAd complexes interact with the signal peptide of PhoD. 3. TatAd-PhoD complexes are targeted to membrane localised TatCd and PhoD is translocated across the membrane.

4.2 Results

4.2.1 Localisation of *E. coli* TatA and *B. subtilis* TatAd

The localisation of the TatA protein of *E. coli* and TatAd protein of *B. subtilis* was determined. Wild-type *E. coli* MC4100 cells and *E. coli ΔtatABCDE* (*Δtat*) cells that were expressing TatABCs from the plasmid pBAD-ABCs were fractionated into cytosolic and membrane samples. Cells fractions were run on SDS-PAGE gels before immunoblotting with specific anti-TatA antibodies. As a control and to confirm the strict membrane localisation of *E. coli* TatB, immunoblots were also performed using anti-TatB antibodies. Also tested were cell fractions prepared from *E. coli ΔtatABCDE* cells expressing TatAdCd from plasmid pBAdCds. Here immunoblots were probed with anti-TatAd antibodies. The results are shown in Figure 4.2.1. *E. coli* TatA is detected in both membrane (M) and cytosolic (C) fractions in both wild-type *E. coli* cells and in cells expressing TatABC from the pBAD24 plasmid. In fact the blots show that not only is TatA found in the cytosol as well as the membrane, but a greater proportion is seen in the cytosolic fraction. The observation that TatA in wild-type cells is found in the cytoplasm is important as it demonstrates that the dual localisation of TatA is not simply due to over expression of the protein. (*E. coli* TatA runs aberrantly on SDS-gels and is seen migrating to the 16.5 kDa marker). The data therefore confirms the reported cytosolic localisation of TatA in *E. coli* (Berthelmann *et al.*, 2008).

In contrast, a recent study using confocal microscopy to image YFP fused to the *E. coli* TatA protein found that the TatA protein is localised exclusively to the plasma membrane when expressed at native levels *in vivo* (Leake *et al*., 2008).

The *E. coli* TatB immunoblot shows the TatB protein to localise to the membrane fraction, exactly as expected, given its tight association with TatC. This demonstrates quite nicely that the fractionation was ‘clean’ and that the cytosolic fraction was not contaminated with membrane proteins.

Finally the TatAd immunoblot confirms the dual localisation of TatAd to both membrane and cytosolic compartments.

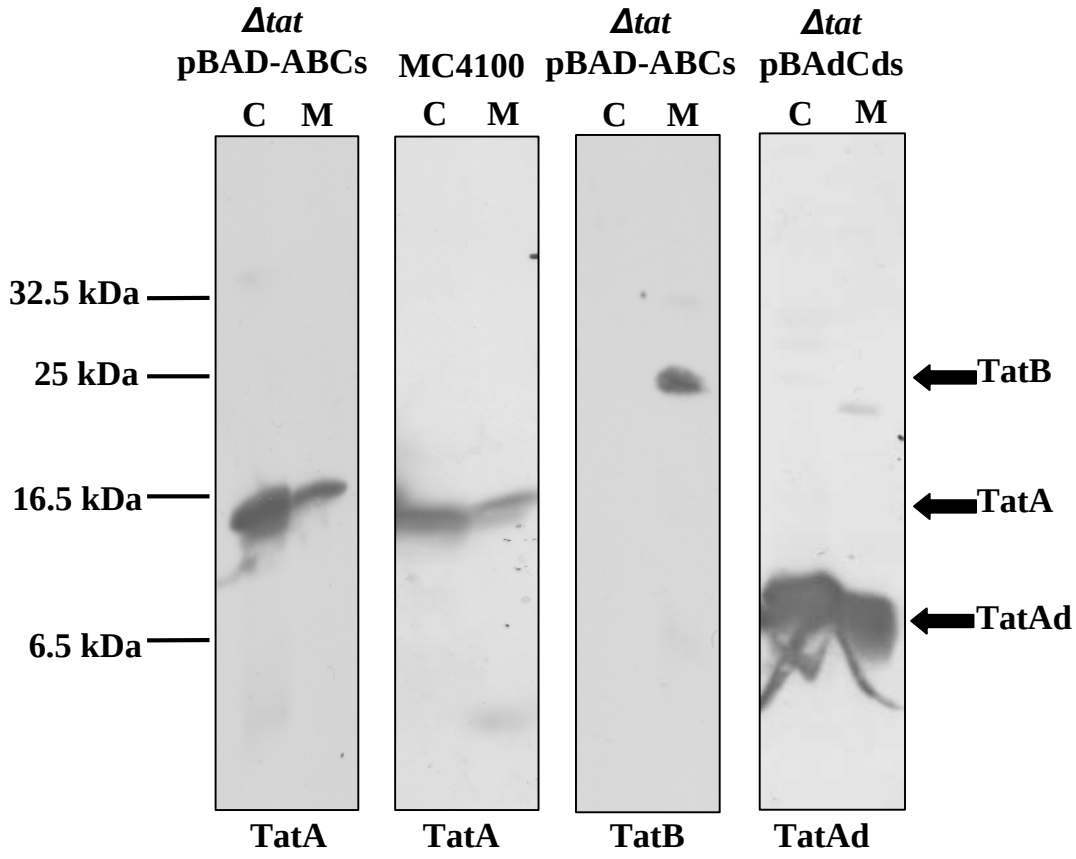

Figure 4.2.1 Localisation of *E. coli* TatA and TatB and *B. subtilis* TatAd
E. coli MC4100 cells, and *ΔtatABCDE* (*Δtat*) cells expressing *E. coli* TatABC or *B. subtilis* TatAdCd from the pBAD24 plasmid, were separated into cytoplasmic and membrane fractions. Cell fractions were applied to SDS-PAGE gels and gels immunoblotted with antibodies against *E. coli* TatA and TatB, and *B. subtilis* TatAd. Positions of the Tat proteins are presented on the right of the figure whilst molecular weight markers are shown to the left.

4.2.2 Purification of TatAd complexes from membrane and cytosolic fractions

One of the aims of this work was to produce highly purified Tat complexes for structural analysis. With this in mind the TatAd complexes were purified from both membrane and cytosolic compartments. *E. coli ΔtatABCDE* cells expressing TatAd-*his* (from the plasmid pBAdh), were fractionated and the cytosolic and membrane fractions collected. Membranes were solubilised using the detergent digitonin and this detergent was used throughout the purification. No detergent was used for the purification of TatAd-*his* from the cytoplasm. Samples were first purified using a 10 ml Q-Sepharose anion exchange column. After application to pre-equilibrated columns, the columns were rinsed with 10 ml of 100 mM NaCl containing buffer to elute weakly bound proteins. The TatAd-*his* protein was eluted in buffer containing

300 mM NaCl. The salt concentration of the eluted samples was diluted down to 150 mM before samples were applied to an equilibrated 4 ml Talon™ metal affinity column (that binds the 6-Histidine tag on TatAd). The columns were rinsed with 20 ml of buffer supplemented with 20 mM imidazole (imidazole competes for binding to the Talon™ affinity resin) to wash weakly bound protein from the columns. Finally TatAd-*his* was eluted from the columns with 5 x 2 ml of buffer containing 150 mM imidazole. All column fractions were run on SDS-PAGE gels before gels were immunoblotted with anti-TatAd antibodies. The peak elution fraction was subsequently analysed silver staining to assess purity (Figure 4.2.2). The immunoblots show the TatAd-*his* protein eluting from the Talon™ columns over fractions E2-E3 with a peak in E2 for both membrane and cytosolic samples. The peak elution fraction from the Talon™ columns (E2) was assessed for purity by silver staining (SS) and the figure shows that the protein in both cases is over 95 % pure.

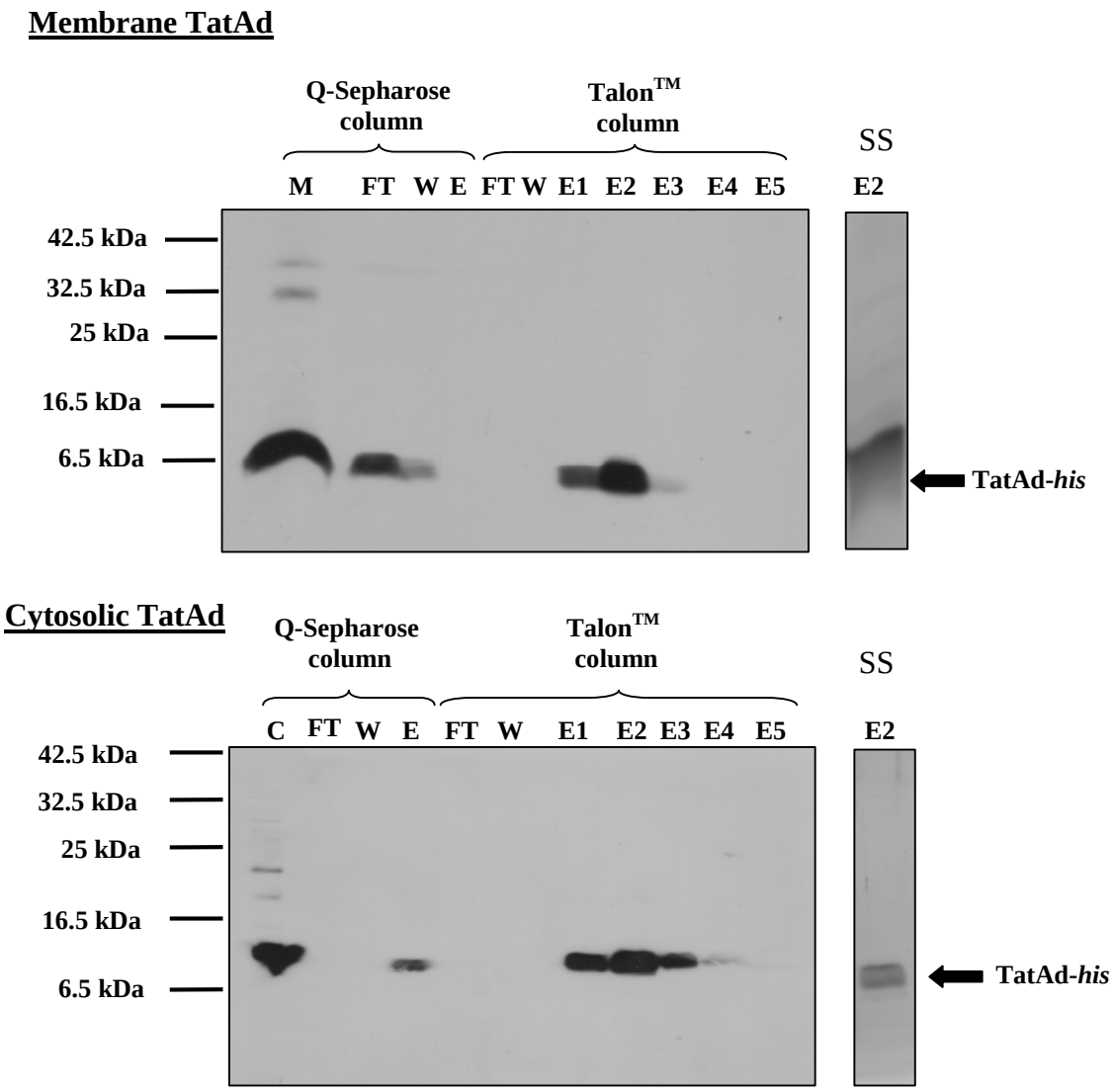

Figure 4.2.2 Purification of TatAd-*his* complexes from cytosolic and membrane localisations.
E. coli ΔtatABCDE cells expressing TatAd-*his* from plasmid pBAdh were separated into membrane (M) and cytosolic (C) samples. Samples were purified by Q-Sepharose anion exchange and Talon™ metal affinity chromatography (as described in chapter 2). Column flow-through (FT), wash (W) and elution (E) fractions were immunoblotted with anti-TatAd antibodies. The peak elution fraction from the Talon™ column (E2) from both purifications was analysed by silver staining (SS) to determine purity. The position of TatAd is presented to the right of the figure and molecular weight markers shown at the left.

4.2.3 Separation of Tat proteins into soluble and insoluble fractions using the detergent Triton X-114

In order to determine whether the cytosolic TatAd protein is a genuinely soluble population of protein it was analysed by phase separation using the detergent Triton X-114 as outlined in chapter 2. One of the properties of detergent solutions is that they undergo a phase separation into detergent and aqueous phases at defined temperatures. For the detergent Triton X-114 this occurs at room temperature. This property of Triton X-114 has been exploited to identify whether proteins are soluble or integral membrane proteins (Bordier, 1981). When a detergent undergoes phase separation membrane proteins will always localise to the detergent phase whilst soluble proteins localise to the aqueous phase.

As a control and to check that in any separations performed the detergent phase was not contaminated with soluble proteins, 3 random soluble proteins were analysed. These were ovalbumin, chymotypsinogen and ribonuclease A. Briefly the lyophilised proteins were mixed with buffer containing 1 % Triton X-114 in the cold. After 30 minutes incubation time, the sample was warmed to 30 °C to cause the detergent (D) and aqueous (Aq) phases to separate. The two phases were collected by centrifugation and samples loaded onto SDS-PAGE gels, that were subsequently stained with instant blue stain. The results shown in Figure 4.2.3A show each of the three proteins had separated to the aqueous phase as expected. There was no contamination of the detergent phase with soluble protein.

To check that the detergent phase was free of contaminating soluble proteins, purified *E. coli* TatABCs and *B. subtilis* TatAdCds were used as markers (since the TatC protein has a strict membrane localisation). Protein was purified from membranes by affinity chromatography using 1 % Triton X-114 in the cold (4 °C), and as above samples were then incubated at 30 °C to allow detergent and aqueous phases to separate. Phases were collected by centrifugation and samples run on SDS-PAGE gels before imunoblotting with antibodies against the *strep*-tag II on TatC and TatCd. The immunoblot in Figure 4.2.3B shows the TatC proteins to localise to the detergent phase as expected. A higher molecular weight band is also present in the detergent lane of the TatABC sample. The identity of this band has not been determined but it

may represent a TatC dimer. A very small amount of the protein was detectable in the aqueous phases. The method employed is therefore a robust way of separating membrane and soluble proteins.

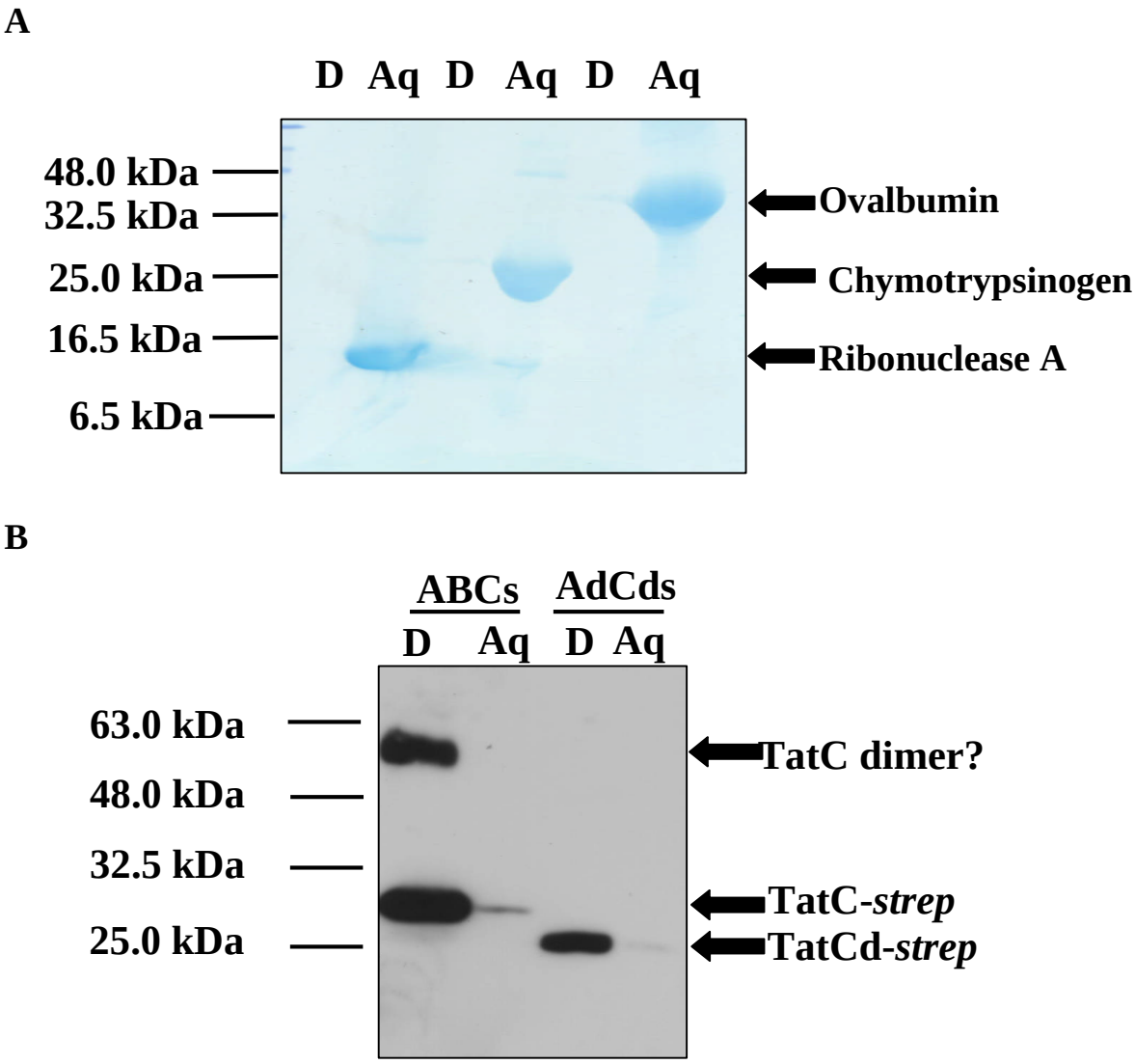

Figure 4.2.3 Separation of soluble and membrane proteins using Triton X-114
A. Three soluble proteins (ovalbumin, chymotrypsinogen, and ribonuclease A), were incubated with 1% Triton X-114 at 4 °C. After ~ 30 minutes samples were warmed to 30 °C to separate detergent (D) and aqueous (Aq) phases. Phases were collected by centrifugation and samples were subjected to SDS-PAGE before staining with Instant Blue stain. Positions of the three proteins are presented on the right whilst molecular weight markers are presented to the left.
B. *E. coli* TatABCs (ABCs) and *B. subtilis* TatAdCds (AdCds) were purified in buffer containing 1% Triton X-114 at 4 °C. Samples were then incubated at 30 °C to separate detergent (D) and aqueous (Aq) phases. Phases were collected by centrifugation and samples subjected to SDS-PAGE. Gels were immunoblotted using antibodies against the *strep*-tag II on TatC and TatCd. Positions of TatC and TatCd are indicated on the right and molecular weight markers shown on the left.

To test whether cytosolic TatAd was a truly soluble population of protein, *E. coli ΔtatABCDE* cells expressing TatAdCds from the pBAD24 plasmid were fractionated and cytosolic samples collected. In addition TatAd-*his* complexes that had been purified from the cytoplasmic fraction were tested. Each of the samples was incubated with 1 % Triton-X-114 on ice for 30 minutes before separation into detergent (D) and aqueous (Aq) phases at 30 °C. Phases were collected by centrifugation and samples from each phase were run on SDS-PAGE gels and immunoblotted with anti-TatAd antibodies. The Figure (4.2.4) shows that both the TatAd and the TatAd-*his* proteins localised to the detergent phase. This was unexpected given that the TatAd protein was isolated from the cytosol and suggests that this population of cytosolic TatAd is mis-localised. Interestingly, significant amounts of TatAd-*his* were also detected in the aqueous phase (unlike TatAd without a *his*-tag present), presumably because the *his*-tag increases the solubility of the protein. Some slower migrating bands are also observed on the blot (indicated by *) and these may represent multimers of the TatAd protein.

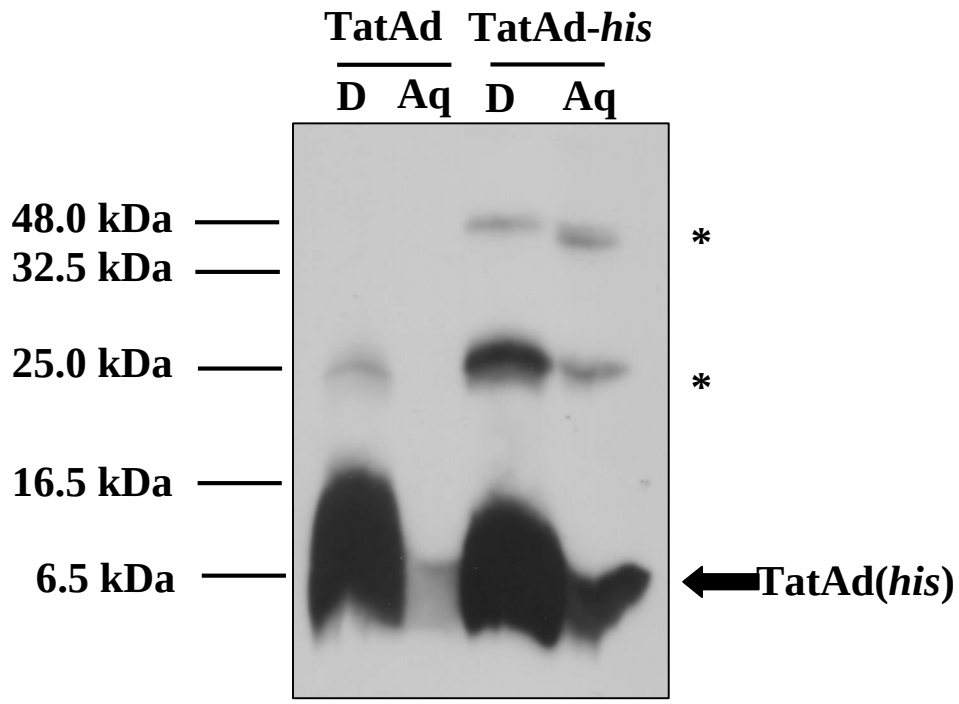

Figure 4.2.4 Triton X-114 phase separation to determine solubility of cytosolic TatAd and TatAd-*his* proteins.
E. coli ΔtatABCDE cells expressing TatAdCd from the pBAD24 plasmid were fractionated and cytosolic samples collected. TatAd-*his* was purified as described above. Samples were incubated with 1% Triton X-114 at 4 °C for ~ 30 minutes before incubation at 30 °C to separate detergent (D) and aqueous (Aq) phases. Phases were collected by centrifugation and samples analysed by SDS-PAGE and subsequent immunoblotting with anti-TatAd antibodies. The position of TatAd and TatAd-*his* is presented on the right whilst molecular weight markers are shown on the left. Some slower migrating bands are also present and these are indicated with *.

4.2.4 Gel filtration chromatography of cytosolic TatAd and TatAd-*his* complexes

The complexes formed by TatAd in the cytosol were analysed by gel filtration chromatography. *E. coli ΔtatABCDE* cells expressing TatAdCds or TatAd-*his* from the pBAD24 plasmid were fractionated and the cytoplasmic fraction collected. Cytoplasmic samples were applied directly to an equilibrated Superose-6 gel filtration column and protein eluted with a single column volume of buffer in 0.6 ml fractions. All fractions were applied to SDS-PAGE gels and gels subsequently immunoblotted with anti-TatAd antibodies (Figure 4.2.5A). Immunoblots were further analysed by densitometry and intensity of band plotted against fraction number. It should be noted that the intensities of the peaks in the graph cannot be directly compared due to differences in the background contrast between the two blots. (Figure 4.2.5B).

The immunoblot shows the TatAd-*his* protein eluting over fractions 27 -29 with a peak in fraction 28. Using the standard curve prepared in chapter 3 (Figure 3.2.10) the mass of the complex eluting in fraction 28 (16.8 ml) is estimated to be 93.5 kDa. This is similar to the size estimate of another study that found cytosolic TatAd-*his* to form homo-oligomeric complexes of between 150-250 kDa by sucrose density gradient centrifugation (Westermann *et al*., 2006).

Unexpectedly, the TatAd protein without a *his*-tag present has a completely different elution profile and elutes with a clear peak in fraction 14. Using the standard curve prepared in chapter 3, this complex can be estimated to have a mass of 3.7 MDa. The cytosolic TatAd protein is therefore forming very large complexes, or possibly aggregates for which a role in translocation cannot be assessed unambiguously. Whilst a *his*-tag on TatAd results in a massive difference in the nature of the cytosolic TatAd complex it causes no apparent difference to the nature of the membrane localised TatAd complex (3.2.7 & 3.2.9). The effect of a *his*-tag on the cytosolic TatAd complex makes this form of TatAd unsuitable for structural analysis.

Importantly despite the effect of the *his*-tag on the nature of the cytosolic TatAd complex, TatAd-*his* is active in *E. coli,* supporting translocation of the *E. coli* Tat substrate TMAO reductase when expressed in *E. coli ΔtatA/E* cells (chapter 6). This

provides further (but indirect) evidence that cytosolic TatAd is not required for translocation.

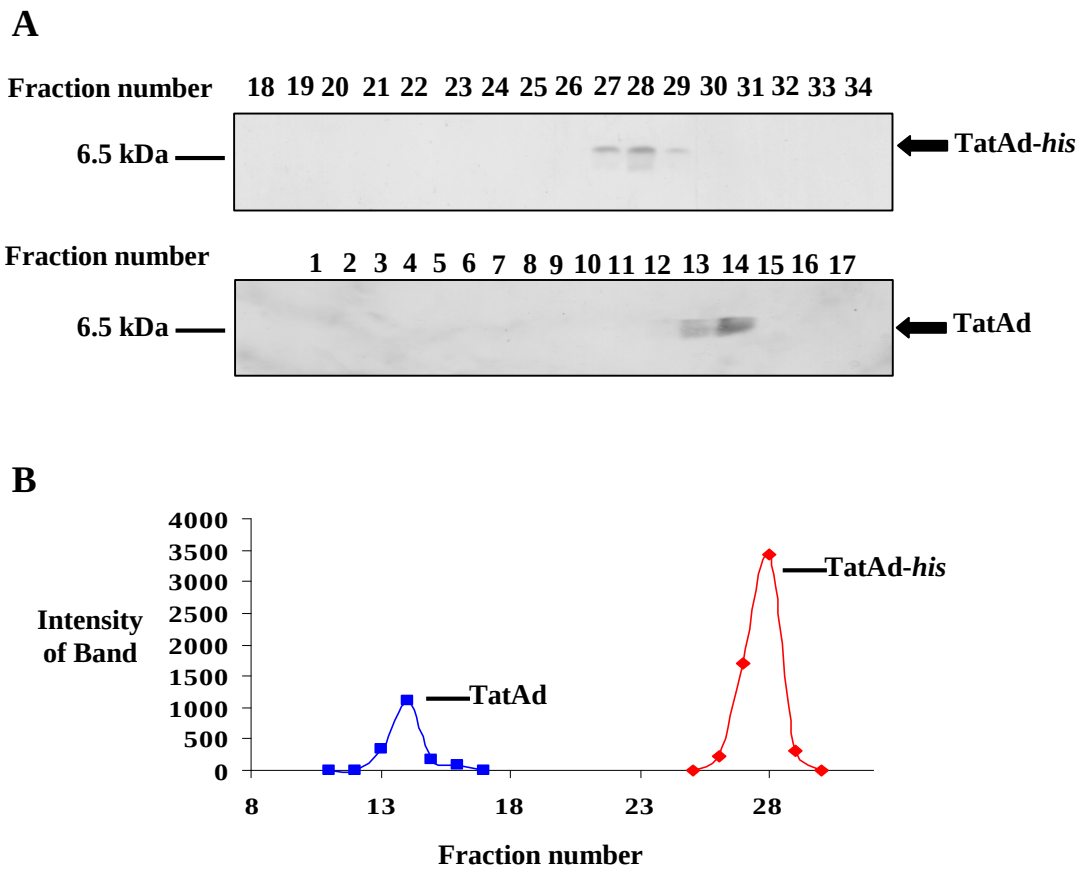

Figure 4.2.5 Gel filtration chromatography of cytosolic TatAd and TatAd-*his* complexes
E. coli ΔtatABCDE cells expressing either TatAdCd-*strep* or TatAd-*his* (from plasmids pBAdCds and pBAdh respectively) were fractionated, and cytoplasmic samples collected. Cytoplasmic samples were applied directly to an equilibrated Superose-6 gel filtration column and protein eluted with a single column volume of buffer in 0.6 ml fractions. **A.** All column fractions were immunoblotted with anti-TatAd antibodies and the peak elution fractions are shown. The position of TatAd is presented on the right whilst molecular weight markers are indicated at the left. **B.** Immunoblots were analysed by densitometry and the intensity of band plotted against fraction number. The elution profile of TatAd is shown in blue and TatAd-*his* in red.

4.3 Discussion

Since the identification of a soluble population of TatAd in *B. subtilis* a great deal of interest has been generated on the role, if any, of this population of TatAd in the Tat pathway. The discovery that soluble TatAd has affinity for the Tat substrate PhoD in *B. subtilis* (Pop *et al*., 2003) led to the suggestion that TatAd is acting as the initial receptor for Tat substrates. A further study by the same group found that cytosolic TatAd has affinity for membrane localised TatCd and it was suggested that the cytosolic TatAd is acting as a guidance factor targeting substrate to membrane localised TatCd (Schrieber *et al*., 2006). This model is completely different from the current *E. coli* model where substrates first interact with a TatBC complex in the membrane (Alami *et al*., 2003). This difference between *E. coli* and *B. subtilis* pointed to a completely different mechanism of Tat dependent translocation in Gram-negative and Gram-positive bacteria. In a further twist the Gram-positive bacterium S*treptomyces lividans* (which unlike most other Gram-positive bacteria has a TatABC type system), was found to have soluble populations of both its TatA and TatB proteins (De Keersmaeker *et al*., 2005).

Although there appeared to be a clear difference between Gram-positive and Gram-negative bacteria it was recently reported that a soluble population of TatA is also present in *E. coli* (Berthlemann *et al.,* 2008) that perhaps suggests that the Tat pathways of these two types of bacteria are more similar than previously thought. This would fit nicely with the data presented in Chapter 3 that shows the *B. subtilis* TatAdCd pathway can function in *E. coli* and translocate a number of *E. coli* Tat substrates.

The dual localisation of TatA is not just restricted to the bacterial Tat pathway. The plant homologue of TatA, Tha4, is present in the thylakoid membrane and also in the chloroplast stroma (Frielingsdorf *et al*., 2008). This stromal Tha4 was found to improve translocation efficiency. The authors of this particular study suggest that rather than acting as a soluble receptor for Tat substrates the soluble TatA may simply act an additional pool of free TatA that inserts into the membrane before exerting its function. The data presented in both this chapter and chapter 3 fit very well with this

idea. The Triton X-114 data demonstrates that cytoplasmic TatAd is not a genuinely soluble population of protein but it certainly could function as an additional pool of protein that inserts into the membrane where it fulfils its role. In addition the gel filtration data shows that whilst a *his*-tag has no effect on membrane localised TatAd complexes it causes a significant shift in the nature of the cytosolic TatAd-*his* complex. Despite this, the *his*-tag has no detectable effect on Tat function. Finally the TatAdCd pathway can translocate TorA in *E. coli*, this substrate not only has its own dedicated chaperone (TorD) in the cytoplasm but has been found to initially interact with membrane localised TatBC (Alami *et al*., 2002).

When taken together the data presented here and in the literature point to an overall conserved mode of action of Tat-dependent translocation between Gram-positive and Gram-negative bacteria with cytosolic TatA most likely representing a mis-localised population of protein or an additional pool of protein that inserts into the membrane before performing its function. Still, more direct experimental approaches are needed to determine unambiguously whether cytosolic TatA represents a truly functional population of protein or not. An *in vitro* translocation assay using *E. coli* inverted inner membrane vesicles would be useful in analysing any role for soluble TatA.

Chapter 5

Functional conservation between Gram-positive Tat systems

5.1 Introduction

Bacillus subtilis has two independent Tat pathways with different substrate specificities (Jongbloed *et al*., 2004). One of these pathways is the TatAdCd pathway that has been discussed in detail previously in this manuscript. The TatAdCd pathway has just a single identified substrate (PhoD) and is only expressed under particular growth conditions (phosphate limitation). Important differences between this pathway and the Tat pathway of the Gram-negative bacterium *Escherichia coli* were identified in chapter 3. The complete absence of any separate TatB component in most Gram-positive bacteria led to the idea that the TatA component in these systems was bifunctional, performing the roles of both *E. coli* TatA and TatB (Jongbloed *et al*., 2006). The finding in chapter 3 that the TatAdCd pathway can function in *E. coli* and translocate *E. coli* Tat substrates strongly supports that idea.

Within *E. coli* the three required Tat proteins form two main types of membrane localised complexes: a 370 kDa TatABC complex (Oates *et al*., 2005) involved in substrate recognition and binding (Alami *et al*., 2003), and separate TatA complexes that are recruited to the TatABC complex to form some kind of channel through which proteins are translocated. The TatA complex was found to vary significantly in mass (with a range of ~100 kDa to 500 kDa) (Oates *et al*., 2005). The different size TatA complexes may function by allowing a wide range of different sized folded substrates to cross the membrane whilst maintaining a tight seal. (Gohlke *et al*., 2005).

As described in chapter 3 the TatAd and TatCd proteins are organised somewhat differently to their *E. coli* counterparts. Like the TatABC systems of Gram-negative bacteria two separate Tat complexes are present within the membrane: a TatAdCd containing complex, and separate TatAd complexes. The TatAdCd complex was found to be considerably smaller than the *E. coli* TatABC complex; just 230 kDa compared to 350 kDa for *E. coli* (as judged by BN-PAGE). This may simply be due to the absence of any TatB component in *B. subtilis* or it might be a result of the TatAdCd complex containing a different number of TatCd and/or TatAd subunits (Barnett *et al*., 2008).

Another major difference concerns the nature of the separate TatA complex. Whilst *E. coli* TatA complexes exhibit a vast range of sizes, the separate TatAd complex is relatively homogeneous in comparison. This implies a mechanism involving a single defined translocon rather than a spectrum of size variants or a more complex mechanism perhaps involving the coalescence of several TatAd or TatAdCd complexes (Barnett *et al*., 2008).

The second minimal Tat system found in *B. subtilis* is encoded by the *tatAy* and *tatCy* genes. These two genes are constitutively expressed in an operon and a single substrate has been identified that is translocated by the TatAyCy pathway (YwbN, a DyP dependent peroxidase (Jongbloed *et al*., 2004)). Since important differences between the TatAdCd and the *E. coli* TatABC pathway have been identified, the TatAyCy pathway was investigated to determine whether the novel features of the TatAdCd system are unique, or if they represent a clear difference between Tat pathways of Gram-positive and Gram-negative bacteria.

The data presented in this chapter provide evidence for a conserved complex organisation in Gram-positive bacteria.

In addition, the clear specificity between TatAdCd and TatAyCy in terms of substrates translocated was further investigated. Evidence is presented that demonstrates similar substrate recognition requirements of TatAdCd and TatAyCy pathways.

5.2 Results

5.2.1 Translocation of TMAO reductase by TatAyCy in *E. coli*

It was shown previously in chapter 3 that the *B. subtilis* TatAdCd pathway can function in *E. coli* and translocate *E. coli* Tat substrates including TMAO reductase (TorA). Since TatAdCd and TatAyCy appear to have different substrate specificities, the ability of the TatAyCy pathway to translocate TorA in *E. coli* was also tested.

E. coli MC4100 cells, *ΔtatABCDE* cells and *ΔtatABCDE* cells expressing TatAdCd or TatAyCy from the pBAD24 plasmid were separated into Periplasm (P), Cytoplasm (C), and Membrane (M) fractions. Samples were subjected to native-PAGE and gels were stained blue with reduced methyl viologen. Upon addition of substrate (TMAO), the methyl viologen becomes oxidised and a clearing of the gel turbidity occurs in the presence of active TorA. Figure 5.2.1 shows that in MC4100 cells, TorA activity is correctly localised to the periplasm as visualised by the presence of a clear white band on the gel in the periplasmic lane. Translocation of TorA has therefore occurred as expected. In *ΔtatABCDE* cells no translocation has occurred as no clear white band is apparent in the periplasmic lane. A very faint band can be seen but this is likely to be due to contamination between lanes since repeated tests show TorA translocation is strictly Tat dependent. As an additional control *ΔtatABCDE* cells expressing TatAdCd were tested and confirming the findings presented in chapter 3, TorA activity is present in the periplasm as shown by a white band in the periplasmic lane. Finally when TatAyCy is expressed in *ΔtatABCDE* cells, no white band is visualised in the periplasmic lane and TorA activity is exclusively found in the cytoplasmic sample. The TatAyCy pathway is thus unable to translocate *E. coli* TorA.

This finding points to different substrate specificities between the TatAdCd and TatAyCy pathways, although the inability of TatAyCy to translocate TorA may be due to the TatAyCy proteins being unable to form an active translocation pathway in *E. coli*, rather than an inability to handle or recognise the TorA substrate. In order to address this point, the ability of TatAyCy system to translocate a substrate comprised of the TorA signal peptide fused to GFP was tested.

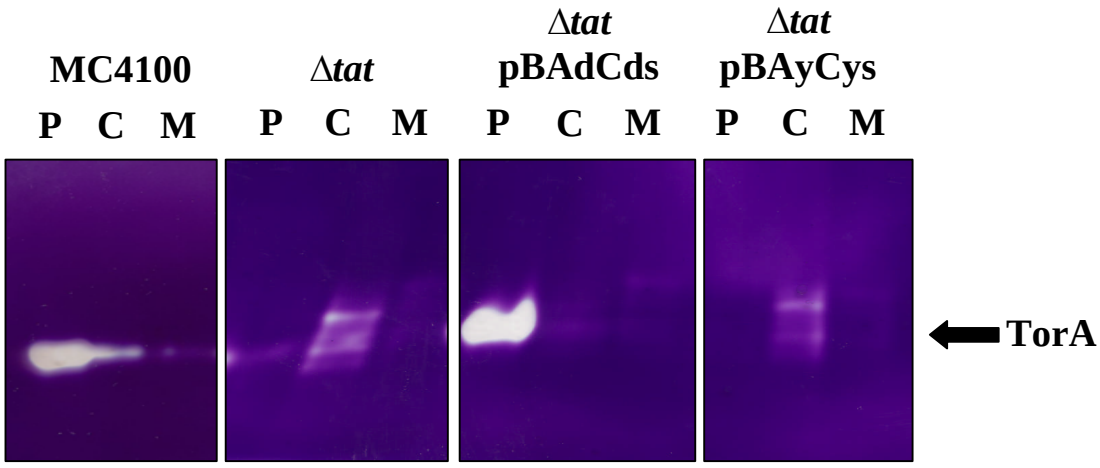

Figure 5.2.1 Translocation of TMAO reductase by TatAdCd and TatAyCy
E. coli MC4100 cells, *ΔtatABCDE* cells, and *ΔtatABCDE* cells expressing TatAdCd or TatAyCy from the pBAD24 plasmid were tested for translocation of TorA. Cellular proteins from the Periplasm (P), Cytoplasm (C), and Membrane (M) compartments were isolated and subjected to native-PAGE and the gel subsequently stained blue with reduced methyl viologen. Upon addition of TMAO, the methyl viologen becomes oxidised where TorA is present and a clearing of the gel turbidity occurs. The position of TorA is shown on the right of the figure by an arrow.

5.2.2 Translocation of TorA-GFP by TatAdCd and TatAyCy in *E. coli*

The TatAdCd pathway is not only able to translocate TMAO reductase in *E. coli* but also TorA-GFP (Chapter 3). Therefore the ability of the TatAyCy pathway to translocate TorA-GFP was tested. Briefly, TorA-GFP was expressed using plasmid pJDT1 in MC4100 cells, *ΔtatABCDE* cells and *ΔtatABCDE* cells expressing TatAdCd or TatAyCy from the compatible pEXT22 plasmid. Cellular proteins from the Periplasm (P), Cytoplasm (C), and Membrane (M) compartments were isolated and samples subjected to SDS-PAGE before immunoblotting with anti-GFP antibodies (Figure 5.2.2). A band corresponding to mature sized GFP is present on the blot in the periplasmic lane of wild-type *E. coli* cells indicating translocation has occurred as expected. Also as expected, no translocation of GFP to the periplasm in *ΔtatABCDE* cells is observed with GFP found exclusively in the cytosolic fraction. Accumulation of GFP in the cytoplasm is not observed and this is perhaps due to degradation of untranslocated GFP. As an additional control and confirming the finding that TatAdCd can translocate TorA-GFP, a mature sized GFP band is present in the periplasmic sample from cells expressing both pJDT1 and pEXT-AdCd plasmids. Finally, no GFP

is observed in the periplasm of cells over expressing TatAyCy alongside TorA-GFP indicating that the TatAyCy pathway is unable to translocate TorA-GFP. Again accumulation of untranslocated GFP is not seen in either the cytoplasmic or membrane compartments. A similar finding has been observed elsewhere and is probably a result of degradation of the untranslocated substrate (Barrett *et al*., 2003).

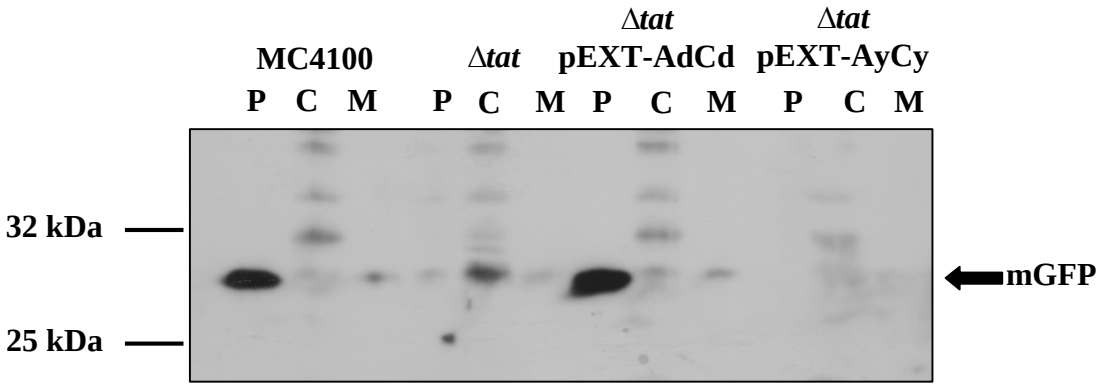

Figure 5.2.2 Translocation of TorA-GFP by TatAdCd and TatAyCy in *E. coli*
TorA-GFP was expressed using plasmid pJDT1 in MC4100 cells, *ΔtatABCDE* cells and in *ΔtatABCDE cells* expressing TatAdCd or TatAyCy from pEXT22 plasmids. Cellular proteins from the Periplasm (P), Cytoplasm (C), and Membrane (M) compartments were isolated. Samples from each fraction were applied to SDS-PAGE gels before immunoblotting with antibodies against GFP. The position of GFP is marked to the right and molecular weight markers shown on the left of the blot.

The inability of the TatAyCy pathway to translocate TorA-GFP was confirmed by confocal microscopy. *E. coli ΔtatABCDE* cells expressing TatAyCy from the pEXT22 plasmid and TorA-GFP from plasmid pJDT1 were observed under the confocal microscope using the 488 nm laser line (Figure 5.2.3). GFP fluorescence is seen throughout the cytoplasm with no halo of fluorescence seen around the periphery of the cell. MC4100 cells and *ΔtatABCDE* cells expressing TorA-GFP from the pJDT1 plasmid were also observed. As expected a halo of fluorescence is observed around the periplasm of wild-type cells whilst in *ΔtatABCDE* cells fluorescence is distributed throughout the cytoplasm. Some WT cells also appear to show an accumlation of GFP at the cell poles. In addition, *ΔtatABCDE* cells expressing both TatAdCd (from the pEXT22 plasmid) and TorA-GFP (from the pJDT1 plasmid) were observed as shown previously in chapter 3. GFP fluorescence here is localised to the periphery of the cell. Also as observed in previous experiments (chapter 3) some variation is observed

between cells with some cells displaying a higher level of GFP flouresence than others.

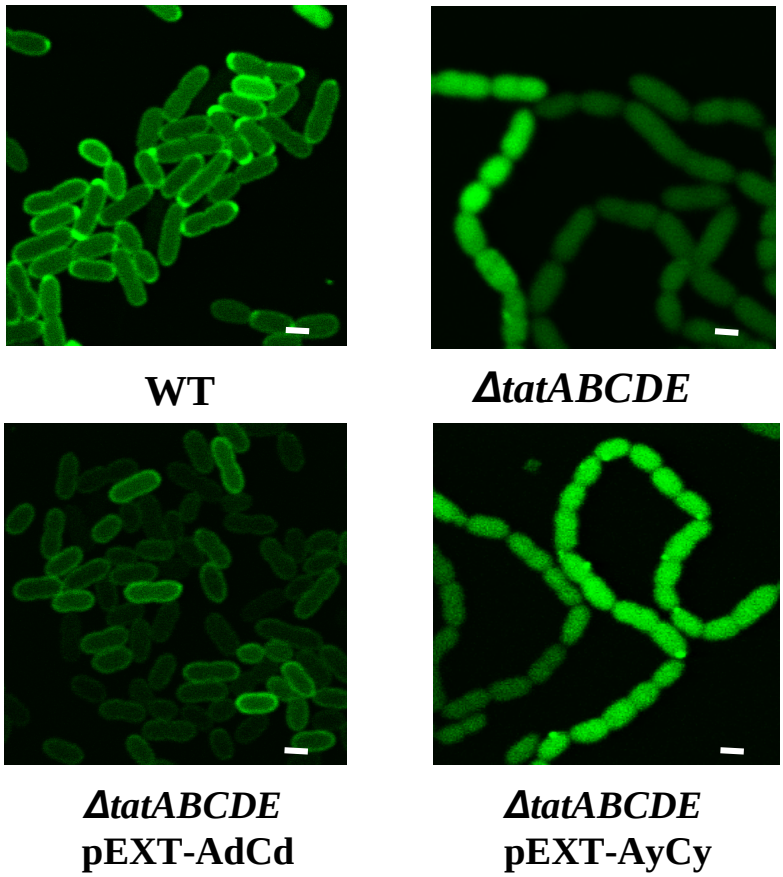

Figure 5.2.3 Translocation of TorA-GFP by TatAdCd and TatAyCy

Plasmid pJDT1 expressing TorA-GFP was expressed in MC4100 cells, *ΔtatABCDE* cells and *ΔtatABCDE* cells expressing TatAdCd or TatAyCy (from compatible pEXT22 plasmids). Cells were examined using confocal microscopy with the 488nm laser line. The scale bar represents 1µm. All experiments were performed in duplicate and a reprentative sample is shown.

5.2.3 Translocation of *E. coli* AmiA and AmiC by the TatAyCy pathway

E. coli Δtat cells exhibit a mutant phenotype where the cells grow in long chain-like filaments. This filamentous phenotype was found to result from the mis-localisation of AmiA and AmiC (two cell wall amidases required for cell division). Both AmiA and AmiC have been found to be *E. coli* Tat substrates (Ize *et al*., 2003; Bernhardt and de

Boer, 2003). In chapter 3 it was found that expression of TatAdCd using pEXT22 plasmids in *E. coli ΔtatABCDE* cells can complement the mutant phenotype and this is also shown above in Figure 5.2.3. *E. coli ΔtatABCDE* cells expressing pEXT-AdCds are seen as single and dividing cells. In contrast when *E. coli ΔtatABCDE* cells expressing pEXT-TatAyCys are observed under the microscope the cells are still visible in long chain like filaments providing indirect evidence that the TatAyCy pathway is unable to translocate AmiA and AmiC of *E. coli*.

5.2.4 Translocation of DmsA-GFP by the TatAdCd and TatAyCy pathways.

There are two possible explanations why the TatAyCy pathway is unable to translocate TorA and TorA-GFP in *E. coli.* Firstly the TatAyCy pathway might simply be inactive when expressed in an *E. coli* background. Secondly it might be because the TatAyCy pathway is active in *E. coli* but unable to handle the two substrates tested. In the latter case this may result from an inability of TatAyCy to recognise the TorA signal peptide, or an inability of the TatAyCy system to accommodate the passenger proteins (TorA and GFP). To try and answer these points the ability of the TatAyCy pathway to translocate another substrate was tested. The substrate chosen was a fusion of the dimethyl sulfoxide reductase (DmsA) signal peptide and GFP. DmsA has been confirmed as a Tat substrate in *E. coli* and DmsA-GFP was previously shown to be translocated by Tat (Ray *et al*., 2003). DmsA-GFP was expressed using pBAD24 plasmids in MC4100 cells, *ΔtatABCDE* cells and *ΔtatABCDE* cells expressing TatAdCd or TatAyCy from the compatible pEXT22 plasmid. Cellular proteins from the Periplasm (P), Cytoplasm (C), and Membrane (M) compartments were isolated and samples run on SDS-PAGE gels that were immunoblotted with anti-GFP antibodies. The data is shown in Figure 5.2.4. A mature sized GFP band can be seen on the periplasmic lane of the blot for MC4100 cells indicating translocation as expected. No periplasmic GFP is observed in *ΔtatABCDE* cells exactly as expected given the strict Tat-dependence of DmsA export. In the *ΔtatABCDE* cells, although translocation does not occur, accumulation of cytosolic DmsA-GFP is not apparent. This has been seen before and is likely due to degradation of the untransported precursor protein (Ray *et al*., 2003). In *ΔtatABCDE* cells expressing both DmsA-GFP and either TatAdCd or TatAyCy, a mature sized GFP band is present in the

periplasmic lanes of the immunoblot indicating translocation of GFP by both TatAdCd and TatAyCy pathways. The TatAyCy pathway is therefore able to form an active translocation pathway in *E. coli* and translocate GFP.

In the membrane lanes of the immunoblot of WT MC4100 cells expressing DmsA-GFP, and in *ΔtatABCDE* cells expressing both DmsA-GFP and either TatAdCd or TatAyCy, a strong precursor sized band is apparent. This band is not observed in the corresponding lane for *ΔtatABCDE* cells indicating that it might represent a population of substrate protein that is interacting with the Tat machinery but remains untransported, perhaps due to saturation of the Tat translocases. In support of this idea in cells where Tat proteins are over expressed (lanes *Δtat* pEXT-AdCd and *Δtat* pEXT-AyCy) a much stronger band is observed compared to WT cells that contain fewer Tat translocases.

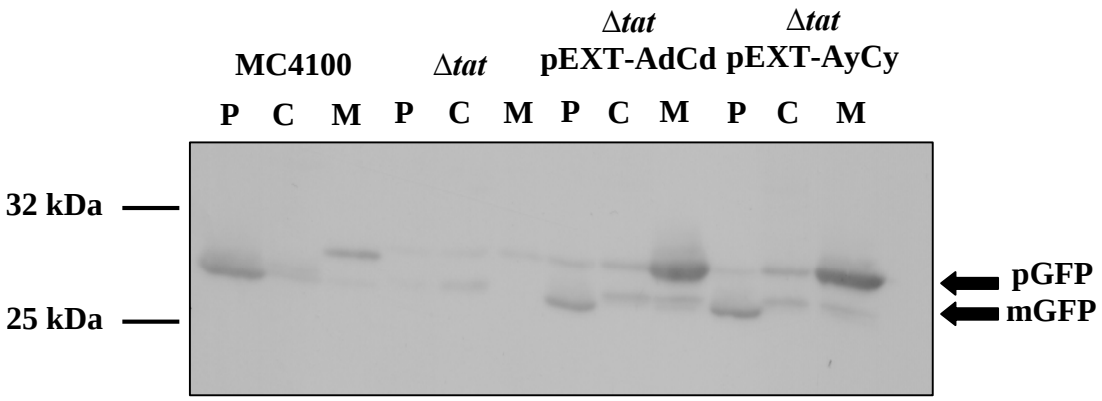

Figure 5.2.4 Translocation of DmsA-GFP by TatAdCd and TatAyCy
DmsA-GFP was expressed using pBAD24 plasmids in *E. coli* MC4100 cells, *ΔtatABCDE* cells, and in *ΔtatABCDE cells* expressing TatAdCd or TatAyCy from pEXT22 plasmids. Cellular proteins from the Periplasm (P), Cytoplasm (C), and Membrane (M) compartments were isolated. Samples from each fraction were analysed by SDS-PAGE followed by immunoblotting with antibodies to GFP. The positions of precursor (pGFP) and mature (mGFP) GFP forms are marked at the right. Molecular weight markers are shown to the left.

5.2.5 DmsA-GFP precursor accumulates at the *E. coli* membrane in the presence of Tat

The membrane associated DmsA-GFP precursor protein identified above (5.2.3) was investigated further by analysing the stability of the protein over time. DmsA-GFP was expressed from the pBAD24 plasmid by induction with 200 µM arabinose for 2 hours in both *E. coli* MC4100 and *ΔtatABCDE* cells. After 2 hours of induction the cells were harvested, washed, and then resuspended using growth medium without arabinose present. Cells were then grown for a further 3 hours. Samples of the cultures were taken every hour during the experiment, fractionated and membrane samples collected. Membranes were run on SDS-PAGE gels before immunoblotting with anti-GFP antibodies. The results are presented in Figure 5.2.5. The immunoblot shows that after 2 hours of induction in both backgrounds a large population of DmsA-GFP precursor is found to be associated with the membrane. After induction was stopped at 2 hours, the DmsA-GFP protein remained largely stable and a significant proportion was still present after the total 5 hours of the experiment in wild-type cells. In contrast after induction of the pBAD-DmsA-GFP plasmid was stopped (at 2 hours) in *ΔtatABCDE* cells, the level of DmsA-GFP protein associated with the membrane decreased until after the total 5 hours of the experiment very little was remaining. Since the precursor form of DmsA-GFP only remains stably associated with the membrane when Tat is present it seems likely that this protein is directly interacting with the Tat machinery and perhaps represents a population of protein that remains untranslocated due to saturation of the Tat translocases.

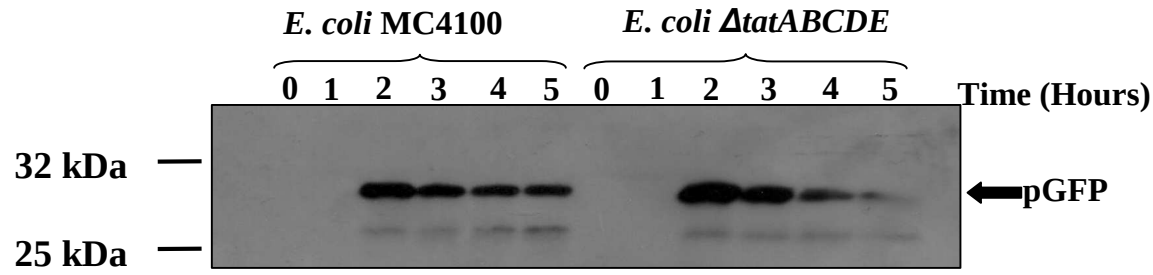

Figure 5.2.5 Stability of membrane associated DmsA-GFP
Plasmid pBAD-DmsA-GFP carried by *E. coli* MC4100 and *ΔtatABCDE* cells was induced for two hours with 200 µM arabinose before induction was stopped by washing cells in fresh growth medium without arabinose. Cells were then grown for a further 3 hours without induction of the plasmid. Every hour during the experiment samples of the culture were taken and cells fractionated. Membrane fractions were analysed by SDS-PAGE and immunoblotting with anti-GFP antibodies. The position of the precursor form of DmsA-GFP (pGFP) is shown to the right of the figure. Molecular weight markers are shown on the left.

5.2.6 Translocation of MdoD-GFP and AmiA-GFP by TatAdCd and TatAyCy

Given the strict substrate specificity between the TatAdCd and TatAyCy pathways in *B. subtilis* it was surprising that both pathways were found to be able to translocate DmsA-GFP in *E. coli*. The specificity between these two pathways was therefore investigated further using two other substrates. MdoD and AmiA have both been identified as Tat substrates in *E. coli* (Ize *et al*., 2003; Lequette *et al*., 2004). AmiA has been mentioned previously in this manuscript, it is a cell wall amidase required for cytokinesis, whilst MdoD is involved in the formation of periplasmic glucan backbone structures. These are extensively branched oligosaccharides that form in the periplasm in response to the low osmorality of the growth medium (Lequette *et al*., 2004). As both the TatAdCd and TatAyCy pathways can translocate GFP, fusions of the signal peptides of these two Tat substrates and GFP were used. Plasmids pBAD-MdoD-GFP or pBAD-AmiA-GFP were expressed in MC4100 cells, *ΔtatABCDE* cells, and *ΔtatABCDE* cells expressing TatAdCd or TatAyCy using compatible pEXT22 plasmids. After induction from both plasmids cellular proteins from the Periplasm (P), Cytoplasm (C), and Membrane (M) compartments were isolated. Cell fractions were subjected to SDS-PAGE and gels immunoblotted with anti-GFP antibodies. The results of the MdoD-GFP translocation assay are shown in Figure 5.2.6A and the

results of the AmiA-GFP translocation assay in Figure 5.2.6B. In both cases a mature sized GFP band can be visualised in the periplasmic lane of the gel for MC4100 cells indicating export. This is important as it is the first time that export of MdoD-GFP and AmiA-GFP by the *E. coli* Tat pathway has been demonstrated. Confirming the strict Tat dependence of these two substrates, in *ΔtatABCDE* cells no GFP is observed in the lanes of the immunoblot corresponding to the periplasmic samples and no translocation has occurred. Some protein is observed in the cytoplasmic lanes that may represent the precursor form of the subsrate and processed forms are also present. The significance of these additional processed bands is not clear but substrate does not appear to accumulate. This is essentially the same as seen with other substrates tested (DmsA-GFP and TorA-GFP) and is most probably due to non-specific degradation of untransported substrate. In *ΔtatABCDE* cells expressing TatAdCd or TatAyCy plus either one of the two substrates being tested, a mature sized GFP band is clearly visible in the periplasmic lanes of the immunoblot; thus demonstrating that both the TatAdCd and TatAyCy pathways can translocate MdoD-GFP and AmiA-GFP in *E. coli.*

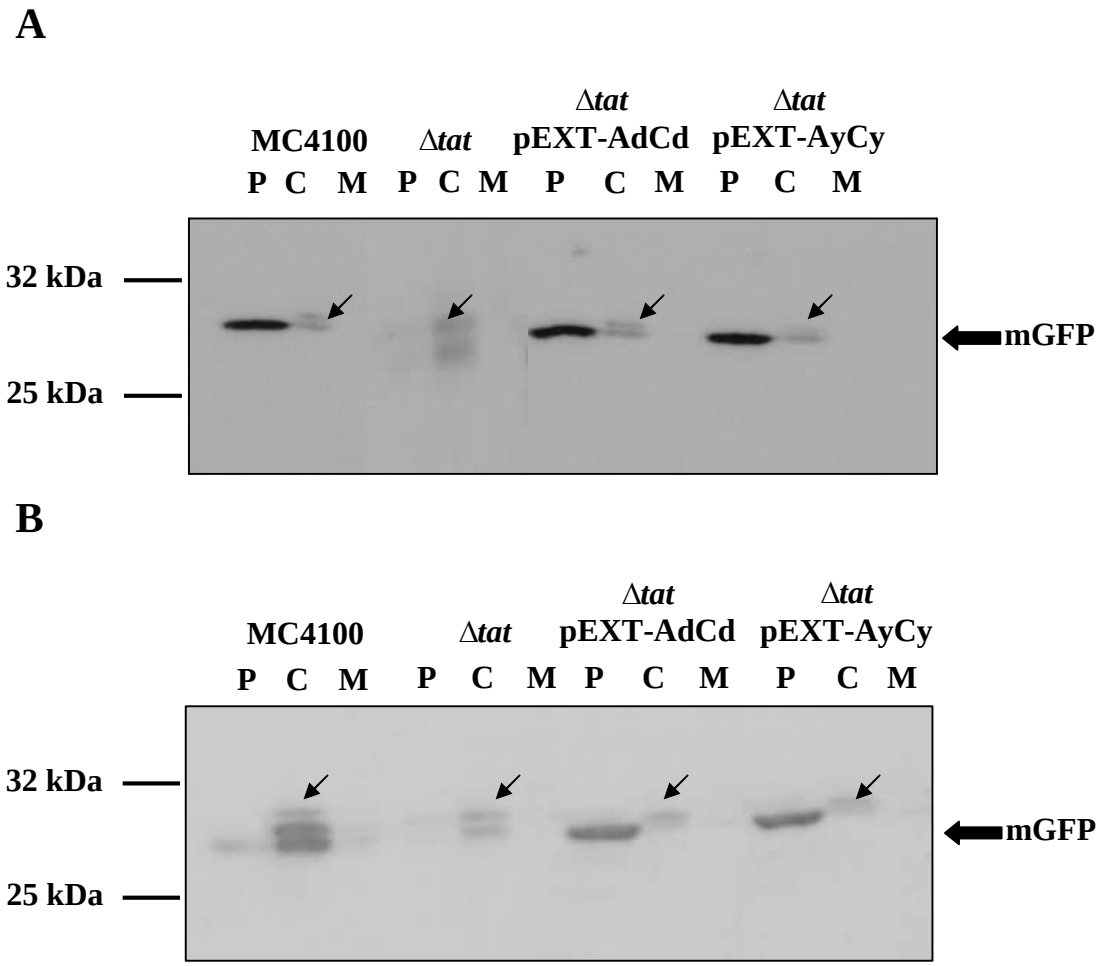

Figure 5.2.6 Translocation of MdoD-GFP and AmiA-GFP by TatAdCd and TatAyCy

A. MdoD-GFP or **B**. AmiA-GFP was expressed using pBAD24 plasmids in MC4100 cells, *ΔtatABCDE* cells and in *ΔtatABCDE cells* expressing TatAdCd or TatAyCy from pEXT22 plasmids. Cellular proteins from the Periplasm (P), Cytoplasm (C), and Membrane (M) compartments were isolated. Samples from each fraction were analysed on SDS-PAGE gels and gels immunoblotted using antibodies against GFP. The position of GFP is marked to the right (mGFP) and molecular weight markers shown to the left. Slower migrating bands that may represent the precursor form of the protein in the cytoplasmic fractions is marked by arrows.

5.2.7 Translocation of *E. coli* SufI

SufI is an *E. coli* Tat substrate that is thought to be involved in cell division (Samaluru *et al*., 2007; Stanley *et al*., 2000). Translocation of this substrate by the TatAdCd and TatAyCy pathways was investigated. *E. coli* MC4100 cells, *ΔtatABCDE* (*Δtat*) cells and *ΔtatABCDE* cells expressing either TatAdCd or TatAyCy proteins from plasmids pBAdCds and pBAyCys respectively were separated into Periplasm (P), Cytoplasm (C), and Membrane (M) samples. Fractions were run on SDS-PAGE gels and subsequently blotted using anti-SufI antibodies for the immunodetection. The data presented in Figure 5.2.7 shows a ~50 kDa band in the periplasmic lane of MC4100 cells showing efficient translocation of this substrate as expected. Also as expected, no translocation is occurring in *Δtat* cells as no SufI is detectable in the periplasmic lane. Expression of TatAdCd or TatAyCy in *E. coli Δtat* cells fails to complement for translocation of SufI. This substrate is clearly not translocated by either of the *B. subtilis* Tat pathways. Within the cytosolic lanes of the immunoblot 3 bands are observed but the significance of these bands is not clear. It seems likely that one of these bands represents the untranslocated precursor form of SufI.

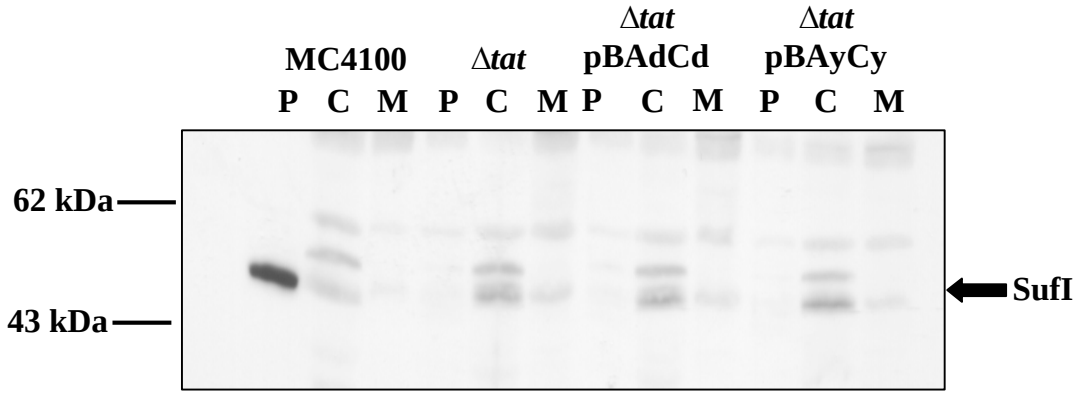

Figure 5.2.7 Translocation of SufI by TatAdCd and TatAyCy
E. coli MC400, *ΔtatABCDE* (*Δtat*), and *Δtat* cells expressing TatAdCd or TatAyCy from pBAdCds and pBAyCys plasmids were separated into Periplasm (P), Cytoplasm (C), and Membrane (M) samples. Samples were analysed by SDS-PAGE and subsequent immunoblotting with anti-SufI antibodies. The position of SufI is indicated to the right and molecular weight markers shown to the left.

5.2.8 Affinity chromatography of TatAyCys

In Chapter 3, the organisation of the TatAd and TatCd proteins were investigated using affinity chromatography. The data show that these proteins form two types of complexes in the plasma membrane; a TatAdCd containing complex and separate TatAd complexes. This result was essentially the same as a similar study in *E. coli* that identified TatABC complexes and separate TatA complexes (Bolhuis *et al*., 2000). In this chapter the organisation of TatAy and TatCy proteins into complexes within the membrane was also analysed by affinity chromatography.

As in previous experiments, the affinity chromatography was performed using a C-terminal *strep*-tag II on the TatC component. *E. coli ΔtatABCDE* cells expressing TatAyCys from plasmid pBAyCys were fractionated and membranes collected. Membranes were solubilised in buffer containing 2 % digitonin before being applied to an equilibrated 4 ml Streptactin^{TM} affinity column (that specifically binds the *strep*-tag II on TatCy). To remove unbound protein the column was washed using 4 x 4 ml of equilibration buffer. Tightly bound protein was eluted in equilibration buffer supplemented with 3 mM desthiobiotin (a biotin derivative that competes for binding to the Streptactin resin) in 6 x 2 ml fractions. All column fractions were analysed by SDS-PAGE and blotting using antibodies to the *strep*-tag II on TatCy and against TatAy for immunodetection. The results are presented in Figure 5.2.8. The anti-*strep* tag II immunoblot indicates that most of the protein bound to the column as very little is detectable in the flow-through (FT) or wash fractions. The TatCy-*strep* then specifically eluted from the column over fractions 2-4 with a peak in fraction 3. The anti-TatAy immunoblot shows a small amount of TatAy co-eluting with TatCy indicating the presence of a TatAyCy-containing complex within the membrane. Most of the TatAy protein is present in the column flow-through and first two wash fractions and had not bound to the column. This suggests the presence of separate TatAy complexes within the membrane and is consistent with similar experiments on the Tat systems from a number of other organisms where two types of membrane-localised Tat complexes are present. A TatABC or TatAC complex and separate TatA complexes (Barnett *et al*, 2008; Bolhuis *et al*, 2000; Oates *et al*, 2003).

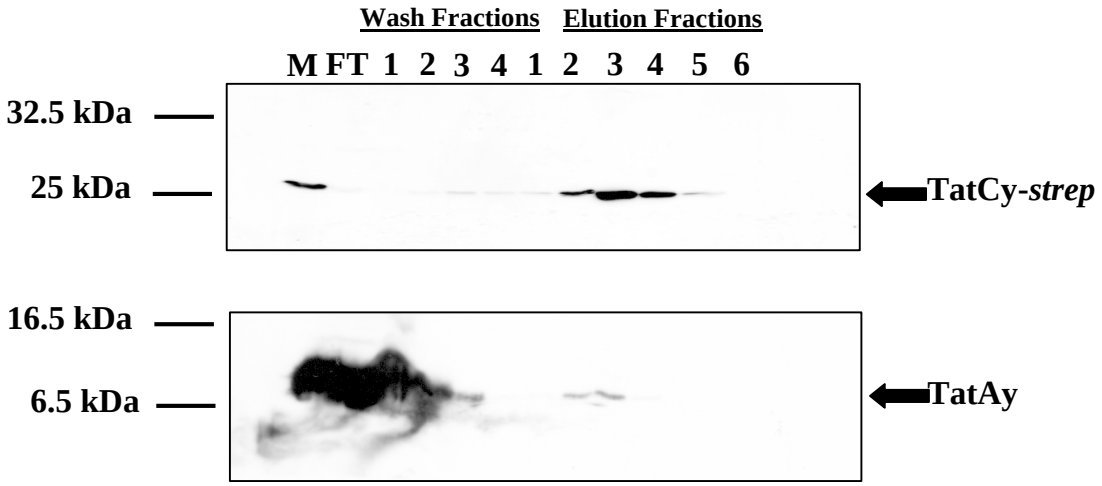

Figure 5.2.8 Affinity chromatography of TatAyCy
E. coli membranes were isolated from *ΔtatABCDE* cells expressing TatAyCy from plasmid pBAyCys. Membranes (M) were solubilised with the detergent digitonin before application to an equilibrated Streptactin™ affinity column and the flow-through (FT) sample collected. Unbound protein was washed through the column with 4 x 4 ml of equilibration buffer before protein was eluted in 6 x ½ column volumes of elution buffer. All column fractions were analysed by SDS-PAGE and blotting with specific antibodies to the *strep*-tag II on TatCy and to TatAy for the immunodetection. The positions of TatCy-*strep* and TatAy are presented to the right. Molecular weight markers are indicated to the left.

The purity of the isolated TatAyCy complexes was determined using SDS-PAGE and subsequent silver staining of the three peak elution fractions from the Streptactin™ affinity column above. The data is presented in Figure 5.2.9. Aside form the TatAy and TatCy bands, a few slower migrating bands are present on the gel but the TatAyCy protein is relatively pure after application to just a single column.

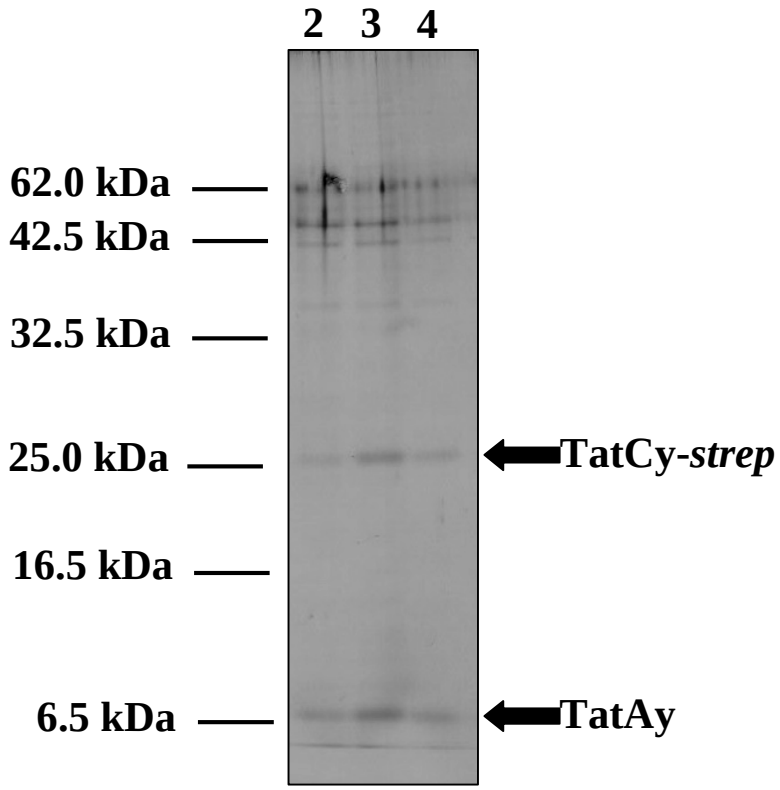

Figure 5.2.9 Silver stain of affinity purified TatAyCys complexes
Samples from the 3 peak elution fractions from the Streptactin™ affinity column above (Fig. 5.2.8) were ran on an SDS-PAGE gel that was subsequently stained with silver. The positions of TatCy-*strep* and TatAy are presented to the right and molecular weight markers are shown on the left.

5.2.9 Gel filtration chromatography of TatAyCy and TatAy complexes

Affinity purified TatAyCys was subjected to gel filtration chromatography to obtain an estimate of complex size. Purified TatAyCys was applied directly to an equilibrated Superose-6 gel filtration column and eluted with a single column volume of buffer in 0.6 ml fractions. The detergent digitonin was used throughout to allow direct comparison with *E. coli* TatABC and *B. subtilis* TatAdCd complexes that were analysed in the same way. All fractions eluted from the column were immunoblotted with antibodies against the *strep*-tag II on TatCy and against TatAy (Figure 5.2.10A). The figure shows TatCy-*strep* eluting over fractions 20-28 with a peak in fraction 25 (15 ml). A small amount of TatAy is co-eluting with the TatCy protein confirming that TatAy and TatCy are tightly associated in a TatAyCy complex. Using the calibration curve in chapter 3 the mass of the TatAyCy complex can be estimated to be ~ 200

kDa; even smaller than the TatAdCd complex that was found to be ~ 350 kDa in mass when analysed in the same way. The small size of the TatAdCd complex was surprising since the TatABC complex of *E. coli* was found to be ~ 600 kDa when analysed by gel filtration using the detergent digitonin. The fact that the TatAyCy complex is also considerably smaller than the *E. coil* TatABC complex suggests that this might be a conserved characteristic of Tat complexes in Gram-positive bacteria and a clear difference to the TatABC complexes of Gram-negative bacteria. The anti-*strep* immunoblot was further analysed by densitometry and the intensity of bands plotted against fraction number (Figure 5.2.10B). The graph shows the complex eluting as a relatively homogeneous species from the gel filtration column.

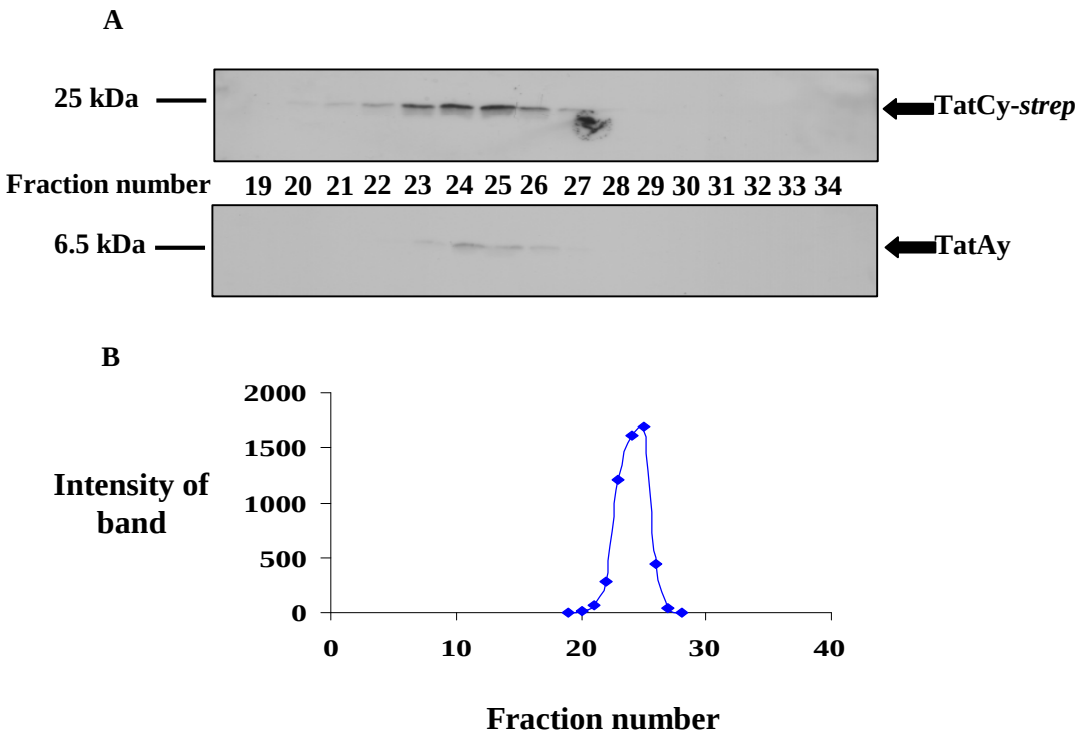

Figure 5.2.10 Gel filtration chromatography of purified TatAyCy complexes.
A. Affinity purified TatAyCys was applied directly to an equilibrated Superose-6 column. Elution of protein was performed using a single column volume of equilibration buffer in 0.6 ml fractions. All column fractions were analysed by SDS-PAGE and Western blotting using antibodies to the *strep*-tag II on TatCy and to TatAy for immunodetection. The positions of TatCy-*strep* and TatAy are presented to the right and molecular weight markers shown on the left.
B. Immunoblots were further analysed by densitometry and intensity of band plotted against fraction number.

5.2.10 Circular Dichroism spectroscopy of purified TatAyCy complexes

In chapter 3, Circular Dichroism (CD) spectroscopy was exploited in order to compare the secondary structural features of *E. coli* TatABC and *B. subtilis* TatAdCd complexes (3.2.12). Both complexes gave similar spectra, displaying minima at 208 and 222 nm indicating a structure rich in alpha-helices. Here CD spectroscopy was also performed on purified TatAyCy complexes as described in chapter 2. The figure (5.2.11) shows a spectrum that is also typical of a structure rich in alpha-helices with minima at 208 nm and 222 nm and rising to a maxima at 190 nm. All three Tat complexes are therefore very similar in terms of overall secondary structure.

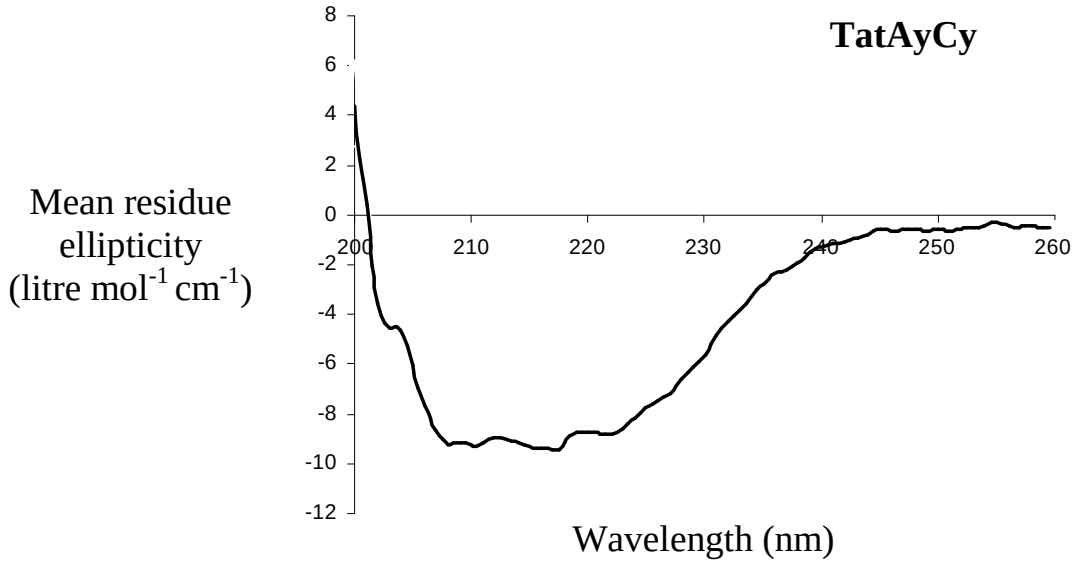

Figure 5.2.11 Circular Dichroism spectra of purified TatAyCys
Purified *B. subtilis* TatAyCy was used to obtain CD spectra over wavelengths of 200 – 260 nm using a Jasco J-185 spectrophotometer as described in chapter 2 (2.11). The spectrum shown is an average taken from 8 consecutive scans.

5.2.11 Gel filtration chromatography of membrane localised TatAy complexes

The *E. coli* TatA complex is highly heterogeneous in nature, ranging from 100 kDa to 500 kDa in mass, (Oates *et al*., 2005). In contrast the TatAd complex of *B. subtilis* was found to be highly homogeneous in nature (Barnett *et al*., 2008). To establish whether the homogeneity of TatAd complex is a unique feature of the TatAdCd pathway or common to other Tat pathways of Gram-positive bacteria, the TatAy complex was further analysed. The flow-through and wash fractions from the Streptactin^{TM} affinity column above (5.2.8) that contained the free TatAy protein were pooled and analysed using size exclusion chromatography. Sample was loaded directly onto a Superose-6 column as in previous experiments and protein eluted with a single column volume of equilibration buffer in 0.6 ml fractions. All column fractions were applied to SDS-PAGE gels before immunoblotting with anti-TatAy antibodies (Figure 5.2.12A). The immunoblot was further analysed by densitometry and intensity of band plotted against fraction number (Figure 5.2.12B).

The immunoblot shows the TatAy protein eluting over fractions 20 – 30 with a peak in fraction 25. This corresponds to an elution volume of 15 ml and using the calibration curve generated in chapter 3 gives a mass estimate of ~200 kDa. This is slightly smaller than the TatAd complex that was estimated to be ~ 270 kDa when analysed in the same way under identical conditions. The graph (Figure 5.2.11B) shows that although not as homogeneous as the TatAd complex, the TatAy complex is still eluting as a relatively tight peak when compared to *E. coli* TatA. It seems that the small homogeneous nature of the TatAd complex may be a common feature of TatA complexes from Gram-positive bacteria.

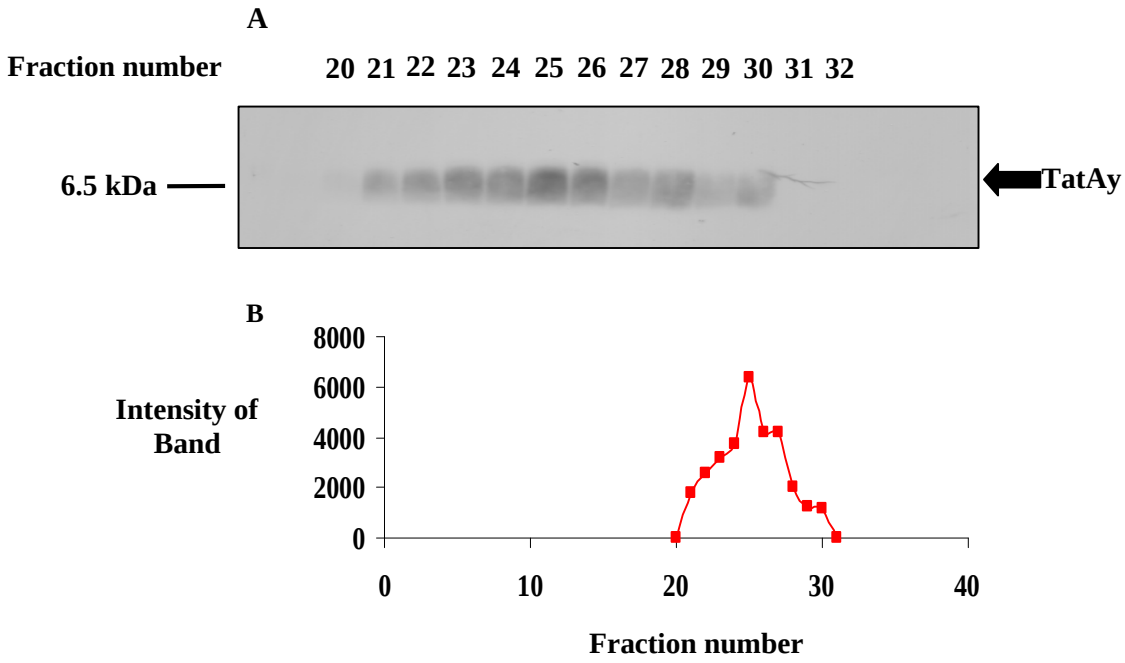

Figure 5.2.12 Gel filtration chromatography of membrane localised TatAy complexes.
A. Free TatAy was prepared by applying *E. coli* membranes from *ΔtatABCDE* cells expressing TatAyCys from plasmid pBAyCys to a Streptactin™ affinity column. Whilst TatAyCys complexes bound the column free TatAy was present in the flow-through and wash fractions (5.2.8). These fractions were pooled and applied directly to an equilibrated Superose-6 column. Elution of protein was achieved with a single column volume of buffer in 0.6 ml fractions. All column fractions were applied to SDS-PAGE gels and immunoblotted using anti-TatAy antibodies. The position of TatAy is indicated to the right and molecular weight markers shown to the left.
B. The immunoblot was further analysed by densitometry and intensity of band plotted against fraction number.

5.2.12 Gel filtration chromatography of the *Listeria monocytogenes* TatA complex

The data presented above point to a clear difference in TatA complex heterogeneity between Gram-negative and Gram-positive bacteria. However the two Gram-positive TatA complexes analysed above (TatAd and TatAy) were from the same organism, (*B. subtilis*). To further investigate whether the homogeneous nature of the TatA complex is a common feature of Tat systems from Gram-positive bacteria the TatA complex from a different organism, *Listeria monocytogenes*, was analysed by gel filtration chromatography.

Rene van der Ploeg from the University of Groningen, The Netherlands, supplied *E. coli* membranes solubilised in the detergent dodecyl maltoside. These membranes had been isolated from *E. coli* cells expressing *L. monocytogenes* TatA-*his* from plasmid pET-tatA-Lmo. Membranes were applied to an equilibrated gel filtration column (Superose-6) and elution of protein was achieved with a single column volume of buffer in 0.6 ml fractions. All column elution fractions were analysed by SDS-PAGE and Western blotting using antibodies against the 6 x histidine tag on the TatA protein for immunodetection. The immunoblot showing the peak elution fractions is presented in Figure 5.2.13A. The TatA-*his* protein is eluting over fractions 24-30 with a peak in fraction 27. This corresponds to an elution volume of 16.2 ml. Using the calibration curve in Chapter 3 the mass of the *L. monocytogenes* TatA complex is estimated to be ~120 kDa. This estimate is slightly smaller than the *B. subtilis* TatAd-*his* complex that when analysed under identical conditions in the detergent dodecyl maltoside gave an estimate of ~160 kDa (Barnett *et al*., 2008). The immunoblot was further analysed by densitometry and intensity of band plotted against fraction number (Figure 5.2.13B). The graph shows the *L. monocytogenes* TatA complex just like the *B. subtilis* TatAd and TaAy complexes is eluting as a relatively tight peak. This further suggests that in contrast to Gram-negative bacteria, the TatA complexes of Gram-positive bacteria are both relatively small and homogeneous in nature.

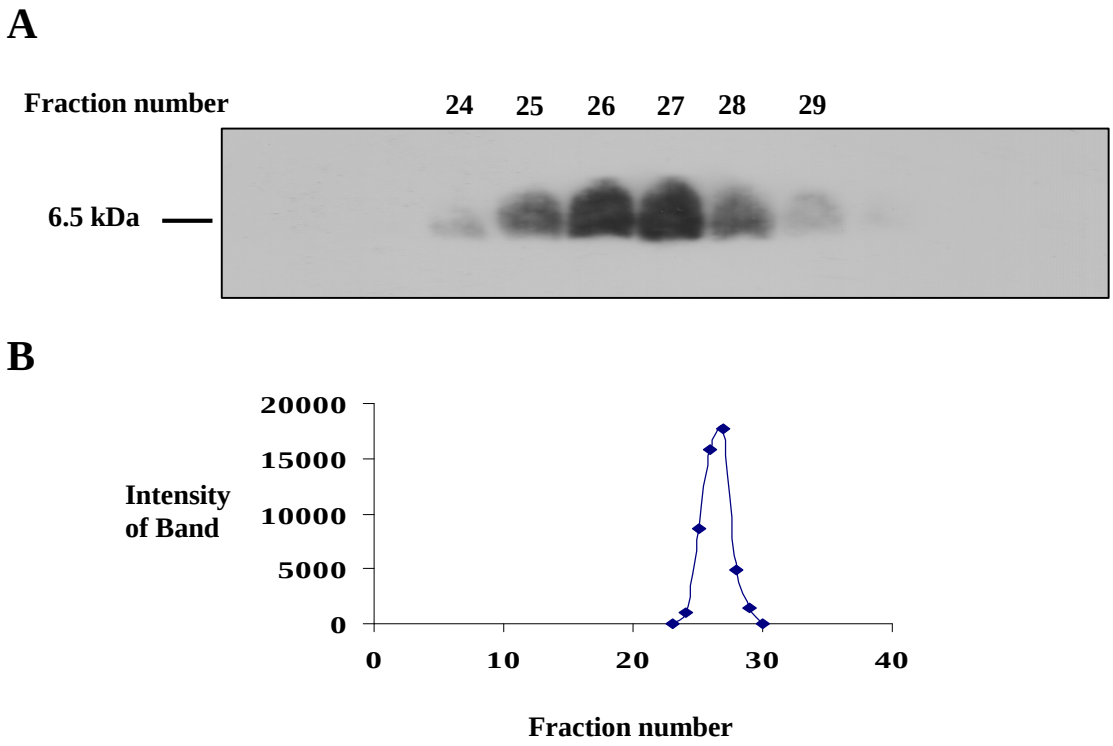

Figure 5.2.13 Gel filtration chromatography of *L. monocytogenes* TatA-*his*
A. *E. coli* membranes were isolated from *ΔtatABCDE* cells expressing *L. monocytogenes* TatA-*his* from plasmid pET-tatA-Lmo. Membranes were solubilised using the detergent dodecyl maltoside and applied directly to an equilibrated gel filtration column (Superose-6). Elution of protein was achieved with a single column volume of buffer in 0.6 ml fractions and all fractions were applied to SDS-PAGE gels before Western blotting using antibodies to the 6-histidine tag that was present on the C-terminus of TatA for immunodetection. The 6.5 kDa molecular weight marker is indicated to the left of the figure.
B. The immunoblot was further analysed by densitometry and intensity of band plotted against fraction number.

5.2.13 Localisation of TatAy

E. coli TatA and *B. subtilis* TatAd are localised to both the plasma membrane and the cytoplasm. Here the localisation of *B. subtilis* TatAy was determined. *E. coli ΔtatABCDE* cells were cultured with expression of TatAyCy proteins from plasmid pBAyCys. Cellular proteins from the Cytoplasm (C), and Membrane (M) compartments were isolated and samples were run on an SDS-PAGE gel that was immunoblotted using antibodies against TatAy (Figure 5.2.14). Just like *E. coli* TatA and *B. subtilis* TatAd, TatAy is localised to both membrane and cytoplasmic fractions.

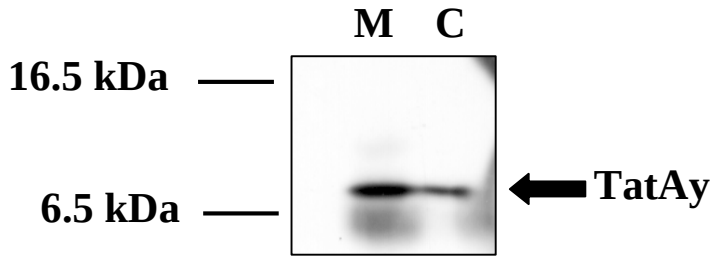

Figure 5.2.14 Localisation of TatAy
E. coli ΔtatABCDE cells expressing TatAyCy from plasmid pBAyCys were fractionated into cytoplasmic (C) and membrane (M) fractions. Cell fractions were run on an SDS-gel that was subsequently immunoblotted using antibodies against TatAy. The position of TatAy is presented to the right and molecular weight markers are presented to the left.

5.2.14 Gel filtration chromatography of cytosolic TatAy

The cytosolic TatAd complex of *B. subtilis* was found to form very large complexes or aggregates. Gel filtration chromatography gave a mass estimate of ~ 3.7 MDa (Barnett *et al.*, 2008). Here an estimate of the mass of the cytosolic TatAy complex was obtained using gel filtration chromatography. *E. coli* cells expressing TatAyCy from plasmid pBAyCys were fractionated and the cytosolic fraction collected. A sample of the cytosolic fraction was applied directly to an equilibrated Superose-6 column. Elution of protein from the column was performed with a single column volume of buffer in 0.6 ml fractions. All eluted fractions were run on SDS-PAGE gels and gels subsequently immunoblotted using anti-TatAy antibodies (Figure 5.2.15A). The immunoblot of the peak elution fractions was analysed further by densitometry and

intensity of band plotted against fraction number (Figure 5.2.15B). The graph also shows the elution profile of the membrane localised TatAy complex to allow a direct comparison. The immunoblot shows cytoplasmic TatAy eluting over fractions 8-11 with a peak in fraction 10. This corresponds to an elution volume of 6 ml and using the calibration curve in chapter 3 gives a size estimate of over 10 MDa. The maximum size of protein complex that can be resolved using the Superose-6 column is 5 MDa so any result greater than that should not be regarded as an accurate determination. However the data still clearly demonstrate that the cytosolic TatAy complex just like the cytosolic TatAd complex is extremely large and may be forming aggregates.

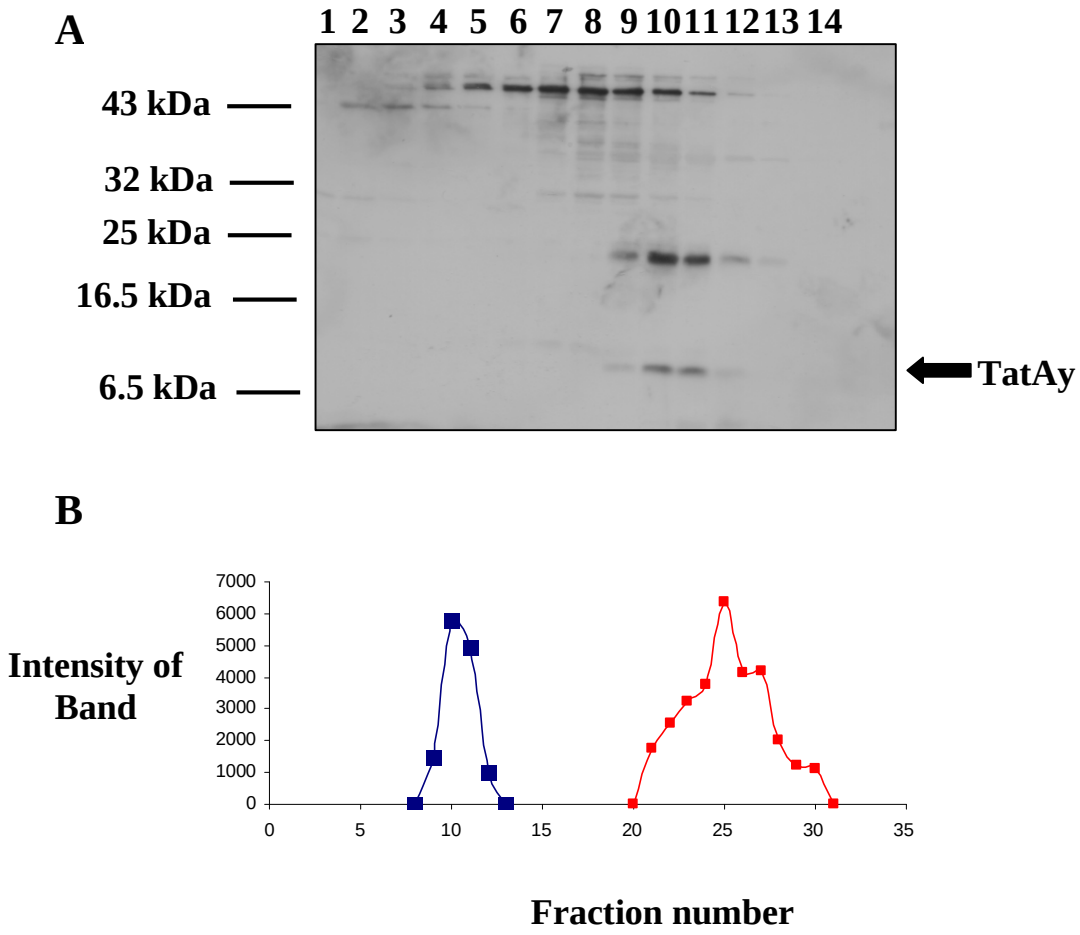

Figure 5.2.15 Gel filtration chromatography of cytosolic TatAy
A. *E. coli ΔtatABCDE* cells expressing TatAyCys from plasmid pBAyCys were fractionated and the cytoplasmic fraction collected. Cytoplasmic sample was run directly onto a gel filtration column (Superose-6) and protein eluted with a single column volume of buffer in 0.6 ml fractions. All column fractions were applied to SDS-PAGE gels before immunoblotting with anti-TatAy antibodies. The position of TatAy is marked to the right of the figure with an arrow and molecular weight markers indicated on the left.
B. The immunoblot was further analysed by densitometry and intensity of band plotted against fraction number. The elution profile of cytosolic TatAy is shown in blue and membrane localised TatAy is shown in red for comparison.

5.3 Discussion

Most studies on the bacterial Tat pathway have used the Gram-negative bacterium *E. coli* as a model organism. Two membrane localised protein complexes have been isolated from *E. coli*, a 370 kDa TatABC complex and 100 kDa -500 kDa TatA complexes (Oates *et al*., 2005). Current evidence points to a model whereby Tat substrates interact first with the TatABC complex (Alami *et al*., 2003) and separate TatA complexes are recruited to form a channel through which protein translocation can occur (Gohlke *et al*., 2005; Mori and Cline, 2002). Studies on other Gram-negative bacteria have resulted in similar conclusions pointing to a conserved mode of action (Oates *et al*., 2003).

In contrast the Tat systems of Gram-positive bacteria appear to be somewhat different. The most notable difference is the absence of a TatB component with the minimal Tat systems in Gram-positive bacteria composed of a single TatA and TatC component (Jongbloed *et al*., 2004). This suggests that the TatA protein in Gram-positive bacteria might be bifunctional carrying out both the TatA and TatB roles. (Jongbloed *et al*., 2006). This is experimentally confirmed in chapter 6 for the TatAd protein of *B. subtilis.*

The TatAdCd pathway of *B. subtilis* was found to have a similar organisation to the *E. coli* TatABC system with the identification of two membrane localised complexes; a TatAdCd containing complex where the TatAd protein presumably takes the place of TatB, and separate TatAd complexes. These two complexes, however, exhibit important differences to their *E. coli* counterparts. The TatAdCd complex was found to be significantly smaller than the TatABC complex of *E. coli*; 230 kDa compared to 370 kDa. This could be due to the absence of a separate TatB component but could also result from a different number of TatA and TatC subunits within the complex. The separate TatAd complex is relatively homogeneous in nature in comparison to the highly heterogeneous *E. coli* TatA complexes (Barnett *et al.,* 2008). Given the TatAdCd pathway is rather unusual it was important to determine whether these differences are unique to the TatAdCd pathway or if they represent a more general difference amongst the Tat pathways of Gram-negative and Gram-positive bacteria.

The TatAyCy pathway like all other Tat pathways analysed in a similar way is found to be organised in the plasma membrane as two separate Tat complexes; a TatAyCy complex and separate TatAy complexes. Gel filtration chromatography found that not only is the TatAyCy complex significantly smaller than the *E. coli* TatABC complex but it is even smaller than the TatAdCd complex of *B. subtilis*. This provides the first evidence of a conserved difference in the nature of the TatC containing complexes of Gram-negative and Gram-positive bacteria in terms of complex size. This size difference could partly be due to the lack of any separate TatB component in Gram-positive bacteria but could also be due to a completely different organisation of TatC and TatA subunits within the complex.

Like the *B. subtilis* TatAd complex, the separate TatAy complex when analysed by gel filtration chromatography (and also the TatA complex from the Gram-positive bacterium *L. monocytogenes*), was found to be relatively homogeneous when compared to the *E. coli* TatA complexes. This provides an indication of a major conserved difference in the TatA complexes of Gram-negative and Gram-positive bacteria.

The TatAy protein was found to have a cytoplasmic as well as a membrane localisation as has been described for TatA proteins of a number of other organisms studied (Berthelmann *et al*., 2008; De Keersmaeker *et al*., 2005; Frielingsdorf *et al*., 2008; Pop *et al*., 2003). This cytosolic population of TatAy just like soluble TatAd is forming large complexes or aggregates for which a role in translocation is difficult to assess (Barnett *et al*., 2008). Further direct experimental methods are required to determine the functional role of this cytosolic pool of TaAy if any in translocation.

The ability of both the TatAdCd and TatAyCy pathways to recognise a similar set of *E. coli* Tat substrates shows that neither pathway is pre-disposed to recognise only a specific set of substrates. The question of why *B. subtilis* has two Tat pathways therefore remains open but it seems likely that the TatAdCd system is providing additional capacity under conditions of phosphate limitation.

The translocation assays performed in his chapter raise another important point. *B. subtilis* is a commercially important bacterium that can be exploited in the production of important protein products that are purified from the growth medium after being secreted from the cells via the Sec pathway. The *B. subtilis* Tat pathway could also prove to be valuable in the production of protein products that are incompatible with the Sec pathway. The data presented in both Chapter 3 and this chapter show the TatAdCd pathway is able to translocate a broader range of substrates compared to the TatAyCy pathway; thus making the TatAdCd pathway the most suitable of the two for biotechnological exploitation.

In summary the data presented in this chapter points towards a conserved complex organisation and similar substrate recognition requirements between the two Tat pathways of *B. subtilis.*

Chapter 6

The Bifunctional TatAd protein of Bacillus subtilis

6.1 Introduction

As already mentioned *E. coli* requires a TatA, a TatB and a TatC protein for Tat function (Bogsch *et al*., 1998; Sargent *et al*., 1998; Sargent *et al.*, 1999). Gram-positive bacteria (except for S*treptomyces species*) have Tat systems that consist of just one TatA and TatC homologue (Jongbloed *et al*., 2004). The absence of a TatB component in these bacteria and the close similarity between TatA and TatB proteins suggested that the TatA proteins in Gram-positive bacteria may be bifunctional, acting as both a TatA and TatB in the translocation mechanism (Jongbloed *et al*., 2006).

TatA and TatB proteins share a similar structural arrangement with an N-terminal periplasmic domain that is limited to just a few amino acids, a transmembrane spanning alpha-helix, and a small amphipathic helix that aligns along the inside surface of the membrane in the cytosol. Following the amphipathic helix is a C-terminal tail that is much larger in TatB than in TatA (Figure 6.1.1). Truncation analysis has found that the C-terminal tails of these two proteins are not required for function (Lee *et al*., 2002; Warren *et al*., 2009), focusing attention on the transmembrane span and amphipathic helix as being the critical domains. Interestingly the TatA proteins of a number of Gram-positive bacteria including TatAd and TatAy of *B. subtilis* are smaller than the *E. coli* proteins and do not have such a large C-terminal extension. A recent study on the *B. subtilis* TatAd protein found it to have a very similar structural arrangement in the membrane to *E. coli* TatA and TatB (Lange *et al*., 2007).

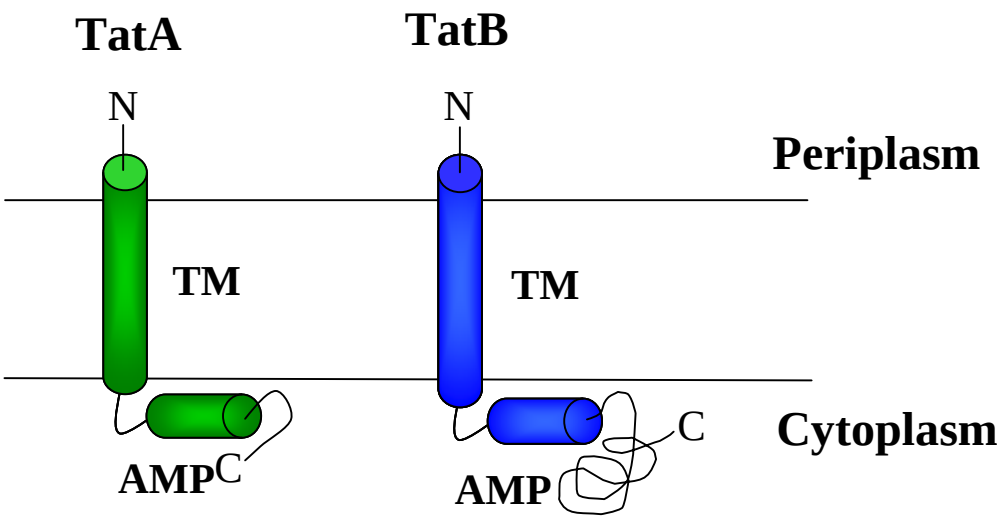

Figure 6.1.1 Schematic representation of the topology of TatA and TatB proteins of *E. coli* in the plasma membrane.
TatA and TatB proteins share a similar structural arrangement consisting of a short N-terminal domain that protrudes into the periplasm, a transmembrane spanning domain (TM), and a small hinge region linking to an amphipathic helix (AMP) lying along the inside (cytoplasmic) face of the membrane. Following the amphipathic helix is an unstructured extension that is larger in TatB than TatA.

The ability of the TatAdCd translocase of *B. subtilis* to translocate *E. coli* Tat substrates including TMAO reductase for which a TatA and TatB component are essential supports the hypothesis that TatA proteins of Gram-positive bacteria are bifunctional (Barnett *et al*., 2008). Another study found that single substitutions of amino acids at the extreme N-terminal periplasmic domain of *E. coli* TatA allowed it to perform the function of *E. coli* TatB and support translocation of a sensitive reporter protein TorA-MalE (Blaudeck *et al*., 2005), and more recently the TorA protein itself in the absence of a TatB component (Barrett *et al*., 2007). Previously it was found that Colicin V is transported by the *E. coli* Tat pathway and that this translocation activity required just TatA and TatC components (Ize *et al*., 2002).

In this chapter a more direct approach was used to determine whether the TatAd protein of *B. subtilis* was bifunctional. The TatAd protein is able to complement both *tatA/tatE* and *tatB* null mutants of *E. coli* for the translocation of TorA; thus confirming the bifunctional nature of the TatAd protein. However whilst the TatAd protein can complement the *E. coli ΔtatAE* and *ΔtatB* mutant strains for translocation of TorA, it cannot complement for translocation of another *E. coli* Tat substrate, SufI, in *ΔtatAE* cells. Similarly whilst TatAd can complement for the increased sensitivity

of *E. coli ΔtatB* cells to the detergent SDS, it cannot complement for the increased sensitivity to SDS of *ΔtatAE* cells.

A sequence alignment showing TatA proteins from Gram-positive bacteria and also *E. coli* TatA/TatB is shown in Figure 6.1.2. The alignment only shows the first 50 – 60 amino acids as the conserved residues all lay within this region. The TatA proteins of Gram-positive bacteria share residues that are conserved amongst both TatA and TatB proteins of Gram-negative bacteria (Jongbloed *et al*., 2006). For example, *E. coli* TatA has a well conserved Phe and Gly residue in the hinge region between the two helices of the protein. TatB shares the conserved Gly residue but this is followed by a conserved Pro residue. Several Gram-positive TatA proteins share all three residues in an FGP motif. The N-terminal ends of the amphipathic helices of the TatA proteins of Gram-positive bacteria contain a highly conserved KLP motif. *E. coli* TatA shares the Lys and Leu residues but not the Pro residue, whilst *E. coli* TatB does not share the conserved Lys residue but does share the Leu and Pro residues.

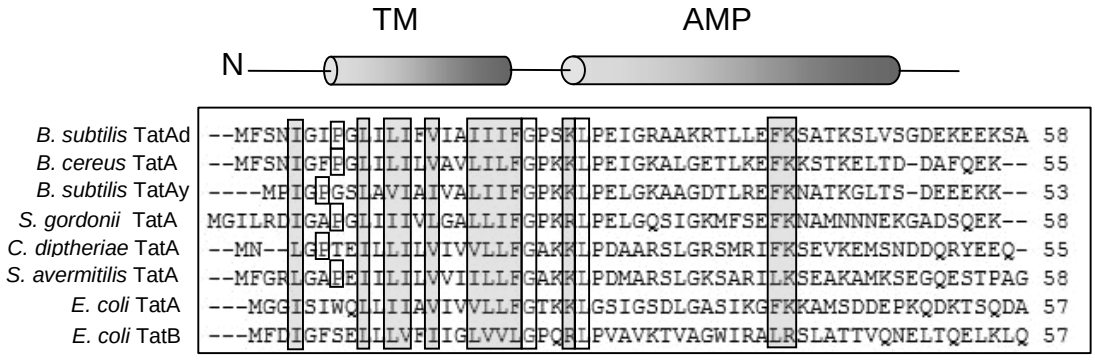

Figure 6.1.2 Sequence alignment of TatA/B proteins from bacteria
The TatA proteins of a number of Gram-positive bacteria and TatA and TatB of *E. coli* were aligned using the ClustalW programme. Only the first 50 – 60 amino acids are shown. Conserved residues are highlighted in white boxes and conservative substitutions highlighted in grey boxes. Also boxed in white is a conserved Proline residue at position 7 or 8 in the Gram-positive TatA proteins. The predicted transmembrane spanning domain (TM) and amphipathic helix (AMP) is indicated above the alignment.

Several mutagenesis studies have been carried out to identify those residues of the *E. coli* TatA/TatB proteins that are required for efficient translocation activity. As mentioned above, truncation from the C-terminal end of TatA and TatB up to the amphipathic helix has no effect on Tat function, (Lee *et al*., 2002; Warren *et al*., 2009). The important regions of TatA/TatB proteins are the transmembrane spanning domain, amphipathic helix, and the small hinge region between them. Single amino acid substitutions within the hinge region and amphipathic helices of *E. coli* TatA and TatB, result in a drastic reduction or complete block in translocation activity. In contrast single substitutions within the transmembrane spans were found to have little if any effect on transport (Barrett *et al*., 2003; Barrett *et al*., 2005a; Barrett *et al* 2005b; Greene *et al*., 2007; Lee *et al*., 2006). This is quite surprising given that this region of both proteins contains the most well conserved residues.

In this chapter the bifunctional TatAd protein of *B. subtilis* was investigated using site-directed mutagenesis to identify residues critical for TatAdCd mediated translocation. In addition the ability of mutant TatAd proteins to complement *E. coli ΔtatAE* and *ΔtatB* strains was used to identify specific TatA or TatB domains within the TatAd protein.

6.2 Results

6.2.1 Complementation of *E. coli ΔtatAE* and *ΔtatB* strains by the TatAd protein of *B. subtilis*: Translocation of TMAO reductase

Here a direct approach to probe the bifunctional nature of the TatAd protein of *B. subtilis* was used. The ability of TatAd to complement *E. coli tatA/E* and *tatB* null mutants in the translocation of the *E. coli* Tat substrate TMAO reductase (TorA) was determined. As a negative control *E. coli ΔtatA/E* and *ΔtatB* mutant strains were tested. Cells were grown for 2 hours, and cellular proteins from the Periplasm (P), Cytoplasm (C), and Membrane (M) compartments were isolated. Samples were subjected to native-PAGE and the gel stained blue with reduced methyl viologen. Upon the addition of TMAO, (the substrate of TorA), and in the presence of the TorA enzyme a clearing of the gel turbidity occurs (visualised as a white band) (Figure 6.2.1). For the two negative controls tested, (*ΔtatAE and ΔtatB*), no white band can be observed in the periplasmic lanes of the gel; thus indicating that no translocation has occurred. This confirms the strict requirement for both a TatA and TatB component for translocation of TorA in *E. coli*. As an additional negative control, *E. coli ΔtatABCDE* (*Δtat*) cells expressing TatAd-*his* from plasmid pBAdh were tested. Again no white band can be seen in the periplasmic lane of the gel indicating that no translocation has occurred. This is important as it demonstrates that the TatAd protein alone is unable to translocate TorA. Finally *E. coli ΔtatAE* and *ΔtatB* cells expressing TatAd from the pBAdh plasmid were tested. In both cases a white band can be visualised in the periplasmic lanes on the gel demonstrating that TorA has been exported. The periplasmic TorA band in *ΔtatAE* cells expressing TatAd is weaker than in *ΔtatB* cells expressing TatAd, however further experiments show very little difference between the two (see later).

This data provides the first direct evidence that the TatAd protein of *B. subtilis* is indeed bifunctional.

In a further note a functional interaction must occur between TatAd and the endogenous *E. coli* Tat components to form an active translocation pathway. This again points towards a conserved mode of action in Tat function in both Gram-negative and Gram-positive bacteria.

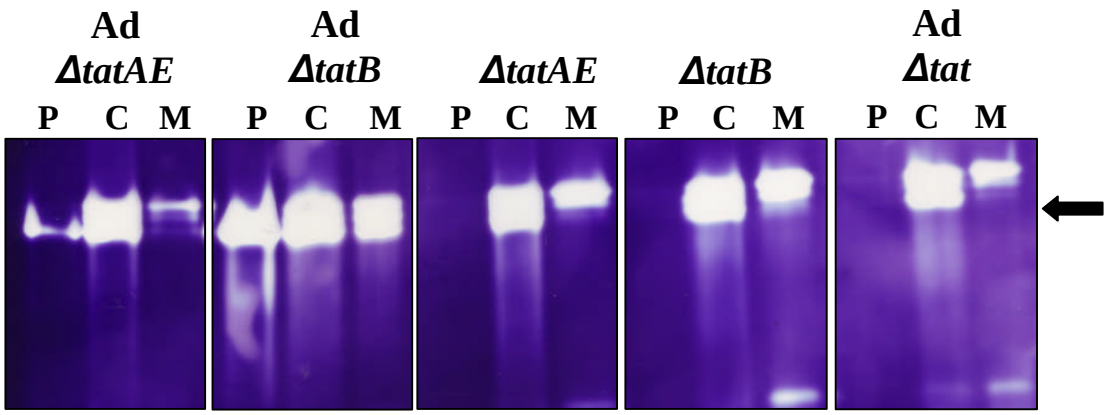

Figure 6.2.1 Complementation of *E. coli ΔtatA/E* and *ΔtatB* mutants by the TatAd protein of *B. subtilis*: Translocation of TMAO reductase
E. coli ΔtatAE, ΔtatB, and *ΔtatAE, ΔtatB* and *ΔtatABCDE* (*Δtat*) cells expressing TatAd-*his* from plasmid pBAdh were grown for 2 hours with induction of the pBAdh plasmid. Cellular proteins from the Periplasm (P), Cytoplasm (C), and Membrane (M) compartments were isolated and samples were subjected to native-PAGE. The gel was stained blue with reduced methyl viologen before being developed by the addition of substrate (TMAO). In the presence of TorA the gel turbidity clears and a white band is observed. The position of TorA is indicated by an arrow.

6.2.2 Complementation of *E. coli ΔtatAE* and *ΔtatB* strains by the TatAd protein of *B. subtilis*: Translocation of SufI

Previously in chapter 5 it was shown that the TatAdCd pathway of *B. subtilis* is unable to translocate SufI (an *E. coli* Tat substrate) (Barnett *et al*., 2008). Given that the TatAd protein can interact with *E. coli* Tat components to form a functioning translocation pathway in *E. coli ΔtatAE* and *ΔtatB* mutant strains, the ability of the TatAd protein to translocate SufI when expressed in these mutant strains was also investigated.

Briefly, *E. coli* cells were grown for two hours with induction of the pBAdh plasmid (where present) before cellular proteins from the Periplasm (P), Cytoplasm (C), and Membrane (M) compartments were isolated. Samples were analysed by SDS-PAGE and Western blotted using anti-SufI antibodies for immunodetection. The data is presented in Figure 6.2.2. As a positive control *E. coli* wild-type MC4100 cells were tested. A clear band can be visualised in the periplasmic lane at around 50 kDa indicating that SufI has been translocated as expected. As a negative control *E. coli ΔtatAE* and *ΔtatB* mutant strains were tested. In both cases no SufI is detectable in the periplasmic lane and no translocation has occurred, again exactly as expected given

the strict requirement of both a TatA and a TatB component for translocation. In a third

negative control the TatAd protein alone could not translocate SufI, *E. coli ΔtatABCDE* cells expressing TatAd were tested; again no SufI is detectable in the periplasmic lane of the immunoblot so no transport of SufI has occurred. When TatAd was expressed in *E. coli ΔtatAE* cells, still no translocation of SufI to the periplasm is observed. This is not too surprising given that TatAdCd was found not to be able to translocate SufI either when expressed in *E. coli ΔtatABCDE* cells. Finally when TatAd was expressed in *E. coli ΔtatB* cells, a clear band in the periplasmic lane running to around 50 kDa is observed. In this case SufI is efficiently translocated to the periplasm. This data shows that whilst the TatAd protein can fulfil a TatB role in SufI translocation it cannot fulfil its TatA role. This may explain why SufI is not translocated by the TatAdCd pathway but it may also be the case that the TatCd protein does not recognise SufI as a Tat substrate.

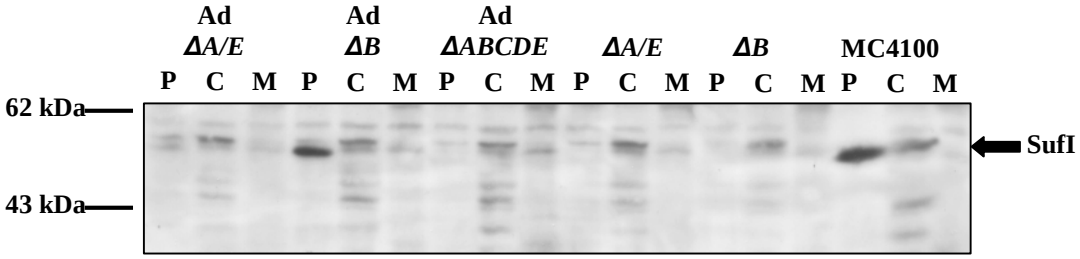

Figure 6.2.2 Complementation of *E. coli ΔtatA/E* and *ΔtatB* mutants by the TatAd protein of *B. subtilis*: Translocation of SufI
E. coli cells (MC4100, *ΔtatAE*, *ΔtatB*, and *ΔtatABCDE*) were grown with induction of the pBAdh plasmid where present for two hours. Cellular proteins from the Periplasm (P), Cytoplasm (C), and Membrane (M) compartments were isolated. Samples were applied to an SDS-PAGE gel and the gel was subsequently immunoblotted using anti-SufI antibodies. The position of SufI is marked on the right and molecular weight markers are shown to the left.

6.2.3 Complementation of *E. coli ΔtatAE* and *ΔtatB* strains by the TatAd protein of *B. subtilis*: Sensitivity to SDS

E. coli tat deletion strains have an increased sensitivity to the detergent SDS. This sensitivity to SDS has been used previously to assay for complementation of *tat* mutants (Ize *et al*., 2003). The TatAd protein was tested to see if it could complement *E. coli ΔtatAE* and *ΔtatB* mutant strains for sensitivity to SDS.

Briefly, overnight cultures of *E. coli* cells were used to inoculate media (to an OD_{600} of 0.05) that had been supplemented with varying concentrations of SDS (0 – 4 % (w/v)). Cells were cultured for 3 hours and the final optical density measured at 600 nm. The final optical density readings were converted into a percentage of the optical density of cells grown in 0 % SDS. This percentage termed % survival was plotted on a graph against SDS concentration (Figure 6.2.3A and B). As positive controls *E. coli ΔtatABCDE* cells expressing *E. coli* TatABC from pBAD24 and pEXT22 plasmids were tested. Cells expressing pEXT-TatABC grew equally well in all SDS concentrations and little effect of SDS on the growth of cells expressing pBAD-ABC was also observed. As a negative control *E. coli ΔtatABCDE* (*Δtat*) cells were tested. In this case the graph shows a significant fall in the % survival of the culture confirming the sensitivity of *Δtat* cells to SDS. The ability of both the TatAdCd and TatAyCy pathways to complement for the SDS sensitivity of *E. coli Δtat* cells was tested by expressing proteins form pBAD24 and pEXT22 plasmids as indicated. Neither TatAdCd nor TatAyCy are able to complement for the increased SDS sensitivity. In fact the graph shows that the cells are as sensitive to SDS as *Δtat* cells without plasmid (Figure 6.2.3A).

The same experiment was then carried out but this time to investigate the ability of the TatAd protein to complement *E. coli ΔtatAE* and *ΔtatB* cells. The data is presented in Figure 6.2.3B. This time WT MC4100 cells were tested as a positive control. The graph shows that the presence of SDS has no effect on cell growth as expected. As negative controls *E. coli ΔtatAE* and *ΔtatB* cells were tested. In both cases the cells are highly sensitive to SDS and a large drop in % survival is observed. Expression of TatAd from plasmid pBAdh in *E. coli ΔtatAE* cells does not complement for the sensitivity to SDS and again a drop in optical density is observed. Expression of TatAd in the *E. coli ΔtatB* cells does however complement the *ΔtatB* cells sensitivity to SDS. This result is similar to that obtained above where TatAd can complement *E. coli ΔtatB* but not *ΔtatAE* cells for translocation of SufI.

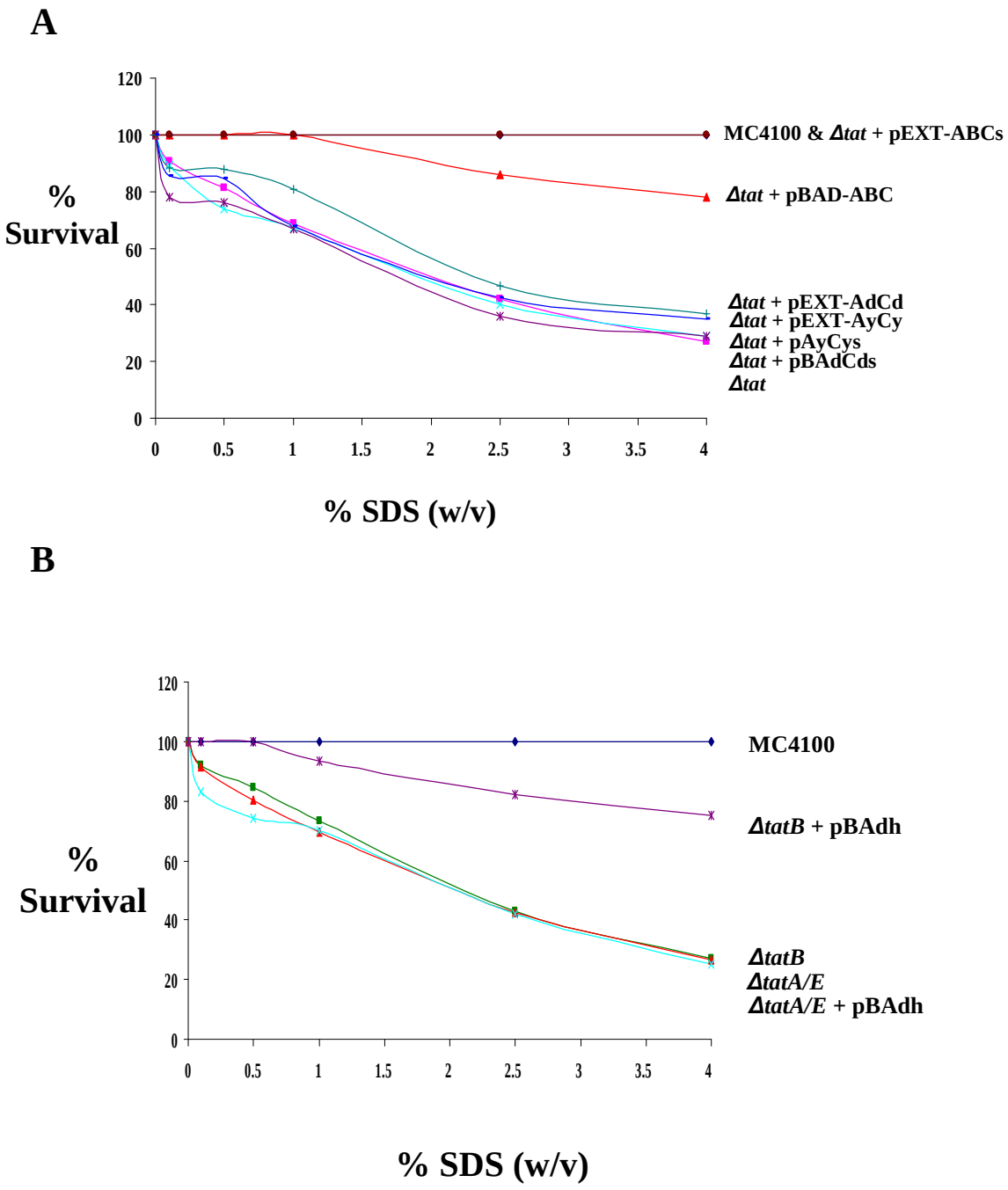

Figure 6.2.3 Complementation of *E. coli Δtat* strains by *B. subtilis* TatAdCd and TatAd: Sensitivity to SDS

E. coli cells (MC4100, *ΔtatAE, ΔtatB* and *ΔtatABCDE*), were grown for 3 hours from a starting culture with an OD_{600} of 0.05 in LB that was supplemented with 0 – 4 % SDS. After 3 hours growth the OD_{600} was measured and converted to a percentage of the OD_{600} of the 0% SDS sample. This percentage (% survival) was plotted against SDS concentration. Also tested were *E. coli ΔtatABCDE* cells expressing pBAD-ABC, pBAdCds, pBAyCys, pEXT-ABC, pEXT-AdCd, and pEXT-AyCy plasmids. Finally *E. coli ΔtatAE* and *ΔtatB* cells expressing TatAd from plasmid pBAdh were tested.

6.2.4 Mutagenesis of TatAd: Identification of residues important for translocation activity

TatA proteins are most highly conserved within the N-terminal half. Residues within this region of TatAd were mutated to Ala to determine those amino acid residues that are critical for function. Mutations were introduced into plasmid pBAdCds using Quickchange Site-specific mutagenesis (see chapter 2). Mutated plasmids were expressed in *ΔtatABCDE* cells and the expression and stability of the mutant TatAd proteins tested. Following expression from the mutated plasmids in *E. coli ΔtatABCDE* cells, cells were run on SDS-PAGE gels and gels immunoblotted with specific anti-TatAd antibodies. Cells expressing wild-type TatAdCd from plasmid pBAdCds were also tested as a control. The results are presented in Figure 6.2.4. The mutant TatAd proteins are expressed at broadly similar levels, the only exception being the L12A mutant. This mutant is expressed at much lower levels or is less stable for unknown reasons.

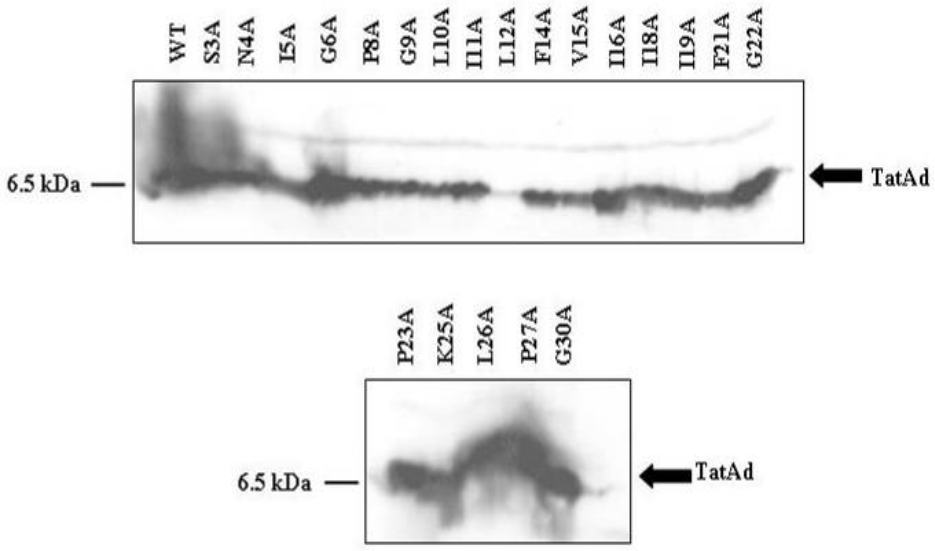

Figure 6.2.4 Expression and stability of mutant TatAd proteins in *E. coli Δtat* cells
ΔtatABCDE cells expressing WT and the mutant versions of the pBAdCds plasmids were cultured, collected, and resuspended in buffer. Samples of whole cells were run on SDS-PAGE gels. The gels were subsequently immunoblotted using specific anti-TatAd antibodies. The position of TatAd is shown on the right and the 6.5 kDa marker shown to the left.

Since the TatAdCd pathway can translocate the Tat substrate TorA, the translocation activity of the mutated forms of the TatAd protein was assayed by detecting translocation of this substrate. The mutated TatAd proteins were expressed along with wild-type TatCd from the pBAdCds plasmid in *E. coli ΔtatABCDE* cells. Cellular proteins from the Periplasm (P), Cytoplasm (C), and Membrane (M) compartments were isolated. Samples were applied to native-PAGE gels that were subsequently assayed for TorA activity as detailed above. The results are presented in Figure 6.2.5.

Four mutations in the extreme N-terminal part of the protein that extends into the periplasm (S3A, N4A, I5A, and G6A), showed no detectable effect on TorA transport. A strong white band is clearly visible in the periplasmic (P) lanes of these samples. This is not too surprising given that the sequence alignment shown in Figure 6.1.2 shows that this region of TatAd is not conserved. The next two residues tested, Pro8 and Gly9, are thought to lay at the beginning of the transmembrane (TM) spanning alpha-helix. Substitution of the Pro8 with Ala, results in a complete block in translocation activity with TorA activity seen only in the cytoplasmic fraction. Interestingly the sequence alignment (Fig. 6.1.2) shows that a Proline residue is conserved at either this position or an adjacent position in Gram-positive TatA proteins. No Proline residue is found in this region of *E. coli* TatA or TatB indicating an important difference between the TatA proteins of Gram-positive and Gram-negative bacteria. Substitution of Gly9 by Ala had no effect on translocation activity and a clear white band is detected in the periplasmic lane of the gel of this sample.

The next three mutants tested were L10A, I11A, and L12A and all three support efficient translocation of TorA as detected by a strong band in the periplasmic lanes of the gels of these samples. The next substitution however, F14A, resulted in a complete block in translocation activity with TorA activity found exclusively in the cytosolic and membrane fractions. A Phenylalanine residue is not conserved at this position in TatA proteins of Gram-positive bacteria so this result was somewhat surprising. A Phenylalanine residue is however found at this position in *E. coli* TatB so could be important for performing a TatB role. Mutation of the following Valine residue to Alanine (V15A) had no effect on the translocation of TorA and a white band can be visualised in the periplasmic lane on the gel of this sample. Three Isoluecine to Alanine substitutions at the C-terminal end of the transmembrane spanning domain

were tested next (I16A, I18A, and I19A). In each case only a very weak periplasmic TorA band can be seen on the gels. These three residues are clearly important for translocation activity. Isoleucine and Leucine residues are well conserved in this part of the transmembrane spanning domains of Gram-positive TatA proteins and they may be important for helix-helix interactions. When using this assay to comment on translocation activity it must be noted that this assay is not quantitative but it allows any drastic changes in translocation activity to be observed.

Next, three amino acids in the hinge region connecting the two helices of TatAd were substituted by Alanine. This region is important for TatA/TatB protein function in *E. coli*, (Barrett *et al*., 2003). In all three cases the substitutions (F21A, G22A, and P23A), cause a complete block in translocation with TorA activity seen exclusively in cytoplasmic samples. Given that this region is important in *E. coli* and these residues are highly conserved amongst all TatA and TatB family proteins, the result is not too surprising. However, mutation of these residues in *E. coli* had a less drastic effect on translocation activity and a low level of translocation activity could still be observed (Greene *et al*., 2007; Lee e*t al*., 2006).

Finally four substitutions at the beginning of the amphipathic helix (the N-terminal end) were tested. These were K25A, L26A, P27A and G30A. All of these mutations except for L26A support transport of TorA as detected by a clear band in the periplasmic lanes of the gels.

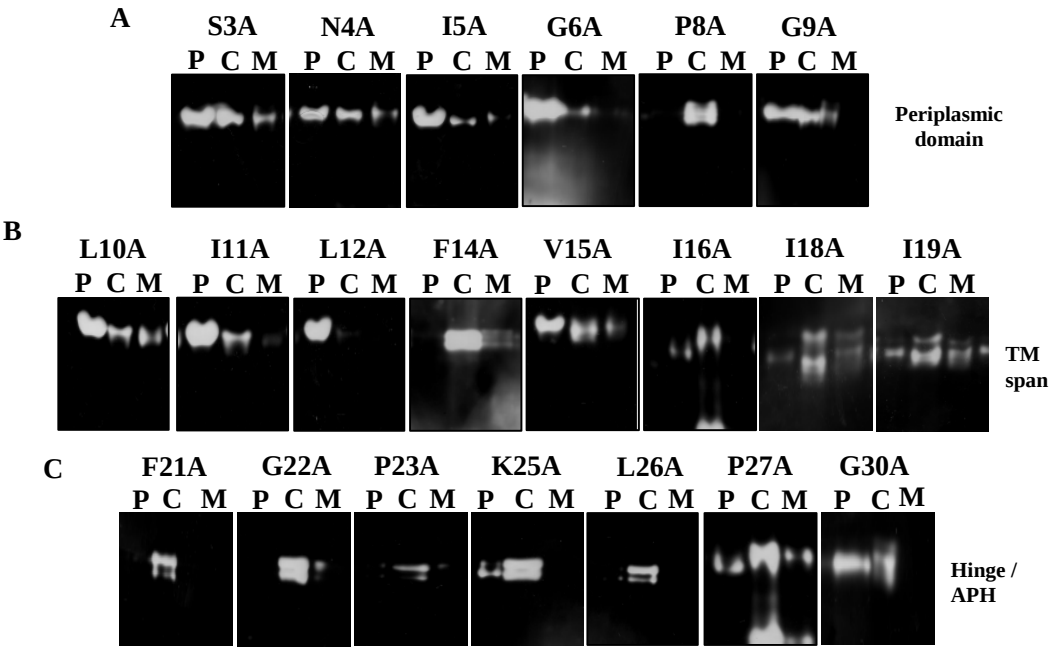

Figure 6.2.5 Translocation of TorA by TatAdCd carrying single amino acid substitutions
Mutant pBAdCd plasmids were expressed in *E. coli ΔtatABCDE* cells and cellular proteins from the Periplasm (P), Cytoplasm (C), and Membrane (M) compartments isolated. Cell fractions were applied to native-PAGE gels that were assayed for the presence of active TorA as detailed in chapter 2. The figure is divided into 3 sections. **A**: substitutions within the periplasmic domain, **B**: substitutions within the transmembrane spanning domain (TM), and **C**: substitutions within the hinge region and amphipathic helix.

The data are summarised in Figure 6.2.6 and overall show that residues throughout the N-terminal half of the TatAd protein (the transmembrane spanning domain, hinge region and amphipathic helix), are all important for TatAdCd function.

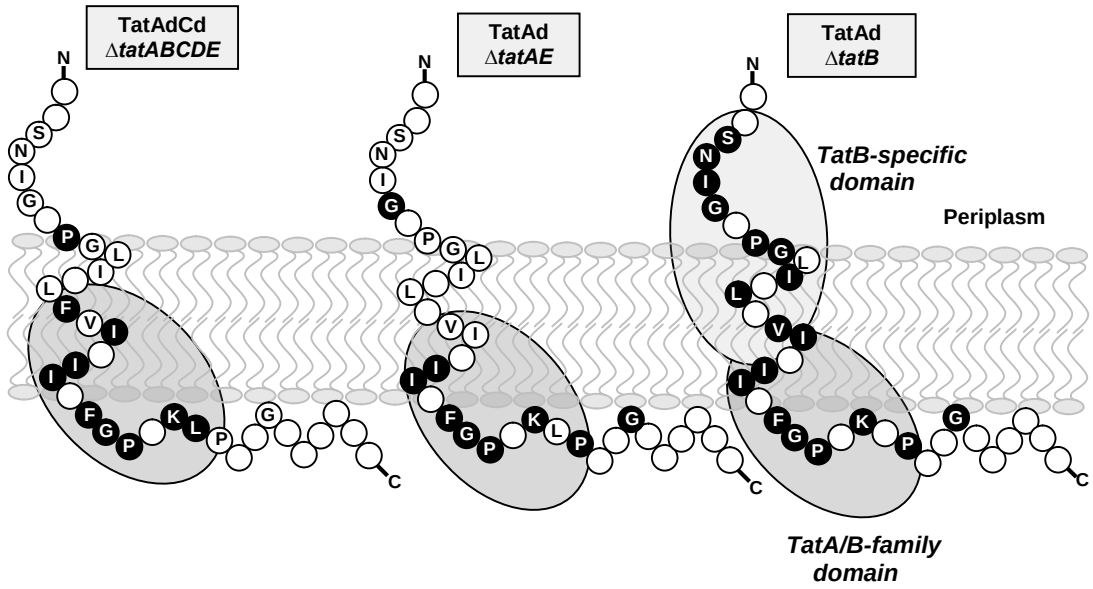

Figure 6.2.6 Identification of residues in TatAd critical for TatAdCd mediated translocation

A diagram showing the topology of the TatAd protein in the plasma membrane (only the N-terminal 36 residues are shown). Substitutions that have a marked effect on translocation activity when TatAd and TatCd are expressed together in *E. coli ΔtatABCDE* cells, and when TatAd is expressed alone in *E. coli ΔtatAE* and *ΔtatB* mutant strains, are shaded in black.

6.2.5 Identification of residues important for the TatA function of the *B. subtilis* TatAd protein

The data presented above shows the effect that single amino acid substitutions within the TatAd protein of *B. subtilis* have on TatAdCd mediated transport in *E. coli*. Since the TatAd protein is bifunctional those residues that are important for the proteins TatA role were determined. The same substitutions that were tested above were introduced into the TatAd protein expressed alone from the pBAdh plasmid. Expression of TatAd from this plasmid has been shown to be able to support translocation of *E. coli* TorA when expressed in both *E. coli ΔtatAE* and *ΔtatB* mutant strains (6.2.1). The pBAdh plasmids carrying single amino acid substitutions were therefore expressed in *E. coli ΔtatAE* cells and the ability of the mutated TatAd proteins to complement the *ΔtatAE* strain for export of TorA determined.

E. coli cells expressing the mutated plasmids were cultured and cellular proteins from the Periplasm (P), Cytoplasm (C), and Membrane (M) compartments were isolated. Samples were applied to native-PAGE gels that were subsequently assayed for the presence of active TorA as described above. The results are shown in Figure 6.2.7. As a negative and positive control *E. coli ΔtatAE* cells and *ΔtatAE* cells expressing wild-type TatAd were tested. As expected the TatAd protein complements *E. coli ΔtatAE* cells in the transport of TorA. Also as expected no translocation is observed in *ΔtatAE* cells without plasmid, again confirming the strict requirement of TatA for translocation of TorA.

As before, four substitutions in the short periplasmic domain of TatAd were tested first (S3A, N4A, I5A, and G6A). The first 3 of these substitutions had no effect on translocation activity and a clear white band can be visualised in the periplasmic lane of the gels. The same mutations also had no effect on translocation when TatAd was expressed with TatCd in *E. coli ΔtatABCDE* cells. In contrast the G6A substitution that had no effect on TatAdCd mediated translocation is unable to support translocation of TorA when TatAd is expressed in *ΔtatAE* cells. TorA activity is localised solely in cytoplasm and membrane compartments. The P8A mutant was tested next, this mutant TatAd protein that was inactive for TatAdCd mediated translocation, is able to complement the *E. coli ΔtatAE* strain as a clear white band can be seen in the periplasmic lane of the gel. This data suggests that this residue may be

important for a TatB role but not for a TatA role, at least in combination with the endogenous *E. coli* TatB and TatC proteins. The G9A substitution that had no effect on TatAdCd directed translocation also has no effect on translocation when TatAd is expressed in *ΔtatAE* cells.

Of the substitutions made in the transmembrane span the L10A, I11A, L12A, V15A, and I16A all support efficient translocation of TorA to the periplasm. In each case a clear white band is detected in the periplasmic lanes of the gels. These same substitutions had no effect on translocation of TorA by TatAdCd with the exception of I16A that allowed only weak transport. The last two substitutions of the transmembrane spanning domain tested were I18A and I19A. These substitutions caused a dramatic reduction in the translocation efficiency of TatAdCd. Here only weak translocation is observed with the I18A mutant and no translocation is observed with the I19A mutant.

The three substitutions in the hinge region were also tested and confirming the importance of this region, all three substitutions analysed, F21A, G22A, and P23A showed no or only very weak TorA activity in the periplasmic lanes of the gels.

Finally the K25A, P27A, and G30A substitutions within the N-terminal end of the amphipathic helix were tested. In each case no TorA activity is detectable in the periplasmic fractions confirming the importance of the amphipathic helix in TatA function.

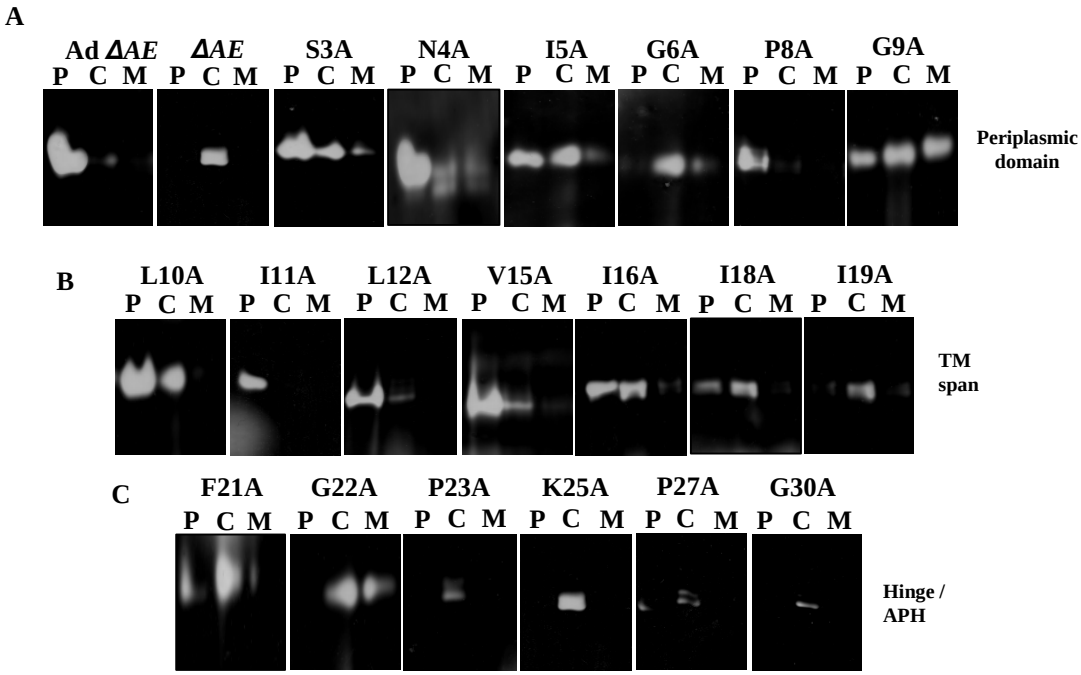

Figure 6.2.7 Complementation of *E. coli ΔtatAE* cells by TatAd carrying single amino acid substitutions

Mutant pBAdh plasmids were expressed in *E. coli ΔtatAE* cells and cellular proteins from the Periplasm (P), Cytoplasm (C), and Membrane (M) compartments were isolated. Cell fractions were applied to native-PAGE gels that were assayed for the presence of active TorA as detailed in chapter 2. The figure is divided into 3 sections. **A**: substitutions within the periplasmic domain, **B**: substitutions within the transmembrane spanning domain (TM), and **C**: substitutions within the hinge region and amphipathic helix.

6.2.6 Identification of residues important for the TatB function of the *B. subtilis* TatAd protein

The TatAd mutants tested above in *E. coli ΔtatAE* cells were also tested in *E. coli ΔtatB* cells to determine those residues that are important for a TatB type role. The TatAd protein and mutant versions were expressed in *E. coli ΔtatB* cells and cellular proteins from the Periplasm (P), Cytoplasm (C), and Membrane (M) compartments were isolated. Samples were applied to native-PAGE gels that were subsequently stained for the presence of active TorA as described above. The data is presented in Figure 6.2.8. Of the substitutions made in the periplasmic domain the S3A, N4A, I5A and G6A are all unable to support translocation of TorA with TorA activity observed only in cytosolic and membrane compartments. Since the S3A, N4A and I5A substitutions had no effect on export when expressed in *ΔtatAE* cells, it seems that this region of the TatAd protein is important for a TatB type function and is not required for its TatA role. The G6A mutant that is inactive in *ΔtatB* cells was also inactive when expressed in *ΔtatAE* cells suggesting that it is unable to interact with the *E. coli* Tat components. The same substitution had no effect on TatAdCd mediated translocation. The P8A and G9A mutants also exhibit no translocation activity when over expressed in *ΔtatB* cells confirming the importance of the N-terminal periplasmic domain for TatB function.

Several of the substitutions made within the transmembrane span also severely affect translocation activity. Only the L10A mutant allows efficient transport of TorA, and the L12A and I18A mutants support only weak translocation activity. The I11A, V15A, I16A and I19A mutants are all blocked in translocation.

Finally the substitutions in the conserved hinge region and N-terminal end of the amphipathic helix were tested. The F21A mutant displays only very weak translocation activity and the remaining mutants, G22A, P23A, K25A, P27A, and G30A are all blocked in export.

All of the data are summarised in Figure 6.2.6 that shows the C-terminal end of the transmembrane span and hinge region is critical under all three conditions tested (i.e. TatAdCd in *ΔtatABCDE*, TatAd in *ΔtatAE*, and TatAd in *ΔtatB*), but substitutions at

the N-terminal end of the protein are critical for the TatB function of the TatAd protein.

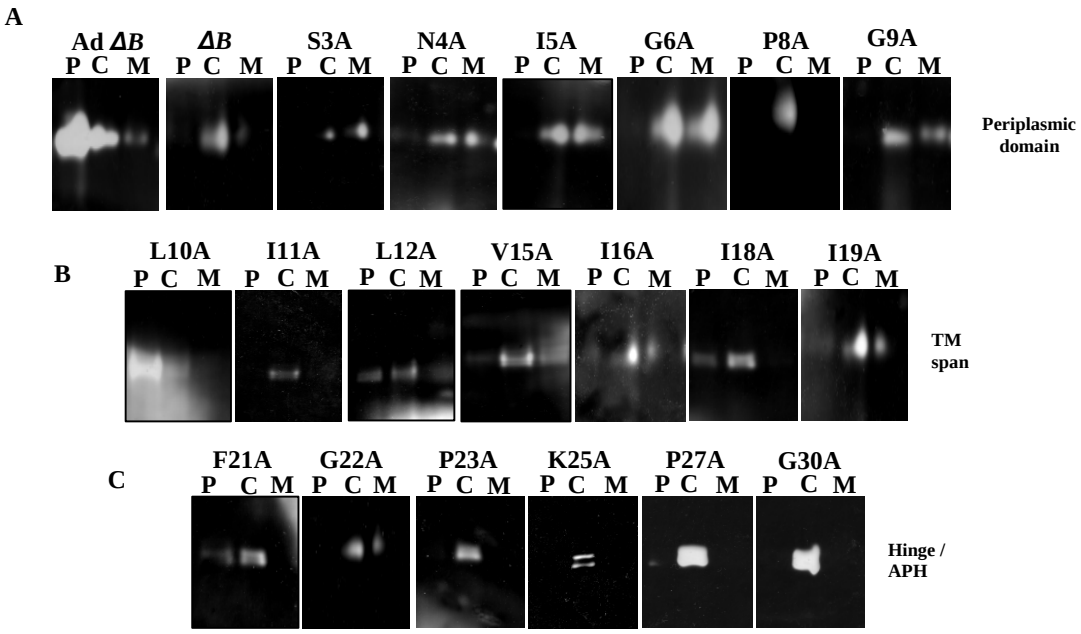

Figure 6.2.8 Complementation of *E. coli ΔtatB* cells by TatAd with single amino acid substitutions

Mutant pBAdh plasmids were expressed in *E. coli ΔtatB* cells and cellular proteins from the Periplasm (P), Cytoplasm (C), and Membrane (M) compartments were isolated. Cell fractions were applied to native-PAGE gels that were assayed for the presence of active TorA as detailed in chapter 2. The figure is divided into 3 sections. **A**: substitutions within the periplasmic domain, **B**: substitutions within the transmembrane spanning domain (TM), and **C**: substitutions within the hinge region and amphipathic helix.

6.3 Discussion

The absence of a TatB protein in Gram-positive bacteria suggested that the TatA protein is bifunctional fulfilling the roles of both TatA and TatB of Gram-negative bacteria (Jongbloed *et al*., 2006). This hypothesis was supported by a study that found *E. coli* TatA with point mutations at the extreme N-terminus could support translocation of a sensitive reporter (TorA-MalE) (Blaudeck *et al*., 2005), and in a separate study also the native TorA protein in cells lacking TatB (Barrett *et al*., 2007). In this chapter the bifunctional nature of the TatAd protein of *B. subtilis* was demonstrated using a more direct approach. The TatAd protein was found to complement *E. coli ΔtatAE* and *ΔtatB* cells in the translocation of the *E. coli* Tat substrate TorA for which a TatA and TatB component is strictly required.

In further tests the TatAd protein was found to be able to complement the *E. coli ΔtatB* strain for translocation of SufI and for its increased sensitivity to the detergent SDS. In contrast the TatAd protein was not able to substitute for TatAE in *ΔtatAE* cells in translocation of SufI or SDS sensitivity. The TatAd protein therefore seems unable to completely functionally substitute for *E. coli* TatA.

Several mutagenesis studies have been performed on the TatA and TatB proteins of *E. coli.* Truncation analysis found the C-terminal tail extensions of these two proteins are dispensable for function (Lee *et al*., 2002; Warren *et al*., 2009). Interestingly the TatA proteins of Gram-positive bacteria are generally smaller than their Gram-negative counterparts and do not have such a large C-terminal tail. The critical regions of *E. coli* TatA and TatB are the transmembrane spanning domain, amphipathic helix and small hinge region between the two helices. Single substitutions within the hinge region and amphipathic helix of TatA and TatB were found to cause a drastic reduction in translocation activity, whilst single substitutions within the transmembrane spanning domains were well tolerated and little effect on transport activity observed (Barrett *et al*., 2003; Barrett *et al*., 2005a; Barrett *et al* 2005b; Greene *et al*., 2007; Lee *et al*., 2006).

Mutagenesis of TatAd demonstrated that the C-terminal part of the TM span, hinge region, and first few residues of the amphipathic helix are critical for function of TatAdCd when expressed in *E. coli ΔtatABCDE* cells. Mutations that had an effect on TatAdCd function also block the ability of the TatAd protein to complement either the *E. coli ΔtatAE* or *ΔtatB* mutant strains. This is nicely summarised in figure 6.2.6 that highlights those residues critical for TatAd function. Whilst similar substitutions in *E. coli* TatA and TatB had an effect on translocation activity, the results were not as dramatic, for example mutations in hinge region of TatA resulted in a drop rather than a complete block in translocation activity (Greene *et al*., 2007; Lee e*t al*., 2006). In conclusion the C-terminal end of the transmembrane span, hinge region and amphipathic helix are critical for TatA/B activity in both Gram-negative and Gram-positive bacteria.

The data also indicates a critical role for the N-terminal periplasmic residues and N-terminal half of the transmembrane spanning domain for TatB function. Several substitutions in this region of TatAd, from S3A to I16A cause a complete block in TorA transport when expressed in *E. coli ΔtatB* cells. The same substitutions tested with the exception of G6A had no effect on TorA transport when TatAd was over expressed in *E. coli ΔtatAE* cells. This data is consistent with a study that found single substitutions at the periplasmic end of *E. coli* TatA allowed translocation of TorA with just a TatC partner (Blaudeck *et al*., 2005).

Whilst several mutations at the N-terminal end of TatAd block translocation of TorA when TatAd is expressed in *E. coli ΔtatB* cells, the same mutations do not have any obvious effects of the transport of TorA by TatAdCd over expressed in *ΔtatABCDE* cells. This difference is perhaps due to the expression levels of the different Tat components. Expression of TatAd mutants from the pBAdCds plasmid may mask effects on translocation activity that are observed when TatAd is expressed in *ΔtatAE* and *ΔtatB* strains of *E. coli*. In the latter case the other Tat components present are only at WT levels of expression. A similar finding has been described in a study on *E. coli* TatB that found that over expression of mutated TatB masks the effects of the mutations on translocation activity (Barrett and Robinson, 2005a).

It would be interesting to further characterise the mutants in terms of complex formation as done previously for the WT protein (chapter 3), and to look at the effects of the mutations on substrate binding to try to determine the exact roles of the different regions of the TatAd protein.

Chapter 7

Final Discussion

7.1 Discussion

A great deal of our knowledge about how the bacterial Tat pathway operates originates from studies on the Tat pathway of the Gram-negative bacterium, *E. coli* (Lee *et al*., 2006; Müller and Klösgen, 2005; Robinson and Bolhuis, 2004; Sargent *et al*., 2006). The Tat pathway of *E. coli*, like other Gram-negative Tat systems, is comprised of TatA, TatB and TatC, (three essential integral membrane proteins) (Bogsch *et al*., 1998; Sargent *et al*., 1998; Sargent *et al.*, 1999). The organisation of these proteins into functional complexes within the plasma membrane has been widely studied and two major types of complex identified: a 370 kDa TatABC complex and separate TatA complexes that vary from below 100 kDa to in excess of 500 kDa (Oates *et al*., 2005). Current data point to a model whereby Tat substrates interact initially with the TatABC complex (with TatB and TatC being the critical components) (Alami *et al*., 2003) triggering recruitment of separate TatA complexes (Mori and Cline, 2002). This transient association of the TatABC and TatA complexes results in the formation or opening of a channel through which substrates can cross the membrane. This channel seems most likely to be mainly (if not completely) composed of TatA. The ability of the TatA protein to form channel like complexes of varying sizes explains the ability of the Tat system to transport folded proteins that differ enormously in terms of size and shape across what is an energy coupled membrane (Gohlke *et al*., 2005). Investigations into the Tat systems of other Gram-negative bacteria have found a degree of structural and functional conservation to the *E. coli* Tat pathway indicating that the *E. coli* Tat pathway is representative of other Gram-negative Tat systems (Oates *et al*., 2003).

The Tat pathways of Gram-positive bacteria differ in their organisation. In almost all cases (the only exception being *Streptomyces* species), the minimal Tat system is comprised of a single TatA and TatC component (Dilks *et al*., 2003; Yen *et al*., 2002). The absence of a TatB component suggests a different organisation and possibly mechanism to the TatABC systems of Gram-negative bacteria. In this study the Tat pathway of a Gram-positive bacterium, the commercially important organism *B. subtilis*, was characterised in detail for the first time. *B. subtilis* is unusual in that it has two distinct Tat pathways that operate in parallel with different substrate specificities

(Jongbloed *et al*., 2004).. The first of these two pathways studied is composed of the two genes, *tatAd* and *tatCd* (Pop *et al*., 2002). These two genes are co expressed in an operon with the Tat substrate *phoD*. PhoD is the only identified substrate of the TatAdCd pathway.

The TatAd and TatCd proteins were expressed in an *E. coli ΔtatABCDE* strain and found to translocate the *E. coli* Tat substrate TMAO reductase (TorA), and a fusion of the TorA signal peptide to GFP (Barnett *et al*., 2008). This result strongly suggests a certain degree of functional conservation amongst the Tat systems of *E. coli* and *B. subtilis*. Furthermore, this result provides some indirect evidence in support of the hypothesis that the TatAd protein is bifunctional. The absence of TatB in Gram-positive bacteria led to the suggestion that the TatA proteins in these bacteria might be bifunctional with both TatA and TatB roles. The ability of TatAdCd to translocate *E. coli* TorA for which a TatA and TatB component is strictly essential supports this hypothesis. More direct evidence for the bifunctional nature of TatAd was obtained by testing the TatAd proteins ability to complement the *E. coli ΔtatAE* and *ΔtatB* mutant strains for translocation of TorA. In both cases TatAd restores export of TorA confirming it can perform both TatA and TatB roles (Barnett *et al*., 2008).

Several mutagenesis studies have been carried out on the *E. coli* TatA and TatB proteins to identify those regions of the proteins that are critical for function. Truncation of the C-terminal ends of the proteins show that the C-terminal tail extensions of these two proteins are not required for function and that the important regions are the transmembrane spanning domain, hinge region, and amphipathic helix (Lee *et al*., 2002). Single amino acid substitutions within the transmembrane spanning domain of both proteins are well tolerated but single substitutions within the hinge region and amphipathic helix can cause a dramatic reduction in translocation activity (Barrett *et al*., 2003; Barrett *et al*., 2005a; Barrett *et al* 2005b; Greene *et al*., 2007; Lee *et al*., 2006). In chapter 6 several point mutations were introduced into the TatAd protein that were then expressed with TatCd in *E. coli ΔtatABCDE* cells. The effect of these mutations on TorA translocation was assessed. As with *E. coli* TatA/TatB, mutations in the hinge region and the first few residues of the amphipathic helix caused a dramatic reduction in translocation activity confirming the importance of this region of the protein for TatA/B function. In addition several amino acid substitutions

in the transmembrane spanning domain also caused a reduction or complete inhibition of translocation activity. Of particular note was the substitution of Pro8 with Ala. This mutation resulted in a complete block in translocation of TorA. A proline residue is conserved amongst Gram-positive TatA proteins at this position or immediately adjacent to it, but no Proline residue is found in this area of the *E. coli* TatA or TatB proteins.

The same mutations were also introduced into the TatAd protein expressed alone and the ability of the mutant TatAd proteins to perform either a TatA or TatB role was determined. Mutations within the C-terminus of the transmembrane span, the hinge region, and the first few residues of the amphipathic helix had significant effects on the ability of TatAd to complement both *E. coli ΔtatAE* and *ΔtatB* mutant strains. This demonstrates the importance of this region for TatA and TatB function. In addition, several mutations at the extreme N-terminus of TatAd and within the N-terminal half of the transmembrane spanning domain caused either a complete block or significant reduction in translocation activity when expressed in *E. coli ΔtatB* cells but not *ΔtatAE* cells. This data points to the N-terminal end of the TatAd protein as having a specific TatB role. This fits nicely with a study that described single N-terminal amino acid substitutions within *E. coli* TatA that allowed the export of TorA in the absence of TatB (Blaudeck *et al*., 2005).

The organisation of TatAd and TatCd into complexes within the plasma membrane was determined and similarities to as well as important differences from the *E. coli* Tat complexes discovered. Like the *E. coli* Tat system, two types of membrane localised Tat complexes were isolated. A TatAdCd containing complex and separate TatAd complexes. Gel filtration chromatography found the TatAdCd complex to be relatively homogenous with a mass of ~ 350 kDa. This is significantly smaller than the *E. coli* TatABC complex that, when analysed in the same way, was found to have a mass of ~ 600 kDa (Bolhuis *et al*., 2001). This difference in size could be caused by the absence of a TatB component in *B. subtilis* but might be caused by the presence of a different number of TatCd and/or TatAd containing units within the complex. This point warrants further investigation and the use of highly purified TatAdCd for single particle analysis may help to address this question.

The second and perhaps most notable difference to the *E. coli* Tat system concerns the separate TatAd complex. The *E. coli* TatA complex is highly heterogeneous and varies in size from below 100 kDa to in excess of 500 kDa (Oates *et al*., 2005). This variation has been linked to the flexibility of the *E. coli* Tat system that allows it to accommodate substrates that vary in size (Gohlke *et al*., 2005). In contrast the TatAd complex was found to be both small and homogeneous in nature displaying none of the size variation of *E. coli* TatA. Gel filtration chromatography gives a size estimate of ~ 160 kDa for the TatAd complex. Despite this difference, the TatAdCd pathway is still able to translocate substrates of different sizes, from GFP at ~ 27 kDa to its own substrate PhoD ~62 kDa, to one of the largest of the *E. coli* Tat substrates TorA ~90 kDa. The homogeneity of the TatAd complex points to a mechanism involving a single defined translocon rather then the spectrum of different sizes as described for *E. coli*. The translocation mechanism might also be more complicated than previously thought and perhaps involves the coalescence of several TatAd and TatAdCd complexes.

The TatAdCd pathway is an unusual translocation pathway, the *tatAd* and *tatCd* genes are only expressed under specific growth conditions (phosphate limitation), and PhoD is the only substrate of this pathway that has been identified in *B. subtilis* (Pop *et al*., 2002). This led to the question of whether the novel features of the TatAdCd and TatAd complexes described above are unique to this system or conserved amongst other Gram-positive Tat systems. To try to address this point the complexes formed by the second Tat pathway of *B. subtilis*, the TatAyCy pathway were characterised. The TatAyCy pathway is comprised of the *tatAy* and *tatCy* genes that are co-expressed in an operon. Unlike the *tatAd* and *tatCd* genes, these genes are constitutively expressed, but the only substrate that has been identified for this pathway is YwbN (Jongbloed *et al*., 2004). The TatAyCy pathway like TatAdCd can function in an *E. coli* background, providing further evidence for a degree of functional conservation between the Tat pathways of Gram-negative and Gram-positive bacteria (Barnett *et al*., 2009).

Affinity chromatography revealed that the TatAy protein, (just like the TatAd protein), is organised into two types of complex within the membrane, a TatAyCy complex and separate TatAy complexes. This organisation into two complexes is a common feature of all Tat systems analysed in a similar way to date (Oates *et al*., 2003; Barnett *et al*.,

2008; Barnett *et al*., 2009). The TatAyCy complex size was estimated using gel filtration chromatography that gives a size estimate even smaller than the TatAdCd complex; ~ 200 kDa compared to 350 kDa for TatAdCd, and ~ 600 kDa for *E. coli* TatABC (Barnett *et al*., 2009). Again this small size compared to *E. coli* TatABC may simply be due to the absence of a TatB component but might also be because of a different number of TatCy and/or TatAy containing units. The separate TatAy complex was also analysed by gel filtration chromatography and again just like the separate TatAd complex it is both small (~200 kDa) and highly homogeneous when compared to *E. coli* TatA. This provides the first evidence of conserved differences in the Tat complexes from Gram-negative and Gram-positive bacteria (Barnett *et al*., 2009).

One of the aims of this work was to produce highly purified Tat complexes for structural analysis by both X-ray crystallography and electron microscopy. The relatively homogeneous nature of the Tat complexes of *B. subtilis* make them an attractive target for such studies and structural work is ongoing.

As mentioned above the two Tat pathways of *B. subtilis* have different substrate specificity. The TatAdCd pathway is solely responsible for translocation of PhoD, and TatAyCy responsible for the transport of YwbN. Two additional Tat substrates of *B. subtilis* were recently identified using a facile reporter system but it remains to be determined whether these are translocated by TatAdCd, TatAyCy or both pathways (Widdick *et al*., 2008). The apparent specificity between the two Tat pathways was investigated in chapter 5. Both pathways (at least when expressed in *E. coli*), are actually able to translocate a very similar set of Tat substrates, although a degree of specificity was apparent. For example, the TatAdCd pathway can translocate TorA but the TatAyCy pathway cannot. It seems likely that this is because the TatAyCy pathway cannot recognise the TorA signal peptide, as TorA-GFP is also not transported. GFP when targeted by other *E. coli* Tat signal peptides, those of DmsA, MdoD, and AmiA, was exported by both TatAdCd and TatAyCy pathways. The TatAdCd pathway is able to handle a broader range of substrates than the TatAyCy pathway although, at least one Tat substrate tested, SufI, was not exported by either TatAdCd or TatAyCy (Barnett *et al*., 2009). The question of why *B. subtilis* has two independent Tat pathways remains open but the similar substrate specificities of both

TatAdCd and TatAyCy suggests that the TatAdCd pathway simply provides additional capacity under conditions of phosphate limitation.

Finally the localisation of the TatA proteins was determined. It was reported in the literature that the TatAd protein of *B. subtilis* has a cytosolic as well as a membrane localisation. Furthermore this soluble population of TatAd was found to have affinity for the Tat substrate PhoD (Pop *et al*., 2003). This led to the proposal of a completely different mechanism of Tat dependent translocation in *B. subtilis* where substrate binds first to cytosolic TatAd. It was proposed that after binding to cytosolic TatAd, the substrate is targeted to membrane localised TatCd through the affinity of TatAd for TatCd (Schreiber *et al.,* 2006). This model is completely different to the current *E. coli* model where substrates bind initially to the TatABC complex within the plasma membrane. In chapter 4 the dual localisation of TatAd was confirmed and in addition *E. coli* TatA and *B. subtilis* TatAy were also found both in the cytosol and plasma membrane. However phase separation experiments using the detergent Triton X-114 strongly suggest that the soluble TatAd protein is mislocalised, and gel filtration experiments found cytosolic TatAd forming massive complexes or possibly aggregates (Barnett *et al*., 2008). The TatAdCd pathway is also found to be active when expressed in *E. coli* and translocate the *E. coli* Tat substrate TorA (Barnett *et al*., 2008) that not only has its own dedicated cytosolic chaperone TorD (Genest *et al*., 2006), but has been shown to interact initially with *E. coli* TatBC in the membrane (Alami *et al*., 2003). Another study has found 3 distinct targeting determinants in *E. coli* Tat signal peptides that are equally important for TatAdCd mediated translocation (Mendel *et al*., 2008). The data presented in this thesis is consistent with the TatAdCd pathway operating in a manner more closely resembling the current *E. coli* model, a schematic representation of our proposed model is shown in Figure 7.1. A remaining challenge is to use more direct experimental methods to determine the physiological role of cytosolic TatAd in the translocation mechanism if any.

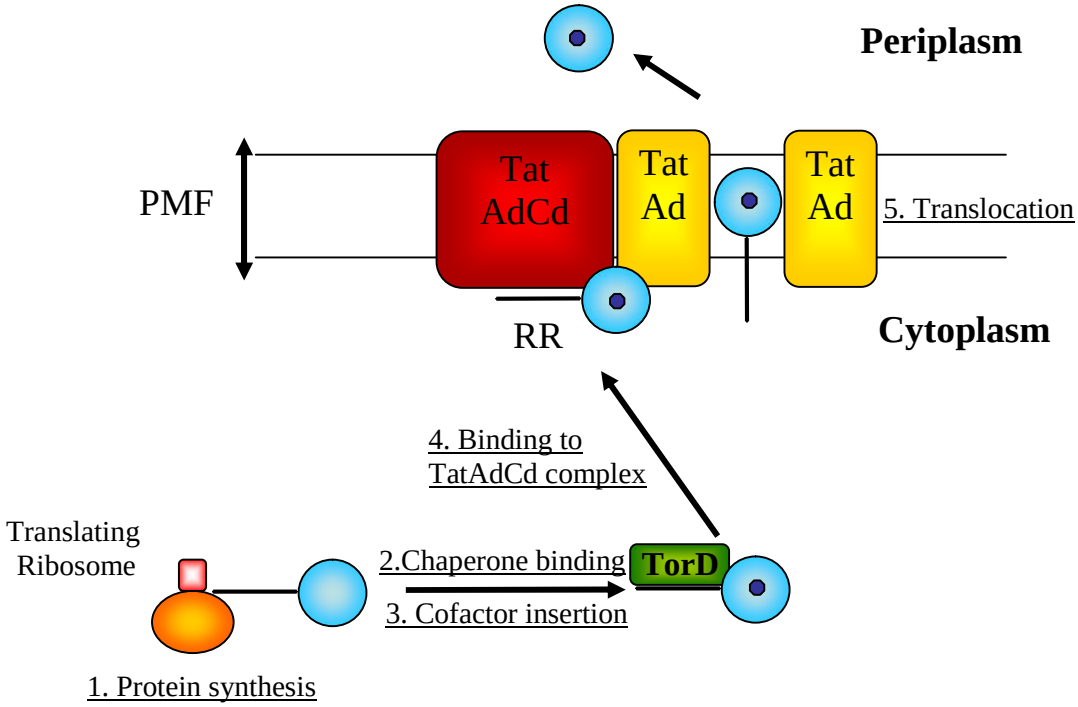

Figure 7.1 Model of TatAdCd dependent translocation in *E. coli*.
1. The Tat substrate TorA is synthesised in the cytoplasm. 2. The chaperone TorD binds to the signal peptide of TorA to prevent premature interaction with the Tat machinery. 3. The molybdenum cofactor is inserted into the protein. 4. The TorA signal peptide binds to the TatAdCd complex within the membrane. Within this complex the TatAd component is performing the role of *E. coli* TatB. 5. Separate TatAd complexes are recruited to form an active translocon and the TorA protein crosses the plasma membrane. Finally the Tat system is reset for another round of translocation.

Chapter 8

References

References

Akiyama, Y., and Ito, K. (1987). Topology analysis of the SecY protein, an integral membrane protein involved in protein export in *Escherichia coli*. *EMBO J.* **6**, 3465-3470.

Alami, M., Luke, I., Deitermann, S., Eisner, G., Koch, H. G., Brunner, J., and Muller, M. (2003). Differential interactions between a twin-arginine signal peptide and its translocase in *Escherichia coli*. *Mol. Cell.* **12**, 937-46.

Alami, M., Trescher, D., Wu, L. F., and Muller, M. (2002). Separate analysis of twin-arginine translocation (Tat)-specific membrane binding and translocation in *Escherichia coli*. *J. Biol. Chem.* **277**, 20499-503.

Allen, S. C., Barrett, C. M., Ray, N., and Robinson, C. (2002). Essential cytoplasmic domains in the *Escherichia coli* TatC protein. *J. Biol. Chem.* **277**, 10362-6.

Bachmann, J., Bauer, B., Zwicker, K., Ludwig, B., and Anderka, O. (2006). The Rieske protein from Paracoccus denitrificans is inserted into the cytoplasmic membrane by the twin-arginine translocase. *FEBS J.* **273**, 4817-30.

Bageshwar, U. K., and Musser, S. M. (2007). Two electrical potential-dependent steps are required for transport by the Escherichia coli Tat machinery. *J. Cell. Biol.* **179**, 87-99.

Barnett, J. P., Eijlander, R. T., Kuipers, O. P. and Robinson, C. (2008) A minimal Tat system from a Gram-positive organism: A bifunctional TatA subunit participates in discrete TatAC and TatA complexes. *J. Biol. Chem.* **283**, 2534-42.

Barnett, J.P., van der Ploeg, R., Eijlander, R. T., Nenninger, A., Mendel, S., Rozeboom, R., Kuipers, O. P., van Dijl, J. M., and Robinson, C. (2009) The twin-arginine translocation (Tat) systems from Bacillus subtilis display a conserved mode of complex organization and similar substrate recognition requirements. *FEBS J.* **276**, 232-43.

Barrett, C. M., Freudl, R., and Robinson, C. (2007). Twin arginine translocation (Tat)-dependent export in the apparent absence of TatABC or TatA complexes using modified Escherichia coli TatA subunits that substitute for TatB. *J. Biol. Chem.* **282**, 36206-13.

Barrett, C. M., Mangels, D., and Robinson, C. (2005a). Mutations in subunits of the Escherichia coli twin-arginine translocase block function via differing effects on translocation activity or tat complex structure. *J. Mol. Biol.* **347**, 453-63.

Barrett, C. M., Mathers, J. E., Robinson, C. (2003a). Identification of key regions within the *Escherichia coli* TatAB subunits. *FEBS Lett*, **537**, 42-6.

Barrett, C. M., Ray, N., Thomas, J. D., Robinson, C., and Bolhuis, A. (2003b). Quantitative export of a reporter protein, GFP, by the twin-arginine translocation pathway in *Escherichia coli*. *Biochem. Biophys. Res. Commun.* **304**, 279-84.

Barrett, C. M., and Robinson, C. (2005b). Evidence for interactions between domains of TatA and TatB from mutagenesis of the TatABC subunits of the twin-arginine translocase. *FEBS. J.* **272**, 2261-75.

Behrendt, J., Lindenstrauss, U., and Brüser, T. (2007). The TatBC complex formation suppresses a modular TatB-multimerization in *Escherichia coli*. *FEBS Lett*. **581**, 4085-90.

Behrendt, J., Standar, K., Lindenstrauss, U., and Bruser, T. (2004). Topological studies on the twin-arginine translocase component TatC. *FEMS Microbiol. Lett.* **234**, 303-8.

Berks, B. C. (1996). A common export pathway for proteins binding complex redox factors? *Mol. Microbiol.* **22**, 393-404.

Berks, B. C., Palmer, T., and Sargent, F. (2003). The Tat protein translocation pathway and its role in microbial physiology. *Advances in Microbial Physiology* **47**, 187-254.

Bernhardt, T. G., and de Boer, P.A. (2003). The *Escherichia coli* amidase AmiC is a periplasmic septal ring component exported *via* the twin-arginine transport pathway. *Mol. Microbiol.* **48**, 1171-82.

Berthelmann, F., and Brüser, T. (2004). Localization of the Tat translocon components in *Escherichia coli*. *FEBS Lett.* **569**, 82-8.

Berthelmann, F., Mehner, D., Richter, S., Lindenstrauss, U., Lünsdorf, H., Hause, G., and Brüser, T. (2008). Recombinant expression of tatABC and tatAC results in the formation of interacting cytoplasmic TatA tubes in *Escherichia coli*. *J. Biol. Chem*. **283**, 25281-9.

Blaudeck, N., Kreutzenbeck, P., Freudl, R., and Sprenger, G. A. (2003). Genetic analysis of pathway specificity during posttranslational protein translocation across the *Escherichia coli* plasma membrane. *J. Bacteriol.* **185**, 2811-9.

Blaudeck, N., Kreutzenbeck, P., Muller, M., Sprenger, G. A., and Freudl, R. (2005). Isolation and characterisation of bifunctional Escherichia coli TatA mutant proteins that allow efficient tat-dependent protein translocation in the absence of TatB. *J. Biol. Chem.* **280**, 3426-32.

Bogsch, E., Brink, S., and Robinson, C. (1997). Pathway specificity for a ΔpH-dependent precursor thylakoid lumen protein is governed by a 'Sec-avoidance' motif in the transfer peptide and a 'Sec-incompatible' mature protein. *EMBO J.* **16**, 3851-9.

Bogsch, E. G., Sargent, F., Stanley, N. R., Berks, B. C., Robinson, C. and Palmer, T. (1998) An essential component of a novel bacterial protein export system with homologues in plastids and mitochondria. *J. Biol. Chem*. **273**, 18003-18006.

Bolhuis, A., Bogsch E. G., and Robinson, C. (2000) Subunit interactions in the twin-arginine translocase complex of Escherichia coli. *FEBS Lett.* **472**, 88-92.

Bolhuis, A., Mathers, J. E., Thomas, J. D., Barrett, C. M., and Robinson, C. (2001). TatB and TatC form a functional and structural unit of the twin-arginine translocase from *Escherichia coli*. *J. Biol. Chem.* **276**, 20213-9.

Bordier C. (1981). Phase separation of integral membrane proteins in Triton X-114 solution. *J. Biol. Chem*. **256,** 1604-1607.

Breyton, C., Haase, W., Rapoport, T. A., Kuhlbrandt, W. and Collinson, I. (2002). Three-dimensional structure of the bacterial protein-translocation complex SecYEG. *Nature*. **418**, 662-5.

Brundage, L., Hendrick, J. P., Schiebel, E., Driessen, A. J. and Wickner, W. (1990). The purified *E. coli* integral membrane protein SecY/E is sufficient for reconstitution of SecA-dependent precursor protein translocation. *Cell*. **62**, 649-57.

Brüser, T. (2007). The twin-arginine translocation system and its capability for protein secretion in biotechnological protein production. *Appl. Microbiol. Biotechnol*. **76**, 35-45.

Buchanan, G., Leeuw, E., Stanley, N. R., Wexler, M., Berks, B. C., Sargent, F., and Palmer, T. (2002). Functional complexity of the twin-arginine translocase TatC component revealed by site-directed mutagenesis. *Mol. Microbiol.* **43**, 1457-70.

Buchanan, G., Maillard, J., Nabuurs, S. B., Richardson, D. J., Palmer, T., and Sargent, F. (2008). Features of a twin-arginine signal peptide required for recognition by a Tat proofreading chaperone. *FEBS Lett.* **582**, 3979-84.

Buchanan, G., Sargent, F., Berks, B. C., and Palmer, T. (2001). A genetic screen for suppressors of *Escherichia coli* Tat signal peptide mutations establishes a critical role for the second arginine within the twin-arginine motif. *Arch, Microbiol,* **177**, 107-12.

Cabelli, R. J., Dolan, K. M., Qian, L. P., and Oliver, D. B. (1991). Characterization of membrane-associated and soluble states of SecA protein from wild-type and SecA51(TS) mutant strains of *Escherichia coli. J. Biol. Chem.* **266**, 24420-7.

Casadaban, M. J., and Cohen, S. N. (1980). Analysis of gene control signals by DNA fusion and cloning in *Escherichia coli*. *J. Mol. Biol.* **138**, 179-207.

Chan, C. S., Zlomislic, M. R., Tieleman, D. P., and Turner, R. J. (2007). The TatA subunit of *Escherichia coli* twin-arginine translocase has an N-in topology. *Biochemistry*. **46**, 7396-404.

Chun, S. Y., and Randall, L. L. (1994). In vivo studies of the role of SecA during protein export in *Escherichia coli. J. Bacteriol*. **176**, 4197-203.

Cline, K., Ettinger, W. F., and Theg, S. M. (1992). Protein-specific energy requirements for protein transport across or into thylakoid membranes. Two lumenal proteins are transported in the absence of ATP. *J. Biol. Chem.* **267**, 2688-2696.

Cline, K., and Mori, H. (2001). Thylakoid ΔpH-dependent precursor proteins bind to a cpTatC-Hcf106 complex before Tha4-dependent transport. *J. Cell. Biol.* **154**, 719-29.

Creighton, A. M., Hulford, A., Mant, A., Robinson, D., and Robinson, C. (1995). A monomeric, tightly folded stromal intermediate on the ΔpH-dependent thylakoid protein import pathway. *J. Biol. Chem.* **270**, 1663-1669.

Cristóbal, S., de Gier, J. W., Nielsen, H., and von Heijne, G. (1999). Competition between Sec- and TAT-dependent protein translocation in *Escherichia coli*. *EMBO J.* **18**, 2982-90.

Czjzek, M., Dos Santos, J. P., Pommier, J., Giordano, G., Méjean, V. and Haser, R. (1998) Crystal structure of oxidized trimethylamine N-oxide reductase from Shewanella massilia at 2.5 A resolution. *J. Mol. Biol*. **284**, 435-447.

Dabney-Smith, C., Mori, H. and Cline, K. (2006) Oligomers of Tha4 organize at the thylakoid Tat translocase during protein transport. *J. Biol. Chem*. **281**, 5476-5483.

De Buck, E., Lammertyn, E., and Anné, J. (2008). The importance of the twin-arginine translocation pathway for bacterial virulence. *Trends Microbiol*, **16**: 442-53.

De Buck, E., Vranckx, L., Meyen, E., Maes, L., Vandersmissen, L., Anné, J., and Lammertyn, E. (2007). The twin-arginine translocation pathway is necessary for correct membrane insertion of the Rieske Fe/S protein in *Legionella pneumophila. FEBS Lett.* **581**, 259-64.

De Keersmaeker, S., Van Mellaert, L., Schaerlaekens, K., Van Dessel, W., Vrancken, K., Lammertyn, E., Anné, J., and Geukens, N. (2005). Structural organization of the twin-arginine translocation system in *Streptomyces lividans. FEBS Lett*. **579**, 797-802.

De Leeuw, E., Porcelli, I., Sargent, F., Palmer, T., and Berks, B. C. (2001). Membrane interactions and self-association of the TatA and TatB components of the twin-arginine translocation pathway. *FEBS Lett.* **506**, 143-8.

DeLisa, M. P., Samuelson, P., Palmer, T., and Georgiou, G. (2002). Genetic analysis of the twin arginine translocator secretion pathway in bacteria. *J. Biol. Chem.* **277**, 29825-31.

Dilks, K., Rose, R. W., Hartmann, E., and Pohlschroder, M. (2003). Prokaryotic utilization of the twin-arginine translocation pathway: a genomic survey. *J. Bacteriol.* **185**, 1478-83

Ding, Z., and Christie, P. J. (2003). *Agrobacterium tumefaciens* twin-arginine-dependent translocation is important for virulence, flagellation, and chemotaxis but not type IV secretion. *J. Bacteriol.* **185**, 760-71.

Driessen, A. J. (1992). Precursor protein translocation by the *Escherichia coli* translocase is directed by the proton motive force. *EMBO J*. **11**, 847-53.

Duong, F and Wickner, W. (1997). Distinct catalytic roles of the SecYE, SecG and SecDFyajC subunits of preprotein translocase haloenzyme. *EMBO J*. **16**, 2756-68.

Duong, F., and Wickner, W. (1998). Sec-dependent membrane protein biogenesis: SecYEG, preprotein hydrophobicity and translocation kinetics control the stop-transfer function. *EMBO J*. **17**, 696-705.

Eder, S., Shi, L., Jensen, K., Yamane, K., and Hulett, F. M. (1996). A Bacillus subtilis secreted phosphodiesterase/alkaline phosphatase is the product of a Pho regulon gene, phoD. *Microbiol.* **142**, 2041-7.

Eijlander, R. T., Jongbloed, J. D., and Kuipers, O. P. (2009). Relaxed specificity of the Bacillus subtilis TatAdCd translocase in Tat-dependent protein secretion. *J. Bacteriol*. **191**, 196-202.

Feilmeier, B. J., Iseminger, G., Schroeder, D., Webber, H., and Phillips, G. J. (2000). Green fluorescent protein functions as a reporter for protein localization in *Escherichia coli*. *J. Bacteriol.* **182**, 4068-76.

Frielingsdorf, S., Jakob, M., and Klösgen, R. B. (2008). A stromal pool of TatA promotes Tat-dependent protein transport across the thylakoid membrane. *J. Biol. Chem*. **283**, 33838-45. 45.

Genest, O., Seduk, F., Ilbert, M., Méjean, V. and Iobbi-Nivol, C. (2006) Signal peptide protection by specific chaperone. *Biochem. Biophys. Res. Commun*. **339**, 991-995.

Gill, D. R., and Salmond, G. P. (1990). The identification of the *Escherichia coli ftsY* gene product: an unusual protein. *Mol. Microbiol*. **4**, 575-83.

Gohlke, U., Pullan, L., McDevitt, C. A., Porcelli, I., de Leeuw, E., Palmer, T., Saibil, H. R. and Berks, B. C. (2005) The TatA component of the twin-arginine protein transport system forms channel complexes of variable diameter. *Proc. Natl. Acad. Sci. U. S. A.* **102,** 10482-10486.

Gouffi, K., Gerard, F., Santini, C. L., and Wu, L. F. (2004). Dual topology of the *Escherichia coli* TatA protein. *J. Biol. Chem.* **279**, 11608-15.

Greene, N. P., Porcelli, I., Buchanan, G., Hicks, M. G., Schermann, S. M., Palmer, T., and Berks, B. C. (2007). Cysteine scanning mutagenesis and disulfide mapping studies of the TatA component of the bacterial twin arginine translocase. *J. Biol. Chem*. **282**, 23937-45.

Hanada, M. , Nishiyama, K. I., Mizushima, S., and Tokuda, H. (1994). Reconstitution of an efficient protein translocation machinery comprising SecA and the three membrane proteins, SecY, SecE, and SecG (p12). *J. Biol. Chem.* **269**, 23625-31.

Hartl, F. U., Lecker, S., Schiebel, E., Hendrick, J.P., and Wickner, W. (1990). The binding cascade of SecB to SecA to SecY/E mediates preprotein targeting to the *E. coli* plasma membrane. *Cell*. **63**, 269-79.

Hatzixanthis, K., Clarke, T. A., Oubrie, A., Richardson, D. J., Turner, R. J., and Sargent, F. (2005a). Signal peptide-chaperone interactions on the twin-arginine protein transport pathway. *Proc. Natl. Acad. Sci. U.S.A.* **102**, 8460-5.

Hatzixanthis, K., Palmer, T., and Sargent, F. (2003). A subset of bacterial inner membrane proteins integrated by the twin-arginine translocase. *Mol. Microbiol*. **49**, 1377-90.

Hatzixanthis, K., Richardson, D. J., and Sargent F. (2005b). Chaperones involved in assembly and export of N-oxide reductases. *Biochem. Soc. Trans*. **33**, 124-6.

Hicks, M. G., de Leeuw, E., Porcelli, I., Buchanan, G., Berks, B. C., and Palmer, T. (2003). The *Escherichia coli* twin-arginine translocase: conserved residues of TatA and TatB family components involved in protein transport. *FEBS Lett.* **539**, 61-7.

Hinsley, A. P., Stanley, N. R., Palmer, T., and Berks, B. C. (2001). A naturally occurring bacterial Tat signal peptide lacking one of the 'invariant' arginine residues of the consensus targeting motif. *FEBS Lett.* **497**, 45-9.

Holzapfel, E., Eisner, G., Alami, M., Barrett, C. M., Buchanan, G., Lüke, I., Betton, J., Robinson, C., Palmer, T., Moser, M. and Müller, M. (2007) The entire N-terminal half of TatC is involved in twin-arginine precursor binding. *Biochemistry*. **46**, 2892-2898.

Hynds, P. J., Robinson, D., and Robinson, C. (1998). The sec-independent twin-arginine translocation system can transport both tightly folded and malfolded proteins across the thylakoid membrane. *J. Biol. Chem.* **273**, 34868-74.

Ilbert, M., Méjean, V., Giudici-Orticoni, M. T., Samama, J. P., and Iobbi-Nivol, C. (2003). Involvement of a mate chaperone (TorD) in the maturing pathway of molybdoenzyme TorA. *J. Biol. Chem.* **278**, 28787-28792.

Ingatova, Z., Hörnle, C., Nurk, A., and Kasche, V. (2002). Unusual signal peptide directs penicillin amidase from *Escherichia coli* to the Tat translocation machinery. *Biochem. Biophys. Res. Commun.* **291**, 146-149.

Ize, B., Gerard, F., and Wu, L. F. (2002a). *In vivo* assessment of the Tat signal peptide specificity in *Escherichia coli*. *Arch. Microbiol.* **178**, 548-53.

Ize, B., Gérard, F., Zhang, M., Chanal, A., Voulhoux, R., Palmer, T., Filloux, A., and Wu, L. F. (2002b). In vivo dissection of the Tat translocation pathway in Escherichia coli. *J. Mol. Biol*. **317**, 327-35.

Ize, B., Stanley, N. R., Buchanan, G., and Palmer, T. (2003). Role of the *Escherichia coli* Tat pathway in outer membrane integrity. *Mol. Microbiol.* **48**, 1183-93.

Jack, R. L., Buchanan, G., Dubini, A., Hatzixanthis, K., Palmer, T., and Sargent, F. (2004). Coordinating assembly and export of complex bacterial proteins. *EMBO J.* **23**, 3962-3972.

Jack, R. L., Sargent, F., Berks, B. C., Sawers, G., and Palmer, T. (2001). Constitutive expression of *Escherichia coli* tat genes indicates an important role for the twin-arginine translocase during aerobic and anaerobic growth. *J. Bacteriol.* **183**, 1801-4.

Jongbloed, J. D., Grieger, U., Antelmann, H., Hecker, M., Nijland, R., Bron, S., and van Dijl, J. M. (2004). Two minimal Tat translocases in Bacillus. *Mol. Microbiol.* **54**, 1319-1325.

Jongbloed, J. D., Martin, U., Antelmann, H., Hecker, M., Tjalsma, H., Venema, G., Bron, S., van Dijl, J. M. and Müller, J. P. (2000) TatC is a specificity determinant for protein secretion via the twin-arginine translocation pathway. *J. Biol. Chem*. **275**, 41350-41357.

Jongbloed, J. D., van der Ploeg, R., and van Dijl, J. M. (2006). Bifunctional TatA subunits in minimal Tat protein translocases. *Trends Microbiol*. **14**, 2-4.

Kol, S., Nouwen, N., and Driessen, A. J. (2008). Mechanisms of YidC-mediated insertion and assembly of multimeric membrane protein complexes. *J. Biol. Chem*. **283**, 31269-73.

Kreutzenbeck, P., Kröger, C., Lausberg, F., Blaudeck, N., Sprenger, G. A., and Freudl, R. (2007). *Escherichia coli* twin arginine (Tat) mutant translocases possessing relaxed signal peptide recognition specificities. *J. Biol. Chem*. **282**, 7903-11.

Kumamoto, C. A. (1991). Molecular chaperones and protein translocation across the Escherichia coli inner membrane. *Mol. Microbiol*. **5**, 19-22.

Kumamoto, C. A., and Francetić, O. (1993). Highly selective binding of nascent polypeptides by an Escherichia coli chaperone protein in vivo. *J. Bacteriol*. **175**, 2184-8.

Laemmli, U. K. (1970). Cleavage of structural proteins during the assembly of the head of bacteriophage T4. *Nature.* **227,** 680-5.

Lange, C., Müller, S. D., Walther, T. H., Bürck, J., and Ulrich, A. S. (2007). Structure analysis of the protein translocating channel TatA in membranes using a multi-construct approach. *Biochim. Biophys. Acta*. **1768**, 2627-2634.

Lavander, M., Ericsson, S. K., Bröms, J. E., and Forsberg, A. (2006). The twin arginine translocation system is essential for virulence of Yersinia pseudotuberculosis. *Infect. Immun*. **74**, 1768-76.

Leake, M. C., Greene, N. P., Godun, R. M., Granjon, T., Buchanan, G., Chen, S., Berry, R. M., Palmer, T., and Berks, B. C. (2008). Variable stoichiometry of the TatA component of the twin-arginine protein transport system observed by in vivo single-molecule imaging. *Proc. Natl. Acad. Sci. U.S.A.* **105**, 15376-81.

Lee, P. A., Buchanan, G., Stanley, N. R., Berks, B. C., and Palmer, T. (2002). Truncation analysis of TatA and TatB defines the minimal functional units required for protein translocation. *J. Bacteriol.* **184**, 5871–9.

Lee, P. A., Orriss, G. L., Buchanan, G., Greene, N. P., Bond, P. J., Punginelli, C., Jack, R. L., Sansom, M. S., Berks, B. C., and Palmer, T. (2006). Cysteine-scanning mutagenesis and disulfide mapping studies of the conserved domain of the twin-arginine translocase TatB component. *J. Biol. Chem.* **281**, 34072-85.

Lee, P. A., Tullman-Ercek, D., and Georgiou, G. (2006). The bacterial Twin-arginine translocation pathway. *Annu. Rev. Microbiol.* **60**, 373-95.

Lequette, Y., Odberg-Ferragut, C., Bohin, J. P., and Lacroix, J. M. (2004) Identification of mdoD, an mdoG paralog which encodes a twin-arginine-dependent periplasmic protein that controls osmoregulated periplasmic glucan backbone structures. *J. Bacteriol.* **186**, 3695-3702

Li, W., Schulman, S., Boyd, D., Erlandson, K., Beckwith, J., and Rapoport, T. A. (2007). The plug domain of the SecY protein stabilizes the closed state of the translocation channel and maintains a membrane seal. *Mol. Cell.* **26**, 511-21.

Luirink, J., High, S., Wood, H., Giner, A., Tollervey, D., and Dobberstein, B. (1992). Signal-sequence recognition by an *Escherichia coli* ribonucleoproetin complex. *Nature.* **359**, 741-3.

Luirink, J., ten Hagen-Jongman, C. M., van der Weijden, C. C., Oudega, B., High, S., Dobberstein, B., and Kusters, R. (1994). An alternative protein targeting pathway in *Escherichia coli*: studies on the role of FtsY. *EMBO J.* **13**, 2289-96.

Maillard, A. P., Lalani, S., Silva, F., Belin, D., and Duong, F. (2007). Deregulation of the SecYEG translocation channel upon removal of the plug domain. *J. Biol. Chem.* **282**, 1281-7.

Mangels, D., Mathers, J., Bolhuis, A., and Robinson, C. (2005) The core TatABC complex of the twin-arginine translocase in *Escherichia coli*: TatC drives assembly whereas TatA is essential for stability. *J. Mol. Biol.* **354**, 415-23.

Matos, C. F., Di Coli, A., and Robinson, C. (2009). TatD is a central component of a Tat-initiated quality control system for exported FeS proteins in *E. coli*. *EMBO Rep.* **10**, 475-9.

Matos, C. F., Robinson, C., and Di Cola, A. (2008). The Tat system proofreads FeS protein substrates and directly initiates the disposal of rejected molecules. *EMBO J.* **27**, 2055-63.

McDevitt, C. A., Buchanan, G., Sargent, F., Palmer, T., and Berks, B. C. (2006). Subunit composition and in vivo substrate-binding characteristics of *Escherichia coli* Tat protein complexes expressed at native levels. *FEBS. J.* **273**, 5656-68.

Meissner, D., Vollstedt, A., van Dijl, J. M. and Freudl, R. (2007) Comparative analysis of twin-arginine (Tat)-dependent protein secretion of a heterologous model protein (GFP) in three different Gram-positive bacteria. *Appl. Microbiol. Biotechnol*. **76**, 633-642.

Méjean, V., Iobbi-Nivol, C., Lepelletier, M., Giordano, G., Chippaux, M., and Pascal, M. C. (1994). TMAO anaerobic respiration in *Escherichia coli*: involvement of the tor operon. *Mol. Microbiol.* **11**, 1169-79.

Mendel, S., McCarthy, A., Barnett, J. P., Eijlander, R. T., Nenninger, A., Kuipers, O. P., and Robinson, C. (2008). The *Escherichia coli* TatABC and a Bacillus subtilis TatAC-type system recognise three distinct targeting determinants in Twin-srginine signal peptides. *J. Mol. Biol*. **375**, 661-72.

Miller, J. D., Bernstein, H. D., and Walter, P. (1994). Interaction of *E. coli* Ffh/4.5S ribonucleoprotein and FtsY mimics that of mammalian signal recognition particle and its receptor. *Nature*. **367**, 657-9.

Mitra, K., Schaffitzel, C., Shaikh, T., Tama, F., Jenni, S., Brooks, C. L., Ban, N. and Frank, J. (2005). Structure of the *E. coli* protein-conducting channel bound to a translating ribosome. *Nature*. **438**, 318-24.

Mori, H. and Cline, K. (2002) A twin arginine signal peptide and the pH gradient trigger reversible assembly of the thylakoid [Delta]pH/Tat translocase. *J. Cell. Biol*. **157**, 205-210.

Mori, H., Summer, E. J., Ma, X., Cline, K. (1999). Component specificity for the thylakoidal Sec and ΔpH-dependent protein transport pathways. *J. Cell. Biol.* **146**, 45-56.

Mould, R. M., and Robinson, C. (1991). A proton gradient is required for the transport of two lumenal oxygen-evolving proteins across the thylakoid membrane. *J. Biol. Chem.* **266**, 12189-93.

Müller, M., and Klösgen, R. B. (2005). The Tat pathway in Bacteria and Chloroplasts (Review). *Mol. Membr. Biol*. **22**, 113-21.

Müller, J. P., and Wagner, M. (1999). **Localisation** of the cell wall-associated phosphodiesterase PhoD of Bacillus subtilis. *FEMS. Microbiol. Lett*. **180**, 287-96.

Nishiyama, K., Hanada, M., and Tokuda, H. (1994). Disruption of the gene encoding p12 (SecG) reveals the direct involvement and important function of SecG in the protein translocation of Escherichia coli at low temperature. *EMBO J*. **13**, 3272-7.

Oates, J., Barrett, C. M., Barnett, J. P., Byrne, K., Bolhuis, A. and Robinson, C. (2005) The Escherichia coli twin-arginine translocation apparatus incorporates a distinct form of TatABC complex, spectrum of modular TatA complexes and minor TatAB complex. *J. Mol. Biol*. **346**, 295-305.

Oates, J., Mathers, J., Mangels, D., Kuhlbrandt, W., Robinson, C., and Model, K. (2003). Consensus structural features of purified bacterial TatABC complexes. *J. Mol. Biol.* **330**, 277-86.

Ochsner, U. A., Snyder, A., Vasil, A. I., and Vasil, M. L. (2002). Effects of the twin-arginine translocase on secretion of virulence factors, stress response, and pathogenesis. *Proc. Natl. Acad. Sci. U. S. A.* **99**, 8312-7.

Orriss, G. L., Tarry, M. J., Ize, B., Sargent, F., Lea, S. M., Palmer, T., and Berks, B. C. (2007). TatBC, TatB, and TatC form structurally autonomous units within the twin arginine protein transport system of *Escherichia coli*. *FEBS. Lett*. **581**, 4091-7.

Palmer, T., Sargent, F., and Berks, B. C. (2005). Export of complex cofactor-containing proteins by the bacterial Tat pathway. *Trends Microbiol*. **13**, 175-80.

Phillips, G.J., and Silhavy, T. J. (1992). The *E. coli* ffh gene is necessary for viability and efficient protein export. *Nature*. **359**, 744-6.

Pool, M. R. (2005). Signal recognition particles in chloroplasts, bacteria, yeast and mammals (review). *Mol. Membr. Biol.* **22**, 3-15.

Pop, O., Martin, U., Abel, C., and Muller, J. P. (2002). The Twin-arginine signal peptide of PhoD and the TatAd/Cd proteins of Bacillus subtilis form an autonomous Tat translocation system. *J. Biol. Chem*. **277**, 3268-3273.

Pop, O. I., Westermann, M., Volkmer-Engert, R., Schulz, D., Lemke, C., Schreiber, S., Gerlach, R., Wetzker, R., and Muller, J. P. (2003). Sequence specific binding of prePhoD to soluble TatAd indicates protein mediated targeting of the Tat export in *Bacillus subtilis*. *J. Biol. Chem*. **278**, 38428-36.

Porcelli, I., De Leeuw, E., Wallis, R., Van Den Brink-Van Der Laan, E., De Kruijff, B., Wallace, B. A., Palmer, T., and Berks, B. C. (2002). Characterization and membrane assembly of the TatA component of the *Escherichia coli* twin-arginine protein transport system. *Biochemistry.* **41**, 13690-13697.

Pugsley, A. P. (1993). The complete general secretory pathway in Gram-negative bacteria. *Microbiol. Rev.* **57**, 50-108.

Punginelli, C., Maldonado, B., Grahl, S., Jack, R., Alami, M., Schröder, J., Berks, B. C., and Palmer T. (2007). Cysteine scanning mutagenesis and topological mapping of the *Escherichia coli* twin-arginine translocase TatC Component. *J. Bacteriol*. **189**, 5482-94.

Randall, L. L. (1983). Translocation of domains of nascent periplasmic proteins across the cytoplasmic membrane is independent of elongation. *Cell*. **33**, 231-40.

Randall, L. L., and Hardy, S. J. (1986). Correlation of competence for export with lack of tertiary structure of the mature species: a study *in vivo* of maltose-binding protein in *E. coli*. *Cell.* **46**, 921-8.

Ray, N., Nenninger, A., Mullineaux, C. W., and Robinson, C. (2005). Location and mobility of twin arginine translocase subunits in the *Escherichia coli* plasma membrane. *J. Biol. Chem*. **280**, 17961-8.

Ray, N., Oates, J., Turner, R. J., and Robinson, C. (2003). DmsD is required for the biogenesis of DMSO reductase in *Escherichia coli* but not for the interaction of the DmsA signal peptide with the Tat apparatus. *FEBS Lett.* **534**, 156-60.

Robinson, C., and Bolhuis, A. (2004). Tat-dependent protein targeting in Prokaryotes and Chloroplasts. *Biochim. Biophys. Acta*. **1694**, 135-47.

Rose, R. W., Bruser, T., Kissinger, J. C., and Pohlschroder, M. (2002). Adaptation of protein secretion to extremely high-salt conditions by extensive use of the twin-arginine translocation pathway. *Mol. Microbiol.* **45**, 943-50.

Saier, M. H. (2006). Protein secretion and membrane insertion systems in Gram-negative bacteria. *J. Membr. Biol*. **214**, 75-90.

Samaluru, H., SaiSree, L., and Reddy, M. (2007) Role of SufI (FtsP) in cell division of Escherichia coli: evidence for its involvement in stabilizing the assembly of the divisome. *J. Bacteriol*. **189**, 8044-8052.

Sambasivarao, D., Turner, R. J., Simala-Grant, J. L., Shaw, G., Hu, J., and Weiner, J. H. (2000). Multiple roles for the twin arginine leader sequence of dimethyl sulfoxide reductase of *Escherichia coli. J. Biol. Chem.* **275**, 22526-31.

Sambrook, J., Fritsch, E. F., and Maniatis, T. (1989). *Molecular Cloning :A Laboratory Manual*, New York: Cold Spring Harbour Laboratory Press

Samuelson, J. C., Chen, M., Jiang, F., Möller, I., Wiedmann, M., Kuhn, A., Phillips, G. J., and Dalbey, R. E. (2000). YidC mediates membrane protein insertion in bacteria. *Nature*. **406**, 637-41.

Samuelson, J. C., Jiang, F., Yi, L., Chen, M., de Gier, J. W., Kuhn, A., and Dalbey, R. E. (2001). Function of YidC for the insertion of M13 procoat protein in *Escherichia coli*: translocation of mutants that show differences in their membrane potential dependence and Sec requirement. *J. Biol. Chem*. **276**, 34847-52.

Santini, C. L., Ize, B., Chanal, A., Muller, M., Giordano, G., Wu, L. F. (1998). A novel sec-independent periplasmic protein translocation pathway in *Escherichia coli*. *EMBO J.* **17**, 101-12.

Sargent, F., Berks, B. C., and Palmer, T. (2006) Pathfinders and trailblazers: a prokaryotic targeting system for transport of folded proteins. *FEMS Microbiol. Lett.* **254**, 198-207.

Sargent, F., Bogsch, E. G., Stanley, N. R., Wexler, M., Robinson, C., Berks, B. C. and Palmer, T. (1998) Overlapping functions of components of a bacterial Sec-independent protein export pathway. *EMBO J*. **17,** 3640-3650.

Sargent, F., Gohlke, U., De Leeuw, E., Stanley, N. R., Palmer, T., Saibil, H. R., and Berks, B. C. (2001). Purified components of the *Escherichia coli* Tat protein transport system form a double-layered ring structure. *Eur. J. Biochem.* **268**, 3361-7.

Sargent, F., Stanley, N. R., Berks, B. C. and Palmer, T. (1999) Sec-independent protein translocation in Escherichia coli. A distinct and pivotal role for the TatB protein. *J. Biol. Chem*. **274**, 36073-36082.

Schagger, H., Cramer, W. A., and von Jagow, G. (1994). Analysis of molecular masses and oligomeric states of protein complexes by blue native electrophoresis and isolation of membrane protein complexes by two-dimensional native electrophoresis. *Anal. Biochem.* **217**, 220-30.

Schagger, H., and von Jagow, G. (1991). Blue native electrophoresis for isolation of membrane protein complexes in enzymatically active form. *Anal. Biochem.* **199**, 223-31.

Schatz, P. J., Riggs, P. D., Jacq, A., Fath, M. J., and Beckwith, J. (1989). The secE gene encodes an integral membrane protein required for protein export in Escherichia coli. *Genes Dev*. **3**, 1035-44.

Schreiber S., Stengel R., Westermann M., Volkmer-Engert R., Pop O. I., and Muller J. P. (2006). Affinity of TatCd for TatAd elucidates its receptor function in the *Bacillus subtilis* Twin-srginine trasnslocation (Tat) translocase system. *J. Biol. Chem.* **281**, 19977-19984.

Scotti, P. A., Urbanus, M. L., Brunner, J., de Gier, J. W., von Heijne, G., van der Does, C., Driessen, A. J., Oudega, B., and Luirink J. (2000). YidC, the *Escherichia coli* homologue of mitochondrial Oxa1p, is a component of the Sec translocase. *EMBO J*. **19**, 542-9.

Serek, J., Bauer-Manz, G., Struhalla, G., van den Berg, L., Kiefer, D., Dalbey, R., and Kuhn, A. (2004). *Escherichia coli* YidC is a membrane insertase for Sec-independent proteins. *EMBO J*. **23**, 294-301.

Settles, A. M., Yonetani, A., Baron, A., Bush, D. R., Cline, K., and Martienssen, R. (1997). Sec-independent protein translocation by the maize Hcf106 protein. *Science.* **278**, 1467-70.

Silvestro, A., Pommier, J., Pascal, M. C., and Giordano, G. (1989). The inducible trimethylamine N-oxide reductase of *Escherichia coli* K12: its localization and inducers. *Biochim. Biophys. Acta.* **999**, 208-16.

Stanley, N. R., Palmer, T., and Berks, B. C. (2000). The twin arginine consensus motif of Tat signal peptides is involved in Sec-independent protein targeting in *Escherichia coli*. *J. Biol. Chem.* **275**, 11591-6.

Stephenson, K. (2005). Sec-dependent protein translocation across biological membranes: evolutionary conservation of an essential protein transport pathway (review). *Mol. Membr. Biol*. **22**, 17-28.

Strauch, E. M., and Georgiou G. (2007). *Escherichia coli* tatC mutations that suppress defective twin-arginine transporter signal peptides. *J. Mol. Biol*. **374**, 283-91.

Summer, E. J., Mori, H., Settles, A. M., and Cline, K. (2000). The thylakoid ΔpH-dependent pathway machinery facilitates RR-independent N-tail protein integration. *J. Biol. Chem.* **275**, 23483-90.

Tam, P. C., Maillard, A.P., Chan, K. K., and Duong, F. (2005). Investigating the SecY plug movement at the SecYEG translocation channel. *EMBO J*. **24**, 3380-8.

Thomas, J. D., Daniel, R. A., Errington, J., and Robinson, C. (2001). Export of active green fluorescent protein to the periplasm by the twin-arginine translocase (Tat) pathway in *Escherichia coli*. *Mol. Microbiol.* **39**, 47-53.

Towbin, H., Staehelin, T., and Gordon, J. (1979). Electrophoretic transfer of proteins from polyacrylamide gels to nitrocellulose sheets: procedure and some applications. *Proc Natl Acad Sci USA* **76**, 4350-4.

Tullman-Ercek, D., DeLisa, M. P., Kawarasaki, Y., Iranpour, P., Ribnicky, B., Palmer, T., and Georgiou, G. (2007). Export pathway selectivity of *Escherichia coli* twin arginine translocation signal peptides. *J. Biol. Chem*. **282**, 8309-16.

Valent, Q. A., Kendall, D. A., High, S., Kusters, R., Oudega, B., and Luirink, J. (1995). Early events in preprotein recognition in *E. coli*: interaction of SRP and trigger factor with nascent polypeptides. *EMBO J*. **14**, 5494-505.

Van den Berg, B., Clemons, W. M., Collinson, I., Modis, Y., Hartmann, E., Harrison, S. C. and Rapoport, T. A. (2004). X-ray structure of a protein conducting channel. *Nature*. **427**, 36-44.

van der Laan, M., Nouwen, N., and Driessen, A. J. (2004). SecYEG proteoliposomes catalyze the Deltaphi-dependent membrane insertion of FtsQ. *J. Biol. Chem*. **279**, 1659-64.

von Heijne, G. (1995). Signal sequences: the limits of variation. *J. Mol. Biol*. **184**, 99-105.

Wagner, S., Baars, L., Ytterberg, A., Klussmeier, A., Wagner, C., Nord, O., Nygren, P., van Wijk, K. and de Gier, J. (2007) Consequences of membrane protein overexpression in Escherichia coli. *Mol. Cell Proteomics*. **6**, 1527-1550.

Walker, M. B., Roy, L. M., Coleman, E., Voelker, R., and Barkan, A. (1999). The maize tha4 gene functions in sec-independent protein transport in chloroplasts and is related to hcf106, tatA, and tatB. *J. Cell. Biol.* **147**, 267-76.

Warren, G., Oates, J., Robinson, C., and Dixon, A. M. (2009). Contributions of the transmembrane domain and a key acidic motif to assembly and function of the TatA complex. *J. Mol. Biol*. **388**, 122-32.

Weiner, J. H., Bilous, P. T., Shaw, G. M., Lubitz, S. P., Frost, L., Thomas, G. H., Cole, J. A., and Turner, R. J. (1998). A novel and ubiquitous system for membrane targeting and secretion of cofactor-containing proteins. *Cell.* **93**, 93-101.

Weiner, J. H., MacIssac, D. P., Bishop, R. E., and Bilous, P. T. (1988). Purification and properties of *Escherichia coli* dimethyl sulfoxide, an iron-sulfur molybdoenzyme with broad substrate specificity. *J. Bacteriol.* **170**, 1505-1510.

Wertman, K. F., Wyman, A. R., and Botstein, D. (1986). Host/vector interactions which affect the viability of recombinant phage lambda clones. *Gene.* **49**, 253-62.

Westerman M., Pop I. O., Gerlach G., Appel T. R., Schlormann W., Schreiber S., and Muller J. P. (2006). The TatAd component of the *Bacillus subtilis* twin-arginine protein transport system forms homo-multimeric complexes in its cytosolic and membrane embedded localisation. *Biochim. Biophys. Acta*. **1758**, 443-451.

Wexler, M., Sargent, F., Jack, R. L., Stanley, N. R., Bogsch, E. G., Robinson, C., Berks, B. C., Palmer, T. (2000). TatD is a cytoplasmic protein with DNase activity. No requirement for TatD family proteins in sec-independent protein export. *J. Biol. Chem.* **275**, 16717-22.

Widdick, D. A., Dilks, K., Chandra, G., Bottrill, A., Naldrett, M., Pohlschröder, M., and Palmer, T. (2006). The twin-arginine translocation pathway is a major route of protein export in Streptomyces coelicolor. *Proc. Natl. Acad. Sci. U.S.A.* **103**, 17927-32.

Widdick, D. A., Eijlander, R. T., van Dijl, J. M., Kuipers, O. P., and Palmer, T. (2008). A facile reporter system for the experimental identification of twin-arginine translocation (Tat) signal peptides from all kingdoms of life. *J. Mol. Biol*. **375**, 595-603.

Xiong, Y., Santini, C. L., Kan, B., Xu, J., Filloux, A., and Wu, L. F. (2007). Expression level of heterologous tat genes is crucial for in vivo reconstitution of a functional Tat translocase in Escherichia coli. *Biochimie.* **89**, 676-85.

Yahr, T. L., and Wickner, W. T. (2001). Functional reconstitution of bacterial Tat translocation *in vitro*. *EMBO J.* **20**, 2472-9.

Yen, M. R., Tseng, Y. H., Nguyen, E. H., Wu, L. F., and Jr Saier, M. H. (2002). Sequence and phylogenetic analyses of the twin-arginine targeting (Tat) protein export system. *Arch. Microbiol.* **177**, 441-50.

Chapter 9

Published Work